Missouri University of Science and Technology
Scholars' Mine

Center for Cold-Formed Steel Structures Library

Wei-Wen Yu Center for Cold-Formed Steel Structures

01 Jun 1965

Effects of cold-forming on light-gage steel members

Kenneth W. Karren

George Winter

Follow this and additional works at: https://scholarsmine.mst.edu/ccfss-library

Part of the Structural Engineering Commons

Recommended Citation

Karren, Kenneth W. and Winter, George, "Effects of cold-forming on light-gage steel members" (1965). *Center for Cold-Formed Steel Structures Library*. 138.
https://scholarsmine.mst.edu/ccfss-library/138

This Technical Report is brought to you for free and open access by Scholars' Mine. It has been accepted for inclusion in Center for Cold-Formed Steel Structures Library by an authorized administrator of Scholars' Mine. This work is protected by U. S. Copyright Law. Unauthorized use including reproduction for redistribution requires the permission of the copyright holder. For more information, please contact scholarsmine@mst.edu.

CCFSS LIBRARY Karren, Kenneth W. Winter,
22 1 * 104 George EFFECTS OF COLD-FORMING
c1 ON LIGH-GAGE STEEL MEMBERS

CCFSS LIBRARY Karren, Kenneth W. Winter,
22 1 * 104 George EFFECTS OF COLD-FORMING
c1 ON LIGH-GAGE STEEL MEMBERS

Technical Library
Center for Cold-Formed Steel Structures
University of Missouri-Rolla
Rolla, MO 65401

Department of Structural Engineering

School of Civil Engineering

Cornell University

Report No. 318

EFFECTS OF COLD-FORMING ON LIGHT-GAGE STEEL MEMBERS

by

Kenneth W. Karren, Research Assistant

George Winter
Project Director

Sixth Progress Report

A Research Project Sponsored by the
American Iron and Steel Institute

Ithaca, New York June, 1965

Wei-Wen Yu
LIBRARY

CONTENTS

ABSTRACT		iii
1.	INTRODUCTION	1
	1.1 General Background and Scope of the Investigation	1
	1.2 Cold-Forming Methods	3
	1.3 Materials	5
2.	PLASTIC STRESS-STRAIN RELATIONSHIPS	7
	2.1 General Strain Hardening Theory	7
	2.2 Representation of the Strain Hardening Equation by a Power Equation	9
	a. Tensile Test Procedure	9
	b. Discussion of Results	10
	2.3 Plastic Strains in Cold-Formed Corners	11
	a. Theoretical Model	11
	b. Plastic Strains by the Photogrid Method	15
3.	PROPERTIES OF COLD-FORMED CORNERS	18
	3.1 Theoretical Tensile Yield Strength of Corners	18
	a. First Corner Model	18
	b. Second Corner Model	23
	3.2 Corner Tests	27
	a. Tensile Corner Test Procedure	27
	b. Compressive Corner Test Procedure	27
	c. Corner Test Results	29
4.	PROPERTIES OF FLATS FROM COLD-FORMED SECTIONS	34
	4.1 Extension of Corner Plastic Strain Effects Into the Adjacent Flats	34
	a. Test Procedure	34
	b. Discussion of Results	36
	4.2 Other Tests of Flats	38
	a. Tensile Tests of Flat Specimens	39
	b. Compressive Tests of Flat Specimens	40
	c. Results of Tests on Flat Specimens	40
5.	FULL SECTION PROPERTIES	49
	5.1 Full Section Tests	49
	a. Full Section Tension Test Procedure	49
	b. Laterally Supported Full Section Compression Test Procedure	49
	c. Stub Column Test Procedure	51

d. Full Section Tension Test Results 51
e. Laterally Supported Full Section Compression Test Results 55
f. Stub Column Test Results 56
5.2 Prediction of Full Section Yield Strength 63

6. THE EFFECT OF COLD-FORMING ON COLUMN BUCKLING STRENGTH IN THE INELASTIC RANGE 71

6.1 Review of Inelastic Buckling Theory 71
6.2 Column Tests 75
a. Column Test Specimens 75
b. Column Test Procedure 76
c. Discussion of Results 77
6.3 Safety Factors in Column Design 82

7. SUMMARY AND CONCLUSIONS 88

APPENDIX A-NOTATION 99

APPENDIX B-YIELD STRENGTH VERSUS PLASTIC STRAIN RELATIONSHIPS OF UNIDIRECTIONALLY PRE-STRAINED FLAT SHEETS 102

APPENDIX C-LOCATION OF THE NEUTRAL AXIS IN MONO- OR NON-SYMMETRIC CROSS SECTIONS WITH NON-UNIFORM MATERIALS PROPERTIES 104

REFERENCES 106

ABSTRACT

Cold-forming may cause significant increases in tensile and in compressive yield strength in both the corner and flat elements of light-gage cold-formed steel members. The cumulative effects may raise the yield strength to as much as 70% above the virgin yield strength of the as-rolled sheet steel. The yield strength of corners is always considerably higher than that of any other portion of a cold-formed member because of the large plastic deformations which take place in the corners. Thus compact members with a large ratio of corner area to cross sectional area will have the largest increases in yield strength. However, in members with a relatively low ratio of corner area to total cross sectional area the total contribution to the increased yield strength of the member may be larger in the flats than in the corners.

Extensive experimental investigations were conducted to study the mechanical properties of full sections, of corner and flat elements from cold-formed sections, and of the virgin materials from which the sections were fabricated.

A method is presented by which the full section tensile yield strength of light-gage members may be predicted from the results of simple tensile coupon tests rather than of full section tests. This method includes, an equation for the prediction of tensile corner yield strength which is based on basic material properties and on concepts from the

theory of plasticity. An empirical equation relating plastic stresses and strains was found to be valid for all nine sheet steel materials tested. The constants in this equation are related to the tensile yield and ultimate strengths of the virgin sheet and are used in developing the corner yield strength equation.

The inelastic buckling behavior of two different types of cross sections of axially loaded pin-ended columns was also investigated analytically and experimentally. These column sections were fabricated by connecting two singly symmetrical sections to form doubly symmetrical sections. Results of these tests are found to correlate well with theoretical column curves based on a modified form of the tangent modulus equation for inelastic column buckling.

1. INTRODUCTION

1.1 General Background and Scope of the Investigation.

The various methods of cold-forming, such as roll forming, brake forming, and deep drawing, bring about changes in the mechanical properties of steel sheets and plates. Cold working generally increases yield and ultimate strengths and decreases ductility. The nature of these changes is dependent on the chemical makeup of the steel, its prior metallurgical history, its prior history of cold work, and on the type and magnitude of plastic strain caused by the cold work. In the first phase[1] of this continuing investigation, specimens subjected to a simple type of cold work were tested to provide an understanding of the fundamental effects of cold-straining before attempting to investigate the more complex types of cold work caused by the cold-forming of members. These specimens, subjected to unidirectional permanent tensile prestrains of 10, 25, 50, and 100 mils, were tested in tension and in compression both in and transverse to the direction of prestrain. It was concluded that the changes brought about in the mechanical properties of sheet steels can be attributed to three phenomena: strain hardening, strain aging, and the Bauschinger effect.

Included herein are the results of the second phase of the investigation, conducted in order better to understand and better to exploit increases in material strength in cold-

---

1. Superscripts refer to References, pp. 106-107.

formed members. Experimental and theoretical studies of the following are included: (1) empirical plastic stress-strain relationships in terms of true stress and true strain, (2) plastic strains occurring in cold-formed corners, (3) the mechanical properties (i.e. yield strength, ultimate strength, and ductility) of corners, (4) extension of plastic strain effects into the adjacent flat portions of the sections, (5) the mechanical properties of flats and full sections, and (6) the inelastic buckling strength of axially loaded pin-ended columns fabricated from cold-formed members.

The method used for derivation of the tensile yield strength of cold-formed corners is outlined briefly below: (1) A corner model is assumed to be produced by a simplified system of forces, e.g. by pure flexure only. (2) An equation is established for the circumferential strain at an arbitrary point in a corner in terms of the radius to the point and of the ratio of the inside radius to the thickness of the corner. The situation in cold-formed corners being that of plane strain, the longitudinal strain component is zero. From the constant volume concept of plasticity it is determined that the third component, the radial strain, is equal and opposite to the circumferential strain when strains are expressed as natural strains. (3) An empirical equation relating stress to strain is established from the stress-strain curves of several tensile specimens from each sheet steel material. (4) In one strain hardening theory it is assumed that such an empirical function is also applicable to certain states

of strain other than simple tension. (5) Thus, using the parallel concepts of effective stress and effective strain, the function relating stress to strain is integrated over the full area of the corner to obtain the average yield strength of the corner after cold working.

In general, stability of thin walled compression members depends on an interaction between local and general buckling. As the L/r ratio is decreased the general buckling stress of a column increases to meet the maximum stress which plate elements are capable of sustaining. Column tests in the inelastic range were conducted on I-shaped columns fabricated by connecting two roll-formed channels back to back and on columns fabricated by connecting two roll-formed joist chord sections together. The tangent modulus equation for inelastic column buckling is applicable in modified form in spite of the non-uniform distribution of the yield strength in cold-formed sections. The tensile and compressive properties of full sections are utilized to obtain analytical column curves for comparison with column test values. On the basis of these comparisons proposals are made for the selection of values of yield stress for use in column design.

1.2 Cold-forming Methods

Light-gage structural members are cold-formed by a variety of methods falling into two main categories: (1) roll-forming and (2) brake forming. Roll-forming is a mass production process requiring rolling machines with a series of two

or more roll stands. As the section passes successive stations in the rolling machine, it is changed by small stages from a flat sheet into the final desired shape. Roll design and the number of roll passes required depends on a number of factors including the complexity of the shape. Roll design has not been completely reduced to a science, depending considerably on the skill and judgment of the designer. Therefore, it is assumed that the type, amount, and locations of cold work resulting from roll-forming will depend, at least within certain limits, on roll design and on roll wear. Forming by press brake, on the other hand, is a straight bending, semi-manually operated process of more limited production capacity, requiring only a standard set of punches, dies, and tools for most shapes which can be braked. A corner may be either "air" or "coin" press braked, the terms "air" and "coin" being descriptive of what actually happens in the forming process. In coin press braking both the punch and the die match the final shape desired in the corner, the die having been cut to the same angle as is subtended by the flats of the final formed corner. The piece to be formed is "coined" or bottomed in the die to eliminate springback. For "air" press braking there are a variety of shapes which may be used for the dies. The corner is bent sharper than the desired final angle to allow for springback. Air press braking is illustrated in Fig. 1. Bending progresses from the centerline outward in this type of forming. The curvature is not constant in the final

corner, being larger for its middle portion[2], Fig. 1. At the point where bending is occurring, there is considerable pressure on the inside surface. However, this radial pressure is probably not as large as that which may occur in either the roll-forming or coin press braking operations.

The three forming methods used in this investigation were (1) roll-forming, (2) air press braking, and (3) coin press braking.

1.3 Materials.

The nine carbon steels used in the investigation are listed in Table 1. The table contains the main properties of the virgin materials in their as-rolled state prior to further cold working. Chemical compositions are shown for each steel. The first four materials, all being of 16 gage thickness, were furnished by Stran Steel Corporation, while the fifth and seventh of 10 gage thickness and the sixth and eighth of 16 gage thicknesses were furnished by U. S. Steel Corporation. The ninth material of 9 gage thickness was furnished by the Armco Steel Corporation.

The following abbreviations are used herein:

1. CRK16-38.3 - Cold reduced killed 16 gage sheet steel
2. CRR16-36.4 - Cold reduced rimmed 16 gage sheet steel
3. HRSK16-37.5 - Hot rolled semi-killed 16 gage sheet steel
4. HRR16-40.5 - Hot rolled rimmed 16 gage sheet steel
5. HRSK10-37.0 - Hot rolled semi-killed 10 gage sheet steel

6. HRSK16-39.7 - Hot rolled semi-killed 16 gage sheet steel
7. HRSK10-42.8 - Hot rolled semi-killed 10 gage sheet steel
8. HRSK16-40.7 - Hot rolled semi-killed 16 gage sheet steel
9. HRSK9-30.7 - Hot rolled semi-killed 9 gage sheet steel.

The last number in each designation is the tensile yield strength of the virgin sheet in ksi., taken in the direction in which the sheet was rolled. The virgin yield strength is defined as the yield strength of the material in the state which it is in prior to being cold-formed. For example, the first 8 materials were received in the form of flat sheets. The last material (HRSK9-30.7) was received in a curved condition as it was cut directly from the coil. This was done because it was roll-formed into a joist chord directly from the coil without stretcher-straightening. The procedures used in testing these virgin materials are described below in Sections 4.2a and b.

The first five materials were used in the work of the first phase on simple unidirectional prestrain[1]. Tensile and compressive corner yield strengths were determined experimentally for all nine materials.

2. PLASTIC STRESS-STRAIN RELATIONSHIPS

2.1 General Strain Hardening Theory.

One theory of strain hardening[3,4] may be expressed in the form

$$\bar{\sigma} = F(\bar{\varepsilon}) \tag{1}$$

where $\bar{\sigma}$ is a quantity known variously as the generalized stress, equivalent stress, or effective stress which may be determined from the Huber-Mises-Hencky distortion energy yield condition as

$$\bar{\sigma} = \frac{1}{\sqrt{2}} \sqrt{(\sigma_1 - \sigma_2)^2 + (\sigma_2 - \sigma_3)^2 + (\sigma_3 - \sigma_1)^2} \tag{2}$$

where σ_1, σ_2, and σ_3, are the principal stresses. (For large plastic strains, such as will be considered herein, these principal stresses must be expressed in terms of true stress. True stress is defined as load divided by instantaneous area. However, it is customary and convenient to omit reference to true stresses when dealing with three dimensional plasticity problems.) Note that for the condition of uniaxial tension, $\bar{\sigma}$ is equal to σ_1', where the prime indicates that the stress is in terms of true stress. $\bar{\varepsilon}$ is a somewhat analogous quantity variously called the generalized strain, equivalent total strain, or effective strain.

$$\bar{\varepsilon} = \frac{\sqrt{2}}{3} \sqrt{(\varepsilon_1' - \varepsilon_2')^2 + (\varepsilon_2' - \varepsilon_3')^2 + (\varepsilon_3' - \varepsilon_1')^2} \tag{3}$$

where ε_1', ε_2' and ε_3' are the natural principal strains. Natural or logarithmic strain ε' is related to engineering

strain ε by

$$\varepsilon' = \ln (1 + \varepsilon) \qquad (4)$$

For the case of uniaxial stress in the plastic range, taking Poisson's ratio as 1/2 results in $\varepsilon_2' = \varepsilon_3' = - 1/2\ \varepsilon_1'$. The constant in Eq. 3 is chosen such that substitution of these values of principal strains gives an effective strain equal to ε_1'. In Eq. 1, F is a function depending on the characteristics of the metal involved. F may be found, for example, from the stress strain curve of a simple tensile specimen, and is assumed to be valid for other states of stress, subject to some limitations which will be enumerated below.

Eq. 1 is subject to the following assumptions: (1) The material is isotropic under plastic conditions. (2) Elastic strains are negligible in comparison with plastic strains. (3) Shearing stresses are responsible for plastic deformations, but normal stresses are not. (4) The ratios of the principal strains remain constant throughout the straining which takes place, i.e. $\varepsilon_2/\varepsilon_1$ and $\varepsilon_3/\varepsilon_1$ remain constant. (5) The principal axes of successive strain increments do not rotate with respect to the element. (6) The tensile and compressive stress-strain curves coincide when expressed in terms of true stress and true strain. (7) No Bauschinger effect is present. (8) There is no change in volume due to plastic deformation. Assumption (8) has been verified to be quite accurate by a number of investigators. For the large plastic strains occurring in cold-formed corners the elastic

strains, assumption (2), are indeed negligible. Assumptions (4) and (5) are shown below to be true for a somewhat idealized model of a cold-formed corner. Assumption (7) is found below to be reasonable from a theoretical standpoint. Experimental evidence from this investigation and that of Rolfe[5] also appears to justify the use of this assumption. From results obtained in this investigation it will be shown that the cumulative error caused by these and the remaining assumptions ((1), (3), and (6)) is reasonably small.

2.2 Representation of the Strain Hardening Equation by a Power Equation.

For some metals the strain hardening function F of Eq. 1 may be represented in the plastic portion of the stress-strain curve by a power function[4,6,7]

$$\bar{\sigma} = k\,(\bar{\varepsilon})^n \qquad (5)$$

where k is called the strength coefficient, and n is called the strain hardening exponent. This formulation is possible when a plot of the logarithm of $\bar{\varepsilon}$ versus the logarithm of $\bar{\sigma}$ in the plastic domain appears as a straight line which is the case for many steels and some other metals[6,7]. For uniaxial tension Eq. 5 reduces to $\sigma' = k(\varepsilon')^n$ by use of Eqs. 2 and 3. To utilize this equation, it is first necessary to investigate k and n experimentally.

a. Tensile Test Procedure. For determination of plastic stress-strain characteristics, three 15 inch long tensile specimens were prepared for each of the nine materials of

Table 1. These specimens were standard tensile specimens except that the narrow (1/2 inch wide) middle portion was 9 inches long rather than the standard 3 inches. Marks 8 inches apart were accurately punched on the specimens. Dividers were preset to appropriate lengths. When the specimen had elongated such that the distance between punch marks matched the preset dividers, the load was read and recorded. The data was converted to true stress and true strain and plotted on log log paper.

b. Discussion of Results. Typical true stress-strain curves are shown in Fig. 2 for the first three materials. Values of k and n obtained from similar true stress-strain curves for each of the nine materials are given in Table 2. Values of k vary from 70 to 114 ksi, and values of n vary from 0.13 to 0.28.

From the non-dimensional plot of σ_{yc}/k versus σ_u/σ_y of Fig. 3 it can be seen that the empirical formula

$$k = 2.80\ \sigma_u - 1.55\ \sigma_y \qquad (6)$$

gives a good approximation for k where

σ_u = the virgin ultimate strength in ksi. and

σ_y = the virgin tensile yield strength in ksi.

From the plot of Fig. 4 where values of n are plotted versus σ_u/σ_y, it can be seen that values of n tend to increase in a general way with increase in the σ_u/σ_y ratio. These experimental values of n may be approximated by

$$n = 0.225\ \sigma_u/\sigma_y - 0.120 \qquad (7)$$

Eqs. 5, 6, and 7 will prove useful below in Section 3.1 in

deriving equations for predicting the tensile yield strength of cold-formed corners.

2.3 Plastic Strains in Cold-Formed Corners.

Circumferential strains at any point in a cold-formed corner are established for a simplified theoretical model of a corner. The results are compared to experimental evidence obtained by using a photogrid method.

a. Theoretical Model. In order to attempt an analysis of strains in a corner caused by cold work it is helpful to choose a model[3,8] with a somewhat simpler force system acting on it than actually exists in any of the common methods of cold-forming. Such a model, in which application of a pure bending moment to a wide flat sheet produces a uniform curvature and uniform tangential strain, is shown in Fig. 5. A certain amount of radial pressure is present in die bending in addition to bending moment. In coin press braking and in roll-forming, the metal in the corner is even more highly compressed in the radial direction. In spite of these complexities, however, it proves instructive and worthwhile to begin by investigating the simplified model.

It is assumed that sections in the radial direction which are plane before plastic bending remain plane after bending. From symmetry it can be seen that the principal directions for stress and strain will be the radial or r, the tangential or θ, and the longitudinal or z directions. The Levy-Mises theory of plastic flow,[3,4,8] in which it is

assumed that elastic strains are negligible in comparison to plastic strains, relates the deviator stress tensor to the strain-increment tensor by

$$S' d\lambda = dE \tag{8}$$

where S' = deviator stress tensor,

dE = strain increment tensor, and

$d\lambda$ = a scalar factor of proportionality.

The first equation contained in this matric equation may be written as

$$\frac{d\lambda}{3} (2\sigma_z - \sigma_r - \sigma_\theta) = d\,\epsilon_z \tag{9}$$

where σ_z, σ_r, and σ_θ are the principal stresses and ϵ_z is the strain in the longitudinal direction. However, since $\epsilon_z = 0$, and $d\epsilon_z = 0$, this becomes

$$\sigma_z = \frac{\sigma_r + \sigma_\theta}{2} \tag{10}$$

Substituting this in the Huber-Mises-Hencky distortion-energy yield condition

$$(\sigma_z - \sigma_r)^2 + (\sigma_r - \sigma_\theta)^2 + (\sigma_\theta - \sigma_z)^2 = 2\sigma_y^2 \tag{11}$$

gives

$$\sigma_r - \sigma_\theta = \pm 2\,K \tag{12}$$

where

$$K = \sigma_y / \sqrt{3} \tag{13}$$

Note that the use of the Huber-Mises-Hencky yield criterion tacitly assumes isotropy and the absence of the Bauschinger effect.

The equilibrium equation of the element of volume of Fig. 5 is

$$\frac{d\sigma_r}{dr} = \frac{\sigma_\theta - \sigma_r}{r} = \pm \frac{2K}{r} \qquad (14)$$

Separation of variables and integration using the boundary condition $\sigma_r = 0$ at $r = b$, the outside radius, yields

$$\sigma_r / 2K = \ln r/b \quad \text{for } r_n \leq r \leq b \qquad (15)$$

and using the boundary condition $\sigma_r = 0$ at $r = a$, the inside radius, gives

$$\sigma_r / 2K = \ln a/r \quad \text{for } a \leq r \leq r_n \qquad (16)$$

These two expressions must be equal at the neutral surface. Equating them gives the radius to the neutral surface, or fiber of zero stress[3,9]

$$r_n = \sqrt{ab} \qquad (17)$$

It may also be shown that the thickness of the model does not change during the plastic deformation.[3,8] This does not mean that the thickness of the volume element of Fig. 5 does not change. It simply means that the overall thickness from a to b remains constant. Hill showed that the neutral surface (i.e., the surface where $\sigma_\theta = 0$) and the fiber of zero strain are not the same[3]. The neutral surface is initially at the midplane of the sheet. As bending progresses, all fibers on the inside of the neutral surface are compressed and those on the outside stretched. Then, as bending progresses still further and the neutral surface moves toward the inside radius, an area that was under compression is now stretched.

It has been shown experimentally that for large plastic strains the material may be considered incompressible for most metal-forming operations. If the location of a given fiber from the mid-plane of the undeformed sheet is described by y (Fig. 5(b)) where $-t/2 < y < t/2$, the volume constancy principle may be applied to solve for the radius r (Fig. 5 (c)) locating this same fiber in the plastically deformed corner. The area outside the radius r is constant before and after deformation:

$$A_1 = \theta/2\,(b^2 - a^2) = (t/2 - y)\,\ell_o \qquad (18)$$

as is the area inside r:

$$A_2 = \theta/2\,(r^2 - a^2) = (t/2 + y)\,\ell_o \qquad (19)$$

Dividing A_2 by A_1 and simplifying gives

$$r = \sqrt{(a^2 + b^2)/2 + (b^2 - a^2)\,y/t} \qquad (20)$$

as given by Hill.[3]

The relation between the original fiber length ℓ_o and the inside and outside radii may be expressed by equating initial and final corner areas and simplifying to obtain

$$\ell_o = (b + a)\,\theta/2 \qquad (21)$$

The radius to the fiber of zero strain is then given by

$$r_o = (b + a)/2 \qquad (22)$$

The engineering strain in the tangential direction is linear with r, i.e.

$$\varepsilon_\theta = \frac{r - (a + b)/2}{(a + b)/2} = \frac{2r}{a + b} - 1 \qquad (23)$$

At the inner ($r = a$) and outer ($r = b = a + t$) surfaces the tangential strain may be found from[8]

$$\varepsilon_a = -\varepsilon_b = -\frac{1}{2a/t + 1} \tag{24}$$

The volume strain Δ is given by

$$\Delta = (1 + \varepsilon_1)(1 + \varepsilon_2)(1 + \varepsilon_3) - 1 \tag{25}$$

and the logarithmic volume strain Δ' is given by

$$\Delta' = \ln (1 + \Delta) = \varepsilon_1' + \varepsilon_2' + \varepsilon_3' \tag{26}$$

Since $\Delta = 0$ for constant volume,

$$\Delta' = \varepsilon_1' + \varepsilon_2' + \varepsilon_3' = 0 \tag{27}$$

In the case of the purely flexural model which is in a condition of plane strain $\varepsilon_z' = 0$ and, consequently,

$$\varepsilon_r' = -\varepsilon_\theta' \tag{28}$$

Using this in Eq. 3 results in $\bar{\varepsilon} = \frac{2}{\sqrt{3}} \varepsilon_\theta'$, from which

$$\bar{\varepsilon} = \frac{2}{\sqrt{3}} \ln (1+ \varepsilon_\theta) = \frac{2}{\sqrt{3}} \ln \left(\frac{2r}{a+b}\right) \tag{29}$$

Eq. 29 will be used below in Section 3.1 in deriving equations for predicting the tensile yield strength of cold-formed corners.

b. Plastic Strains by the Photogrid Method. An accurately gridded contact negative with divisions of 200 lines per inch and lines of 0.00045 inch width was purchased. The spacing of the lines was reported to be accurate to $\pm$ 0.0001 inch. The edges of the steel sheets were de-burred, and the surfaces were degreased, cleaned and dried. A photographic emulsion was applied to the surfaces of the sheets. They were then exposed to the grid, developed, and

the grid image dyed black. The process provided a satisfactory grid both on the light surface of cold reduced sheets and the dark surface of hot rolled sheets.

Sixteen gage cold reduced rimmed sheets with both surfaces photogridded were air and coin press braked into corners of various radii. Measurement of the maximum plastic strains on the inside and outside surfaces was accomplished by means of a vernier microscope. Thickness to inside radius ratios were obtained by cutting thin sections from the photogridded corners and examining them on a 32 power comparator. Concentric circles were compared with the corner image until the circle which best matched the central part of the inside radius was found. A slight reduction in thickness was observed in most of these corner images. The reduction varied from 0% for the largest to 3% for the smallest a/t ratios.

The experimental plastic strains, measured in the tangential direction on the inside and outside corner surfaces, are shown in Fig. 7. The theoretical strains given by Eq. 24 for the purely flexural model are shown by the dashed lines. The experimental strains are somewhat larger on the tensile surface and slightly smaller on the compressive surface than the theoretical strains given by Eq. 24. The differences between the experimental and the theoretical values are largest for low values of the a/t ratio (i.e. high values of the t/a ratio.) Quite similar results were obtained by Lubahn and Sachs[9] for plastic bending of an aluminum alloy. The theoretical strains shown by the solid

lines will be discussed in Section 3.1b in connection with a second model which includes the effect of radial pressure in addition to bending during the forming of the corner. Note that the correlation of experimental points is better for the second model than for the first. Strains measured in the longitudinal direction of these specimens were negligible. Consequently, a plane strain condition may be considered to exist during and after the plastic condition of cold-forming.

Grids were also applied to the edges of 10 gage sheet so that the distribution of plastic strains over cross sections could be studied as well as on the inside and outside surfaces of sheets bent into corners. When a wide flat plate or sheet is bent by applying equal bending moments to two opposite edges, distortions occur at the two edges where no moment is applied. Thus the application of photogrids to the unrestrained edges of such sheets or plates will not give precise values of the plastic strains which have occurred in the locations in which restraint is present. In spite of such edge distortions, however, the photogridded specimen of Fig. 6 appears roughly to justify the assumption that plane sections before plastic bending remain plane after bending.

3. PROPERTIES OF COLD-FORMED CORNERS

3.1 Theoretical Tensile Yield Strength of Corners

In this section an equation is established to relate the corner yield strength σ_{yc} directly to the fundamental material properties k and n. This will be done for (1) a corner model with purely flexural loads and (2) for a corner model with flexural plus radial pressure loads.

a. First Corner Model. Because of the condition of plane strain it is logical to assume that the Bauschinger effect is not present in the plastically formed corner model of Fig. 5(a). Indeed, a typical volume element located outside the surface of zero strain will have a tensile natural plastic strain in the tangential direction and a compressive natural plastic strain of equal magnitude in the radial direction (as was shown by Eq. 28). Similarly, a volume element located inside the surface of zero strain will have a compressive natural plastic strain in the tangential direction and a tensile natural plastic strain of equal magnitude in the radial direction. In each of these two typical elements the plastic strains ε_θ' and ε_r' of equal size and opposite sign are oriented at right angles to the final direction of testing or loading, the longitudinal z-direction. Thus, considering one strain at a time and superimposing the two effects, there is no net effect on the yield strength in the longitudinal direction from the "inverse

Bauschinger effect".* For example, the increase in tensile yield strength in the longitudinal direction from a compressive plastic strain in the tangential direction is offset by the reduction from the equal tensile plastic strain in the radial direction. Rolfe[5] reported that specimens taken from locations of high plastic deformation in 2 1/2 inch thick HY-80 steel plates cold-formed to different radii exhibited no Bauschinger effect when tested in the longitudinal direction. There is, however, an increase in both tensile and compressive yield strength due to strain hardening.

It is desired to find the stress at which a corner will yield when tested in uniaxial tension. A corner may be considered to be made up of a series of elements each of which has its own characteristic stress-strain curve. Suppose a composite stress-strain curve for the corner were calculated from those of the individual elements. Then the corner yield strength could be determined from this composite curve. (A technique for construction of composite stress-strain curves is given below in Section 5.1d.) However, in this

---

* "The phenomenon that results in an increase in the proportional limit and yield strength by reloading plastically deformed specimens in the same direction, but in a decrease by reloading it in the opposite direction is known as the Bauschinger effect." However, when testing is at right angles to prior cold-straining, a prior tensile strain produces a larger increase in the compressive than in the tensile yield strength. This is called the "Inverse Bauschinger Effect" by Chajes, Britvec, and Winter in a thorough discussion of the Bauschinger effect.[1]

case this is neither practical nor necessary. The corner yield stress may be approximated quite accurately by taking the weighted average of the yield strengths of the elements of the corner. Weighted average versus composite stress-strain yield strengths are discussed in more detail below in Section 5.2 where examples for full sections are given. Now assume that the material has been cold worked to a certain "effective stress" and then unloaded. Next, assume that the material is reloaded by a different system of forces. It should now yield when the "effective stress" of the second loading equals that of the first. For uniaxial tension the effective stress is equal to the applied tensile stress. Since the Bauschinger effect is assumed to be absent, the average corner yield strength is given by the average effective stress attained in cold-forming.

No correction from true stress to engineering stress is required here. If a specimen is loaded plastically in uniaxial tension and then unloaded its area will be reduced. If the specimen has not reached the point where necking begins the reduced area may be found from

$$A = A_o/(1 + \varepsilon) \qquad (30)$$

where A is the final area, A_o the initial area, and ε the strain to which the specimen was taken. (Elastic strains are neglected as being quite small compared to plastic strains.) However, the new area is the initial area for any subsequent loading. Therefore, the true stress of a prior plastic loading is the engineering stress of the

subsequent loading. Furthermore, in the first corner model the area remains constant during plastic deformation. This is true because of the incompressibility of the material with regard to plastic strains and because of the plane strain condition.

While no tests were made on unidirectionally precompressed sheets, it is assumed that Eq. 5 for the plastic tensile strain of a material is also valid for plastic compressive strains of the same material using the values of k and n determined from tensile tests. The average corner yield strength σ_{yc} is obtained by integrating the effective stress from Eq. 5 over the full area of a corner:

$$\ell_o t\ \sigma_{yc} = k \int_A |\bar{\varepsilon}|^n\ dA = k \int_{-t/2}^{t/2} |\bar{\varepsilon}|^n\ \ell_o dy \qquad (31)$$

or

$$_o\sigma_{yc} = k/t \int_{-t/2}^{t/2} |\bar{\varepsilon}|^n\ dy \qquad (32)$$

By taking the derivative of Eq. 20 the change of variable $dy = 2tr/(b^2 - a^2)\ dr$ is obtained. Using this in Eq. 32 gives

$$\sigma_{yc}/k = \int_a^b \frac{2\ |\bar{\varepsilon}|^n\ r\ dr}{(b^2 - a^2)} \qquad (33)$$

Separating this integral into two parts, using Eq. 29 for $\bar{\varepsilon}$ and the change of variable $x = 2r/(a + b)$, yields

$$\sigma_{yc}/k = 1/2(2a/t + 1)\left[\int_{1}^{\frac{2a/t + 2}{2a/t + 1}} \left(\frac{2}{\sqrt{3}} \ln x\right)^n x\,dx + \right.$$

$$\left. + \int_{\frac{2a/t}{2a/t + 1}}^{1} \left|\frac{2}{\sqrt{3}} \ln x\right|^n x\,dx\right] \qquad (34)$$

The integrals in this equation were evaluated numerically by means of Simpson's Rule for values of n held constant. Values of the integrals are given in Table 3 and plotted in Fig. 8(a). The final result is that σ_{yc} is a product of the strength coefficient k and a coefficient determined from Fig. 8(a) as a function of the a/t ratio and the strain hardening exponent n.

For values of a/t less than 10.0 Eq. 34 may be closely approximated by the empirical formula

$$\sigma_{yc} = \frac{kb}{(a/t)^m} \qquad (35)$$

This is true because the plot (Fig. 8(a)) of Eq. 34 on log log paper, holding n constant, approximates a straight line quite closely. Furthermore, using Eq. 35, it was found that the relationships between the constants b and n and between m and n are linear as shown in Figs. 8(b) and (c). The empirical equations for b and m are

$$b = 0.945 - 1.315n \qquad (36)$$

$$\text{and} \quad m = 0.803n \qquad (37)$$

With values of k and n available for sheet materials Eqs. 35, 36, and 37 may be used to establish σ_{yc} values. This will

be discussed further after consideration of the second corner model.

b. Second Corner Model. Radial pressures of unknown magnitudes are present during the plastic bending of corners by air and coin press braking or by roll-forming. The effect of an inside radial pressure during the plastic bending is, therefore, explored analytically. This is done, by means of a second corner model with a uniformly distributed outward radial pressure p on the inside surface of the corner. The uniform radial pressure is equilibrated by circumferential tensile forces equal to pa per unit length of the corner. Cylindrical surfaces will remain cylindrical, but Hill has shown that these conditions cause the neutral surface to displace inward and the thickness of the sheet to decrease[3]. (Note that the maximum decrease in thickness measured for the press braked photogridded corners was 3%.) Integrating Eq. 14 using the corresponding boundary conditions $\sigma_r = -p$ at $r = a$ and $\sigma_r = 0$ at $r = b$, the radial stresses are

$$\sigma_r = -2K \ln b/r, \quad \text{for } r_n \leqq r \leqq b \tag{38}$$

$$\sigma_r = -p - 2K \ln r/a \quad \text{for } a \leqq r \leqq r_n \tag{39}$$

Equating the expressions for σ_r at the neutral surface, the radius to the neutral surface is

$$r_n = \sqrt{abe^{-p/2K}} \tag{40}$$

Comparison with Eq. 17 shows that the neutral surface is closer to the inside surface than for the first model

(subjected to pure flexure only.) Now, if the neutral surface is displaced inward, so will be the fiber of zero strain. Larger strains will be expected on the outside fiber and smaller strains on the inside fiber.

The exact amount of radial pressure produced by any of the three forming methods is not known. However, the location of the axis of zero strain may be adjusted by trial until better agreement is obtained between the experimental and theoretical strains of Fig. 7. In so doing it is assumed that the slight thinning effect can be ignored and that the strain distribution remains linear. If it is thus arbitrarily assumed that the axis of zero strain is located at

$$r_o = \sqrt{ab} \tag{41}$$

the resulting theoretical strains are $e_a = \sqrt{b/a} - 1$ and $e_b = \sqrt{a/b} - 1$ and are shown by the solid lines on Fig. 7. Comparison of Eqs. 41 and 22 shows that the axis of zero strain is closer to the inside surface for the second than for the first corner model.) It appears that this assumption tends to give closer agreement between theoretical and experimental strains than the assumption of pure flexural bending. The effective strain becomes

$$\bar{\varepsilon} = (2/\sqrt{3})\varepsilon_\theta' = (2/\sqrt{3}) \ln r/r_o \tag{42}$$

From the volume constancy relation it may be assumed that an area after deformation is equal to the same area before

deformation. Thus

$$dA = \ell_o = \theta r_o \, dy = \theta r \, dr \tag{43}$$

from which

$$dy = r/r_o \, dr \tag{44}$$

Now, integrating the effective stress over the corner area by substitution in Eq. 31:

$$\sigma_{yc} = k/t \int_a^b |2/\sqrt{3} \ln r/r_o|^n \, r/r_o \, dr \tag{45}$$

With the change in variable $x = r/r_o$

$$\sigma_{yc}/k = r_o/t \int_{a/r_o}^{r_o/a} |2/\sqrt{3} \ln x|^n \, x \, dx \tag{46}$$

Eq. 46 was broken into two parts and evaluated by Simpson's rule in a similar manner to the way Eq. 34 was evaluated. Eq. 46 can also be closely approximated by Eq. 35 provided that the relationships between b and m are now given by

$$b = 1.0 - 1.3n \tag{47}$$

$$\text{and} \quad m = 0.855n + 0.035 \tag{48}$$

In non-dimensional form Eq. 35 may be written as $\sigma_{yc}/\sigma_y = (kb/\sigma_y)/(a/t)^m$. By inspection of Eqs. 6, 7, 47, and 48 it may be seen that the right hand side of this form of Eq. 35 is a function of only two parameters: the σ_u/σ_y and the a/t ratios. This fact made possible the preparation of Fig. 8(d) as an aid to design.

The dashed and solid curves for σ_{yc} versus a/t ratio of Figs. 9-17 were obtained by evaluating Eqs. 35, 36, and 37

for the first corner model and Eqs. 35, 47, and 48 for the second corner model. Experimental values of σ_{yc} are also shown in Figs. 9-17. Values for the materials constants k and n were established for use with Eq. 35 by three different methods: (1) from empirical Eqs. 6 and 7 which require that representative values of σ_u and σ_y be available from standard tension tests, (2) from true stress-strain curves of virgin tensile specimens, carried well into the plastic range as on Fig. 2, and (3) from yield strength-strain curves for uniaxially prestrained and aged sheets (See Appendix B).

Curves of σ_{yc} versus a/t established using k and n values taken directly from true stress-strain curves of tensile specimens (Method 2)) are not shown, but have the same general shape and appearance as the curves shown. However, the natural variations in virgin properties which occur from location to location in any rolled sheet steel cause variations from specimen to specimen in the values of k and n as well as in σ_y and σ_u. Many of these curves based on the k and n values from individual specimens fall below and a few fall above the experimental points. In order to obtain the best correlation using k and n values determined in this way, it would be necessary to take enough specimens from the appropriate locations in a sheet to insure that the averaged values of k and n were truly representative for that sheet. Curves of σ_{yc} versus a/t based on k and n values from uniaxially prestrained and aged specimens (Method (3)) did not correlate well with experimental values. Thus method (1),

the use of Eqs. 6 and 7 to establish k and n values for use in predicting σ_{yc}, gives the best agreement with experimental results with the least experimental and computational effort of the three methods. The σ_{yc} versus a/t curves obtained using Eq. 35, will be discussed further in Section 3.2c where corner test results are treated in detail.

3.2 Corner Tests

Tensile and compressive test specimens for corners, as well as flat specimens, are shown in Fig. 18. Special methods for cutting and testing corner specimens were devised. For each of the types of tensile and compressive corners tested from the first five materials, one or more adjacent flat (series 1) specimens were cut as shown in Fig. 19(a) and tested.

a. Tensile Corner Test Procedure. Tension tests on corner specimens were conducted using self-aligning grips and a standard microformer strain gage of 2 inch gage length. The specimens were made extra long: 16 inches and 18 inches rather than the standard 9 inches ordinarily used for flat sheet specimens, as shown in Figs. 18 (a) and (b). This was considered necessary in order to minimize bending and flattening of the corner in the central portion of the specimen during testing.

b. Compressive Corner Test Procedure. Compression tests were more difficult than tension tests because of the necessity of measuring strains while preventing buckling in

the specimen. Compressive tests such as shown in Figs. 18 (g) through (k) were accomplished by two main methods. In the first, the specimen was greased, wrapped in aluminum foil and enclosed in hydrostone in a pipe tube as in Figs. 18 (g) and (h). (Hydrostone is a proprietary material of white color containing gypsum which hydrates and hardens much more rapidly than portland cement and has ultimate compressive strengths of the order of 9000 psi.) In the second method the specimen was greased and inserted into a special metal jig for corners, Fig. 18(ℓ). For the ten gage specimen shown in Fig. 18 (i), which had an inside radius of 7/16 inch, no jig or hydrostone was necessary since the specimen had an L/r ratio of less than 15 so that buckling was not a problem.

Electric SR-4 foil type strain gages were mounted on one side of each specimen. One test was conducted with strain gages on both sides of the corner specimen. The results from the two gages were so close that it was determined unnecessary to mount two gages on each specimen.

Measurement of the inside radii of the corners was accomplished by use of radius gages.

Corner and flat specimens for the first five materials listed in Table 1 were taken from the cold-formed sections shown in Figs. 24 (a), (b), and (c) and from press braked angles. These sections were made by three forming methods: air press braking, coin press braking, and roll-forming. Corners from the sixth, seventh, and eighth materials of

Table 1 were taken from air press braked angles.

c. Corner Test Results. The appropriate as-formed material properties, such as proportional limit σ_p, yield strength σ_y, tensile ultimate strength σ_u, and percent elongation in 2 in., of each tensile and compressive corner specimen tested are tabulated in Table 4. Yield strength is defined as that stress at which the permanent strain is 0.2% for gradually yielding steels or the level of the yield plateau for sharp yielding steels. Proportional limit is taken as that stress at which the permanent strain is 0.02%. Data for series 1 flat specimens taken as companion specimens to corner specimens are listed in Table 5.

The compressive experimental corner yield strengths are approximately equal to the tensile experimental corner yield strengths in the non-aging CRK16-38.3 material. This tends to check the assumption that the Bauschinger effect is not present in cold-formed corners. On the other hand, for all of the aging materials the compressive corner specimens give from 5 to 15% larger increases in yield strength than tensile specimens.

Typical stress-strain curves for corners are given in Figs. 19 (b) and (c). It is seen that the curves are highest for corners with the smallest a/t ratios, corresponding to the highest amounts of cold work. It is also apparent that as the a/t ratio decreases, the σ_p/σ_y ratio decreases. Corners formed from the CRK16-38.3 steel have the lowest σ_p/σ_y ratios, Table 4, with values varying from 0.65 to 0.87.

Corners formed from the HRSK16-37.5 steel have the highest σ_p/σ_y ratios varying from 0.79 to 0.97. Low values of the σ_p/σ_y ratio indicate gradual yielding stress-strain curves; whereas high values correspond to sharp yielding stress-strain curves. Thus with increasing amounts of cold work even the curves for originally sharp yielding materials become more rounded at the knee or more gradual yielding and do not seem to regain a plateau with aging as many simply prestrained flat specimens do.[1] This is true of both tensile and compressive corner specimens. Possible explanations for this phenomenon follow. The various fibers in a bent corner do not have the same yield strength, having been subjected to varying amounts of cold work. Consequently, as a corner is tested, various elemental portions of it yield at different loads, resulting in a gradual yielding stress-strain curve. The tendency may further be explained by the fact that the amounts of plastic strain in the corners are considerably larger than in the simply prestrained flats of the first phase of the investigation[1]. (In the first phase it was found that the flat specimens for longitudinal compression and transverse tension and compression for the three hot rolled materials which had been subjected to 100 mils of prestretch remained of the gradual yielding type after aging. All the rest of the specimens for the three hot rolled materials regained sharp yielding characteristics after aging.)

The experimental results of tensile and compressive corner tests are given in Figs. 9-17. The dashed and solid

curves in these figures represent the theoretical tensile yield strength based on the first and second corner models. Note that the curves established for the tensile σ_{yc} from Eq. 35 are also plotted with the compressive experimental points for comparative purposes.* Several conclusions may be drawn from these curves: (1) For a/t ratios greater than about five there is very little difference between the solid curves and the dashed curves, the latter being based on the purely flexurally loaded model. For smaller a/t ratios, however, the yield strengths predicted for the second model are up to 9% larger than for the purely flexural model. (2) The theoretical σ_{yc} versus a/t curves of the second model correlate better than those of the first for most of the nine materials tested, i.e. for all but the sixth, seventh and eighth materials. The correlation between the theoretical curves and experimental values is quite good, the curves giving for most of the eight materials conservative, yet reasonable values of σ_{yc}. (3) The calculated curves for σ_{yc} are, in general, more conservative when compared to experimental compressive corner yield strengths than to tensile yield strengths. (4) The variations between experimental values

---

* It is difficult to obtain accurate experimental stress-strain curves in the plastic region for compressive sheet metal specimens. For the purposes of the theoretical analysis for σ_{yc} presented above, it was necessary to assume that the plastic material constants k and n are the same in compression as in tension. Therefore, no theoretical evaluation for compressive corner yield strength was attempted.

in a given sheet material cold-formed into corners by coining, by air press braking, or by roll-forming are not significant. (5) Variations between curves of corner yield strength for different materials are large enough to be of significance.

The majority of experimental points lie above the theoretical (solid) curves, however. How much of this is due to aging, to a different strain distribution than that assumed, or to a combination of causes is uncertain. Other possible sources of difference between the theoretical curves and the experimentally obtained points are:

(1) variation in virgin properties of individual specimens,

(2) lack of uniform curvature and possible deviation from the assumption that plane surfaces remain plane,

(3) anisotropy, which is present in virgin sheet steel and is also caused by the cold-forming operations themselves, and which tends to render the "effective strain" concept somewhat inaccurate,

(4) the fact that no experimental stress-strain curves are available from which compressive values of the constants k and n can be determined,

(5) ignoring the effects of residual stresses, and

(6) the fact that plastic straining in the corners was at right angles to the grain whereas k and n values were established for specimens tested in the direction of the grain. However, comparison of tests and analysis indicates that the total influence of these factors is relatively small.

Thus the tensile corner yield strength σ_{yc} has been successfully related to the a/t ratio and to the fundamental material properties k and n. It should be noted that Eq. 35 should not be used for a/t ratios in excess of about 6.0 without further verification, since no corner specimens were tested beyond that range. With b and m calculated from Eqs. 47 and 48 and k and n from Eqs. 6 and 7, Eq. 35 should be useful in predicting the effects of cold work upon the yield strength of corners within reasonable limits.

In regard to ultimate strength, the percentage increase in the corners is considerably less than the increase in yield strength, with a consequent marked reduction in the spread between yield and ultimate strength. Also, Fig. 20 shows that the percent elongation drops rapidly with increasing amounts of cold work in the corner, indicating a loss of ductility with increasing strength. The reduction in percent elongation as compared to that of the virgin material varies from 20 to as much as 90% in CRK16-38.3 corners.

4. PROPERTIES OF FLATS FROM COLD-FORMED SECTIONS

4.1 Extension of Corner Plastic Strain Effects into the Adjacent Flats.

It is likely that a transition zone should exist between the high plastic deformations in a cold-formed corner and the undeformed material several sheet thicknesses from the edge of the corner. However, since the plastic deformation and the consequent increase in yield strength in this transition zone falls off rapidly with the distance from the corner, it was suspected that the usual variations in the virgin yield strength would tend to obscure any trends that may exist in that zone. Unfortunately, the same specimen cannot be tested both before cold working and afterward. Therefore, this investigation was divided into two parts: (1) an investigation to determine the virgin yield strength distribution in a given sheet of steel and (2) an investigation to determine the extent of the effects of plastic deformation from the corner into the adjacent flats from materials press braked from portions of the same sheet. The information gained from part (1) was utilized to evaluate the increases in yield strength in part (2).

a. Test Procedure. A 14 in. by 60 in. piece of HRSK10-37.0 10 gage steel was selected for this purpose, Fig. 21(a). Five virgin tensile (A, C, E, G, and J) and compressive (B, D, F, H, and K) specimens were taken from each of three longitudinal 1 in. wide strips (marked 1, 2, and 3). Fourteen

virgin tensile specimens were taken from each of three transverse strips (A, E, and J). This left 4 portions of the sheet (CX, CXX, GX, and GXX) to be coin press braked into channel sections. Each of these portions was surrounded by virgin tensile specimens.

Fig. 21(a) shows the distribution of virgin tensile yield strengths for 73 virgin specimens, taken from one 14 x 60 in. sheet. The locations of these specimens are indicated by short horizontal lines. These yield strengths varied from 37.1 ksi to 43.8 ksi, a total variation of 18%. Assuming a Gaussian distribution of these values, the standard deviation from the arithmetic mean value of 39.9 ksi was 1.2 ksi or 3%. Values of tensile ultimate strength for these same 73 specimens varied from 57.7 ksi to 62.6 ksi, a variation of 8%. The arithmetic mean was 60.1 ksi and the standard deviation 1.4 ksi. The yield strength for a total of 15 compressive specimens varied from 39.2 ksi to 46.3 ksi, a variation of 18%. The corresponding arithmetic mean and standard deviation are 42.1 and 2.0 ksi, respectively. These values serve to illustrate just how much the mechanical properties may be expected to vary from point to point in any modest-size sheet prior to cold-forming operations.

The four channels were allowed to age at room temperature for 2 1/2 months after being cold-formed and were then cut into thin rectangular specimens without shoulders as shown on Fig. 21(b). The 1/4 in. wide specimens furthest removed from the corners (i.e. from locations marked 1, 4,

5, and 8) were considered to be unaffected by cold work. Scribe marks were accurately made before specimens were cut and milled so that the distance from the edge of a specimen to the edge of the corner could be accurately determined in the final milled specimen. The specimens, from locations marked 2, 3, 6, and 7, were made with widths which were purposely varied by 0.0300 in. with the edge furthest from the corner being a constant distance from the corner. Thus the increase in yield strength for that portion which two specimens had in common (i.e. the same distance from the corner) could be considered to be the same. The increase in tensile yield strength after cold working for the area not in common for the two specimens was calculated from

$$\sigma_{y\ incr} = [(\sigma_{yf1} - \sigma_{y1})\ A_1 - (\sigma_{yf2} - \sigma_{y2})\ A_2]/(A_1 - A_2) \quad (49)$$

where the subscripts 1 and 2 denote two specimens of different area,

σ_{yf} = the tensile yield strength after cold working of the area represented by the difference in areas $(A_1 - A_2)$,

σ_y = the virgin tensile yield strength of the sheet as determined from the contours of Fig. 21 (a),

$\sigma_{y\ incr}$ = the increase in yield strength above actual virgin yield strength, and

A = the cross sectional area of a specimen.

b. Discussion of Results. The results of computations are shown in Fig. 22 where the increase in yield strength is

plotted versus the distance from the edge of the corner. This curve shows that the increase in yield strength is negligible at a distance of one sheet thickness from the edge of the corner. To take a numerical example, the increase in the force required to yield a 90° corner with inside radius of 1/8 in. and t = 0.14 in. would be 0.043 sq. in. times 34 ksi = 1.46 kips. The average value of increase in the yield strength from a corner edge to a distance one thickness away is 11.1 ksi, giving for the two adjacent flat areas an increase in the force required to cause yielding of 2 x 0.14 x 0.14 x 11.1 = 0.44 kips. This is 30% of the increase attributable to the corner alone. Put another way, the "effective corner area" in this case could be considered to be 1.3 times the actual corner area which includes a distance of 0.46 times the sheet thickness on each side of the corner.

It will be shown in Section 4.2c that in some press braked sections this transition range is extremely small. On the other hand, there are substantial increases in yield strength in "adjacent flat specimens" (i.e. specimens from locations immediately adjacent to corners) taken from roll-formed sections. Consequently, the increase in yield strength in adjacent flat specimens from roll-formed sections may be attributed primarily to the normal pressure of the rolls on these flats rather than to the extension of plastic bending strains from the corners into the flats.

4.2 Other Tests of Flats.

In addition to the tests described in Section 4.1, two additional series of tests were conducted on flats of cold-formed members: (1) The series 1 flat tests included tensile and compressive specimens taken as companion specimens to nearly all of the corner specimens tested. These specimens were all taken from locations adjacent to corners. However, a scarf distance of approximately 1/8 in. was left between corners and these specimens as shown in Fig. 19(a). An additional 0.095 in. was cut out on tensile specimens to allow for the standard shoulder (wider area at the grips). It was originally intended that these flat specimens serve to explore the possible extent of the transition zone from high plastic bending strains in the corners to elastic strains in the flats. However, it is apparent from the results of the previous section that a scarf distance of 1/8 in. is larger than the width of the transition zone. Nevertheless, the series 1 flat tests did furnish some data which proved to be of value as is discussed more fully below. (2) The series 2 flat tests were conducted to determine how cold-forming changes the tensile and compressive mechanical properties of the flats of members made from four of the test steels. These specimens were taken from locations distributed throughout the flat portions of the cross sections. Not only was it desired to investigate the general magnitude of such changes, but also to investigate the magnitude of the changes at varying locations throughout flat portions

of the cold-formed members.

a. Tensile Tests of Flat Specimens. Tensile series 1 flat specimens were the standard 9 inch coupons illustrated in Fig. 18(c).

Tensile series 2 flat specimens were 1/4 in. wide by 10 in. long strip specimens cut from the cross sections of the cold-formed shapes indicated on Figs. 25(a), 27(a), 28(a), and 29(a). These specimens were made narrow and without shoulders in order to obtain the desired test information reasonably close to the corners and to get more points in the flats between the corners than would have been possible with standard width tensile coupons. The specimens were tested with the middle three inches of length exposed between the grips. Very few of these non-standard tensile specimens failed in the jaws of the self-aligning tension grips, the majority breaking in the desired middle portion of the specimen. Strains were measured with an autographic microformer gage. Final elongation in 2 inches was taken.

The virgin tensile properties of the first 8 materials of Table 1 were established by using the standard 9 in. coupons shown in Fig. 18(c). Three tensile coupons for the ninth material, HRSK9-30.7, were cut directly from a length of unstraightened sheet coil of 4 5/8 in. width. The material had a radius of curvature of approximately 18.2 in. These tensile coupons were standard except for the longitudinal curvature. Two SR-4 strain-gages were mounted on opposite sides of each of these three specimens. The gages were

connected so as to eliminate bending strains from the strain readings. The specimens were tested in the curved condition, the force of the testing machine gradually straightening them as testing progressed. The resulting stress-strain curves are somewhat gradual yielding due to the bending stresses caused by the curvature. The stress-strain curves show a definite flattening out at the yield plateau so that the yield point is not difficult to determine.

b. Compressive Tests of Flat Specimens. Flat rectangular specimens 0.57 in. by 3.57 in. were taken for the series 1 compression tests. Specimens 0.57 in. by 3.57 in. were cut from the cross section of the cold-formed hat sections and specimens 0.50 in. by 3.00 in. from the 10 gage channel and 16 gage track sections for the series 2 compression tests. These flat specimens were tested in a steel jig to keep them from buckling in the weak direction. A microformer gage was mounted on the protruding edges of the specimen. See Figs. 18(e) and (f) for illustration of specimens and jig. The assembled jig, specimen, and microformer gage were placed into a subpress to ensure maximum axiality of loading during testing.

c. Results of Tests on Flat Specimens. The data for all series 1 flat specimens taken as companion specimens to corner specimens are shown in Table 5. The level of yield strengths for these flat specimens was above the virgin yield strength for all of the aging materials and below for the non-aging CRK material. However, these changes in strength

are much less than in the corners, ranging from -3 to 22% in compression and from -5 to 16% in tension. All of the stress-strain curves for these specimens exhibit a sharp knee at the yield point (see Fig. 19(d) for typical curves) except those for the CRK16-38.3 steel which were of the gradual yielding type.

Figs. 25(b), 26(b), 27(b), 28(b), and 29(b) show the distribution of tensile yield and ultimate strengths in the corners as well as the flat portions (series 2 flats) of the cross sections. The yield and ultimate strengths are plotted as ordinates, and the locations of the elemental strip specimens are shown on the abscissa. The virgin tensile yield and ultimate strengths of the material are indicated as solid horizontal lines.

The values for corner strengths are plotted as equal for all of the corners shown for each particular type of member. In each case the values of yield and ultimate strength of the corners can easily be identified because they are so much higher than the values for the flat material. In fact, the yield strength values for the cold worked corners are significantly above the virgin ultimate strength of the material in all cases.

From the average tensile values for series 2 flats shown on Table 6 the following conclusions may be drawn. First, if it is assumed that the virgin values of yield and ultimate strengths are reasonably representative, then it may be concluded that changes in the yield and ultimate strengths of

the flats of the CRK16-38.3 press braked section, Fig. 25(b) are negligible. Second, the increase in yield strength of the HRSK16-37.5 press braked hat flats, Fig. 26(b), is measurable, being on the order of 6%. Third, roll-forming as conducted upon the three HRSK sections of Figs. 27(a), 28(a), and 29(a) increases the yield strength in the flats in the most significant amounts, i.e. averaging 17, 29, and 50%, respectively. Fourth, roll-forming seems to raise the average ultimate strength of the flats by a more significant amount than does press braking.

The general appearance of compressive yield strength distributions (omitted here for brevity) is quite similar to that of their respective tensile counterparts. As is seen from Table 6, in the CRK16-38.3 hat section the average value of the compressive yield strength of flats was lower than the average tensile yield strength while in all other sections tested the reverse was true.

The change in ductility of cold-formed flats is generally quite small. The largest reduction in percent elongation as compared to that of the virgin material was 26% in the flats of the HRSK9-30.7 roll-formed joist chord.

The increases in yield strength of flats appear to be attributable to strain hardening and aging from several factors:

(1) the strain hardening and aging which occurs after uncoiling (i.e. stretcher-straightening) of stored sheet materials,

(2) the normal pressure of the rolls in roll-forming or of the dies in coin press braking upon the flat portions of the sections being formed,

(3) the extension of the plastic deformations which occur in corners into the flats adjacent to the corners,

(4) the warping of flats with accompanying shearing strains that occur in roll-forming, and

(5) the presence of elastic strains in the flats. These factors will be discussed in some detail in the following paragraphs.

(1) That the stretcher-straightening of sheets (i.e. flattening of the sheet from the coils in which it is stored) may increase the yield strength seems to be substantiated by the fact that the average tensile strength of the 73 virgin specimens of the HRSK10-37.0 sheet described in Section 4.1 was 39.9 ksi while it averaged 37.0 ksi in tests conducted nearly two years earlier. If stretcher-straightening is responsible for the higher values occurring in later tests, then the increase from 37.0 to 39.9 ksi must be attributed to aging. The factor of normal pressure, in addition to all of the factors present in press braking, is present in the roll-forming of flats. Therefore, for simplicity, the properties of flats from press braked sections will be considered first. It has already been shown that the direct influence of plastic bending strains in the corners does not extend for any significant distance into the flats. It has also been pointed out that the virgin properties of sheets

are by no means constant. The influence of this non-uniformity in the original flat sheet is reflected in the variations in the yield strength values for the series 2 flats of Fig. 26(b). No increase occurred in the series 2 flats of the non-aging CRK16-38.3 press braked hat, Fig. 25(b), while increases occurred in the flats of all of the materials which exhibit the property of aging. Therefore, it seems unlikely that such increases are caused entirely by the random variation in virgin properties. Curves for yield strength versus plastic strain of the unidirectionally prestrained flats were given in the first phase of the investigation[10]. These curves showed larger increases due to aging for low values of prestrain than for high values. For example, for HRSK16-37.5 steel prestrained in the longitudinal direction the difference in yield strength of aged and non-aged tensile specimens averaged 3.0, 1.5, and 0 ksi, for 25, 50, and 100 mils of prestrain, respectively. The maximum plastic prestrain caused by stretcher-straightening is low (about 40 mils) compared to that occurring in a corner (up to about 400 mils) and thus is probably the cause of relatively large amounts of aging in those materials which age.

(2) The behavior of the series 2 flat tension strip specimens from the roll-formed track sections was markedly different from those from press braked hat sections from the moment they were cut from the members. Specimens cut from roll-formed track sections at the A, G, K, and Q locations, Fig. 27(a), developed pronounced longitudinal curva-

tures which were concave toward the outside surface of the cross section. For example, one K specimen had a radius of curvature of 20.2 inches. Specimens from the H and J locations were curved, but not quite so much as the A, G, K, and Q specimens. Curvatures for the remaining specimens were negligible. Inspection of the outside surface of specimens from the A, G, K and Q locations showed a narrow band lengthwise along each specimen where the mill scale was partially removed by the rolls as the forming took place. No decrease in thickness as measured by a micrometer was observed in these locations. The shape of the stress-strain curves for the A, G, H, J, K, and Q specimens was unusual, as if each of these specimens were made from two sharp yielding materials, one of which had a higher yield strength than the other. In other words, these stress-strain curves could easily be idealized (up to the strain hardening region) by three straight lines, the first line having a normal modulus of elasticity for steel (i.e., about 29.5×10^6 psi) up to a point somewhat less than the virgin yield strength, the second having a considerably smaller slope or modulus, and, finally, a third (horizontal) line with a zero modulus, Fig. 30. The yield strength of the H and J specimens was not much larger than the virgin yield strength of the material, but the yield strengths of the A, G, K, and Q specimens were significantly larger. This indicates that the pressure of the rolls on the material may change the shape of the stress-strain curve of the material either with or without increasing

the yield strength. While some of the thin strip specimens taken from the 10 gage roll-formed channel did exhibit longitudinal curvatures, none of them had stress-strain curves with the peculiar shape shown in Fig. 30. The thin strip specimens taken from the 9 gage roll-formed joist chord were quite straight.

(3) The third factor does not appear to have a significant influence in the case of the press braked hat sections. The series 2 flat tensile specimens taken without a scarf directly adjacent to the corners ($a/t = 1.06$) of the press braked hat sections of Figs. 25(b) and 26(b) were evidently not affected by any such extension of plastic strains. Compare the yield strength values of the flat specimens from locations next to corners for the roll-formed track section of Fig. 27(b) and for the roll-formed channel of Fig. 28(b). The increases in yield strength in these specimens are significantly above those of specimens located farther from the corners. Thus it may be inferred that the transition zone for extension of plastic strains into the adjacent flats is not appreciable for any of the three forming methods under consideration. Rather, the increase in yield strength observed in the adjacent flats of coin press braked corners and of roll-formed corners is more likely due to the higher normal pressure present in these processes than in the air press braking process. The tensile and compressive stress-strain curves of Fig. 19(d) for hot rolled flat specimens taken from locations adjacent to coin press braked corners

show a tendency for the yield strength of flats fairly distant from the corner to continue increasing with decreasing a/t ratio. This tendency is evident in the flats of coin press braked and roll-formed sections but not in air press braked sections. It cannot be attributed to the extension of corner plastic strain effects this far from the corner, because a scarf distance (approximately 1/8 in. or more, see Fig. 19(a)), wider than the width of the transition zone investigated in the previous section was left between the corner and the flat specimen.

(4) It seems evident that as the flat portions of a roll-formed member pass from station to station in a rolling mill, some of them will be warped and plastic shearing strains will be present. For example, in the roll-formed track section of Fig. 27(a), the two longest sides were probably subjected to shearing strains, and the 1.84 in. side probably was not, because of symmetry. The yield strength values of specimens C, D, E, M, N, and O tend to indicate that these shearing strains do not contribute large increases in yield strength, since these values are about the same as those for the flats of the press braked hat section of Fig. 26(b).

(5) The Levy-Mises Eq. 8 used previously in the model for plastic deformation of a corner is valid only in cases where plastic deformations are so large that elastic deforma-

tions are negligible. The more general equations of Prandtl and Reuss include the effects of elastic and plastic strain components.[3] Thus in the flats where plastic strains are much smaller than in the corners, any elastic strains present must be considered in an analysis of strain hardening.

Of the five factors listed as possibly contributing to strain hardening and aging in the flats of cold-formed members the first two are probably the most significant. The increase in yield strength due to factor (1), stretcher-straightening of stored materials, is assumed to be fairly uniform throughout the flats, both for roll-formed and for press braked members. To determine the magnitude of such increases is a simple matter requiring only a few representative standard tensile tests from the central regions of flat portions of cold-formed members. Factor (2), normal pressure on the flats, as caused by roll-forming may be the cause of increases in yield strength at locations immediately adjacent to corners or at random locations remote from corners. However, increases in yield strength due to this factor are evidently dependent on roll design, adjustments made by the rolling mill operator, wear on the rolls, etc. Accurate predictions of such increases prior to the rolling of a particular member would require a certain amount of experience and judgment. A statistical study might possibly be used to establish limits for mechanical properties of flats after roll-forming for given cross sectional shapes.

5. FULL SECTION PROPERTIES

5.1 Full Section Tests.

a. Full Section Tension Test Procedure. Full section tension tests were performed by welding 1/4 in. plates to the sections in the neutral plane of the member, perpendicular to the axis of symmetry, Fig. 23(a). The end plates were slotted rather than the specimens. This made welding easier and more reliable since the tendency to burn through a thin sheet is reduced when welding in an uncut location rather than along a cut edge. This also had the advantage that welding across the ends of the 1/4 in. plates was unnecessary. Full section tension tests were made on all of the sections shown in Fig. 24.

SR-4 electric wire type strain gages were mounted on each of these full section tensile specimens, Figs. 23(a) and 24. Strains were recorded as long as they could be read. Thereafter, strains were taken visually by means of a scale reading to the nearest hundredth of an inch in a six inch gage length.

b. Laterally Supported Full Section Compression Test Procedure. The first series of full section compression tests was accomplished by casting short lengths of the sections in hydrostone within slightly shorter lengths of 4 in. diameter pipes, Fig. 23(b). The purpose of the hydrostone was to limit local bending of flat portions of the section and to prevent local buckling. SR-4 wire type electric

strain gages were mounted on each specimen as shown by the short dark lines next to the cross sections of Fig. 24. All of the sections shown in Fig. 24 were tested as full section compression specimens with hydrostone lateral support.

Before casting these specimens in the hydrostone, the gages were coated with "Petrosene" wax for waterproofing. To protect them from damage, the waterproofed gages were covered with sections of metal tubing split longitudinally. This assembly was again waterproofed with wax. The specimens were then greased and wrapped in aluminum foil so that they could slide longitudinally within the hydrostone. The ends of the specimens were milled to a plane surface after the hydrostone had hardened. The milled ends were placed against 1 1/2 in. thick bearing plates which were, in turn, seated against the head and table of the testing machine with hydrostone, Fig. 23(b). The hydrostone was allowed to harden for approximately one hour before each test. The spherical-seated compression head was fixed with three shims to insure that it did not rotate during testing. The object of using this procedure is to apply compressive loads such that the strains over all parts of the cross section are as close to equal as possible at a given load. When the described test procedure is carefully followed, the elastic strains given by the various strain gages are nearly equalized from the beginning of the test until yielding occurs.

In addition, specimen C9A, cast in hydrostone, had plates welded across both ends to check the influence of

welding in the full section compression test procedure.

c. Stub Column Test Procedure. Two full section compression tests without lateral support were performed for each of the sections shown in Figs. 24(c), (d), (e), (f), and (g). These tests were conducted in the same manner as shown in Fig. 23(b), except that the hydrostone surrounding the specimen and the 4 in. diameter tubes were omitted.

d. Full Section Tension Test Results. With the arrangement of Fig. 23(a) it was possible to carry tension tests of all of the full section tensile specimens to stresses beyond the yield point; in fact, nearly all specimens could be taken to their ultimate load with necking down and fracture occurring near mid-length of the specimen. However, because of difficulties encountered in welding, it proved impossible to reach the potential ultimate load in the track specimens. Failure did not occur in the central portions of any of these track specimens. In specimen T5 testing was stopped shortly after the yielding process began because the pull plate sections bent out from the specimen and distorted it. The discontinuity which occurs between strains of 2 and 3 mils in specimen T6, Fig. 27(c) was probably caused by a similar distortion. However, the full section curve follows very closely the calculated composite curve (see below) up to a strain of 2.5 mils, indicating that the composite curve is a valid representation of the properties of the section.

To illustrate the performance of the various gages during a typical full section tension test (from HRSK16-37.5

hat specimen T4) the strains of gages 1 and 4 were plotted versus stress P/A on Fig. 26(a). All five of the gages performed in a manner reasonably similar to each other up to approximately the point of virgin tensile yield strength (37.5 ksi). At this point gage 1 began to depart from the straight line of proportionality, i.e. gave a less steep curve, while gage 4 continued in a nearly straight line up to just below the yield point of the full section. The curve of gage 4 went up in a vertical line until it yielded, dropped back down about one ksi and then rose with a slightly decreasing strain until it reached a new high point at 43.0 ksi. (The scale of Fig. 26(a) is too small to show all of the actions of gage 4 in detail.) At that stress the strain increased rapidly and began to catch up with that of gage 1. This indicates that the specimen behaved essentially as an axially loaded tensile member up to the point where yielding in some elements began. At this point, because selective local yielding evidently started near the gage 1 side of the specimen, there existed an axial load and a superimposed bending moment on the remaining elastic section. Yielding then progressed across the section until, finally, all elements had yielded. At this time the section was again essentially in uniform axial tension so that the strains quickly equalized. The differences in strains were quite large at some stages of selective yielding, e.g. at 42.8 ksi gage 1 was at 10.7 mils and gage 4 was at 1.3 mils, and 43.4 ksi gage 1 was at 24.3 mils and gage 4 was at 9.5 mils.

Composite stress-strain curves were also obtained analytically by selecting convenient values of strain and calculating corresponding mean stresses from the stress-strain curves of all the component corner and flat test coupons taken from the particular shape. The mean stress at a given value of strain is found as follows: The cross section to be investigated is divided into several sub-areas, each of which may contain either flats or corners, but not both. The mean stress for the full section at a given strain is obtained by summing the product for each sub-area of the average stress for that sub-area by the ratio of the area to the total cross sectional area. This is rather a tedious procedure and would not be practical for routine use, but it did serve to give an excellent check on full section test values. These composite stress-strain curves compared to full section tension test curves are shown in Figs. 25(c), 26(c), 27(c), 28(c), and 29(c) for the CRK16-38.3 hat, HRSK16-37.5 hat, HRSK16-37.5 track, HRSK10-37.0 channel, and HRSK9-30.7 joist chord sections.

The experimental stress-strain curves from the full section tests as compared to the calculated composite stress-strain curves appear to be within a scatter range defined by the variation which can be expected from specimen to specimen. The small accidental eccentricities which are present in full section tensile specimens in the elastic range will have no serious effect on determining the correct overall yield point since the material being used is ductile. It

may, therefore, be said that the two methods of obtaining full section data confirm each other in obtaining the shape of the stress-strain curve and the tensile yield point of the section. This agreement between the full section tensile and the calculated stress-strain curves indicates that the residual stresses which may be present do not have significant effect on full section stress-strain curves. This conclusion is of importance in determining theoretical buckling loads of cold-formed compression members in the inelastic range and will be utilized further in Chapter 6.

There is no guarantee that a given specimen will not fail prematurely at the end zones which may have been weakened by the welding. The more cold worked material a specimen has, the more liable it is to be weakened by the welding of the end plates. However, the ultimate strength will be attainable for quite a variety of cold-formed shapes by this or similar full section testing methods. (Welding may also decrease the yield strength of compressive specimens. One such specimen is discussed below in connection with full section compression test results.)

The full section tension stress-strain curves for the T3 and T4 HRSK16-37.5 press braked hat sections (see Fig. 26(c) for specimen T4) were more sharp yielding than the calculated composite curves, even though the latter could be considered sharp yielding in and of themselves. For the HRSK16-37.5 roll-formed track section, Fig. 27(c), the HRSK10-37.0 roll-formed channel section, Fig. 28(c), and

the HRSK9-30.7 roll-formed joist chord section, Fig. 29(c), both the calculated composite and the full section stress-strain curves are more gradual yielding than that of the HRSK16-37.5 press braked hat sections. Thus the variation of the yield strength of the cold worked material affects the shape of the stress-strain curve more in roll-formed than in press braked sections.

For the CRK16-38.3 press braked hat the elongation was 50%, for the HRSK10-37.0 roll-formed channel it was 26%, and for the HRSK9-30.7 roll-formed joist chord it was 34%. This shows that the cold work of forming leaves ample amounts of ductility in full sections even though member ductility decreases as the amount of cold worked material in the section increases.

e. Laterally Supported Full Section Compression Test Results. Full section compression stress-strain curves are not included, since the same general shape characteristics and agreement between experimental and calculated curves were obtained in compression as in tension. Yield strengths obtained in laterally supported compressive full section tests are compared to those calculated from strip specimens in Tables 7a and b. Yield strengths of laterally unsupported full section compressive tests are included in Table 7b. From this data it is seen that the compressive full section yield strength values were above the tensile values for all the sections tested except the CRK16-38.3 hat sections. The full section yield strengths for the CRK16-38.3 press

braked hat sections averaged only 4% lower in compression than in tension.

For a compact roll-formed joist chord, Lenzen and Dixon[11] concluded that residual stresses were present in sufficient degree to materially affect the shape of the full section compression stress-strain curves. The agreement of Cornell University full section stress-strain curves calculated from coupon tests with those obtained from full section tests shows that residual stresses in cold-formed members of open shaped cross section do not significantly affect the shape of the full section stress-strain curves. This is true both for tensile and compressive full section test results.

From Table 7b it may be seen that welding plates across the ends of compressive specimen C9A reduced its yield strength by about 6%. This is apparently due to the annealing effect of the welding process in reducing the increases in strength which were caused by the cold work of forming.

f. Stub Column Test Results. Two stub column tests (i.e. laterally unsupported full section compression tests) were conducted for each of the cold-formed shapes shown in Figs. 24(c), (d), (e), (f), and (g). Test results for these specimens are given in Table 7b, and section properties including moments of inertia, w/t ratios, and the form factor Q are shown in Table 7c. (The form factor Q is defined in Section 3.6.1 of Reference 12. Q is used in the design of sections containing one or more flat elements with large w/t ratios. Its purpose is to provide safety against

(1) local buckling and consequent member collapse and (2) excessive local deformations.) Typical stress-strain curves for stub column tests are shown in Figs. 33, 34, and 35.

The compressive behavior of the stub column specimens was as follows: Buckling or failure always began in the flat elements, spreading to the corners after additional loading. Figs. 31 and 32 show the manner in which inelastic local buckling developed. In general, the compressive yield strengths of the laterally unsupported were somewhat lower than the compressive yield strengths of laterally supported specimens (see Table 7b). Evidently, the flats, having a lower yield point, started to buckle locally at an average cross sectional stress at or slightly above their own lower yield point, preventing the higher yield point of the corners from becoming fully effective. The reduction in yield strength was not large, however. For most of these sections the laterally unsupported full section compressive (stub column) yield strength was slightly above the full section tensile yield strength, Table 7b, the only exception to this being for the CRK16-38.3 hat section. Two types of stress-strain curves (Fig. 35) were obtained in these tests. The first, from the more compact shapes, had a long stable yield plateau, and the second, from the less compact shapes, had a maximum load at a low value of plastic strain followed by a relatively rapid drop in load. The behavior of the stub column specimens is treated in detail in the following paragraphs:

The yield strengths for these tests, as shown in Table 7b, were taken either as the 0.2% offset (specimens C9, C16, C12, C21, and C22) or as the maximum load sustained (specimens C10, C11, C13, C14, and C15). Both unsupported HRSK10-37.0 roll-formed channel specimens C9 (Fig. 33) and C16 (Fig. 35) yielded at a stress of 49.1 ksi or 11.5% below supported specimens C7 and C8. Unsupported HRSK9-30.7 roll-formed joist chord specimens C21 (Fig. 34) and C22 yielded at an average of 51.6 ksi. or 3.6% below supported specimen C23. Both unsupported hot rolled 16 gage lipped angle specimens C10 and C11 yielded at 44.7 ksi or 6.1% below supported specimens C19 and C20. On the other hand, unsupported CRK16-38.3 hat section specimens C14 and C15 (Fig. 35) yielded at an average stress of 1.3% above supported specimens C17 and C18. Thus the yield strengths of stub columns were below those of companion laterally supported full section compressive specimens for all except the CRK16-38.3 hat section. The compressive yield strengths of laterally unsupported compression specimens are all above the full section tensile yield strengths for specimens made from hot rolled, or aging sheet steels, and only slightly below for specimens made from the cold reduced killed material. Further experimental verification of the latter trend was given in an investigation[11] of an Armco roll-formed joist chord section. It was found that the maximum stress of four laterally unsupported full section compression tests averaged 71.6 ksi, whereas the 0.2% offset yield stress for two full section tension

tests averaged only 64.4 ksi.

Values of the form factor Q were computed to be 1.0 for all of the stub column specimens except the 16 gage press braked channels, for which Q = 0.72 (Table 7c). If, for the two sections having Q less than 1, the laterally supported full section compressive yield strength is multiplied by Q, a value lower than the laterally unsupported full section compressive yield strength is obtained. (For example, in the 16 gage channel Q times the laterally supported full section compressive yield strength = 0.72 x 44.3 = 31.9 ksi, considerably less than the stub column yield strength which averages 42.2 ksi. This tends to indicate that the form factor requirements of Reference 12 may be quite conservative for some sections with Q less than 1. The following discussion of local buckling in the flats of the stub column specimens gives an additional possible reason for the apparent large difference for the 16 gage channel sections.

The average stresses at which local buckling of the flat plate elements was first noted are given in Table 7b. For the 10 gage cold roll-formed channels C9 and C16, Fig. 31, waving was first noted at a load slightly larger than the 0.2% offset yield strength. Buckling first became visible in the flanges of the HRSK9-30.7 joist chords, specimens C21 and C22, at 98% of the maximum load. For the 16 gage lipped angles, C10 and C11, Fig. 32, local buckling was not visible until after the maximum load was reached. Local buckling was observed in the hot rolled 16 gage channel

specimens, C12 and C13, Fig. 31, at about 95% of the maximum load. In the CRK16-38.3 press braked hats, C14 and C15, Fig. 32, a slight waving in the simple lips was noted at about 80% of the maximum load. At about 90% of the maximum load both the simple lips and the corners began to buckle outward, as can be seen in the photograph of specimen C15, Fig. 32. (Note that the depth of the simple lips of the 16 gage hats more than satisfies the minimum requirement for edge stiffeners of Section 2.3.2.1 of Reference 12). From the above it seems reasonable to assume that at working load levels the deflection of flats would probably not be serious for any of these five sections used in compression members. It is somewhat surprising that buckling became visible in the flats in the 16 gage hats for which Q = 1.00 at a lower percentage of the maximum load than in the 16 gage channels for which Q = 0.72. This may be due, at least in part, to the fact that the simple lips of the 16 gage hats had a much larger aspect ratio (i.e. length to width ratio) than those of the 16 gage channels. It is well known that as the aspect ratio of plates increases the critical buckling load approaches the smallest possible critical load. Perhaps if the 16 gage channels were longer, local buckling would have commenced at lower stresses permitting somewhat less maximum load to be carried by the section.

There is a striking contrast between the stress-strain curves of the most compact and the less compact sections. Curves typical for these two types of sections are shown in

Fig. 35. The curve for 10 gage HRSK10-37.0 roll-formed channel specimen C16 shows not only a long, stable yield plateau, but also a tendency to strain harden. On the other hand, the curve for 16 gage CRK16-38.3 press braked hat specimen C15 shows that instability occurred at a low value of plastic strain. (The last stable strain reading prior to the maximum load for specimen C15 was 4.06×10^{-3} in./in. at a stress of 40.2 ksi. It was not possible to read strains at the maximum stress of 41.6 ksi. because the load dropped before strains stabilized.) The 16 gage channel sections for which Q is less than 1 and the 16 gage press braked lipped angle and hat sections for which Q = 1 reached the ultimate compressive load at strains in the range of from 3 to 5 $\times 10^{-3}$ in./in., after which the load dropped off sharply. The 10 gage roll-formed channel and 9 gage joist chord specimens for which Q = 1 showed long yield plateaus and reached the ultimate load at much higher values of strain (i.e. 16 to 27 $\times 10^{-3}$ in./in.) The behavior of the more compact shapes has significance with regard to safety factors for compression members and is discussed further in Section 6.2.

Reductions in the compressive yield strength of short compression specimens are also suggested by the results of other investigations:

Lenzen and Dixon[11] reported that failure was due to local buckling of the flat plate elements (flanges) in laterally unsupported full section compression tests on a compact Armco roll-formed joist chord section. However, in this

compact section (with a ratio of corner to total cross sectional area of approximately 0.46) the 0.2% offset tensile yield strength (64.4 ksi.) was considerably above the tensile yield strength (49.2 ksi.) of the cold worked flanges.

In compressive tests of short lengths of welded steel tubing, Wolford and Rebolz[13] found that compressive and tensile yield strengths were about equal for small diameter pipe specimens, but that . . ."There was a tendency for tensile yield strengths to run somewhat higher than compressive tests in tubing." . . . In other words, when the D/t ratio was low there was no difference in tensile and compressive yield strengths. This suggests that inelastic local buckling may be responsible for the lowering of the compressive yield strength of tubing and larger sizes of pipe.

In stub column tests performed at Lehigh University on both as received and annealed hot rolled wide flange sections, Huber and Beedle[14] found that the resulting stress-strain curves for the full sections had lower yield plateaus than would have been predicted from a weighted average of compressive coupons taken from all parts of the sections. It was necessary to multiply the average coupon yield strength by a factor of 0.90 to 0.95 to obtain stub column yield strengths. Thus the yield strength of stub column tests of hot rolled, light-gage, and circular tubing sections is lower (by up to 13%) than would be predicted from simple coupon tests.

The main conclusions of the stub column investigation are summarized as follows: The high value of corner yield

strength is not completely effective in laterally unsupported stub column tests of cold-formed sections because of local buckling in the flat plate elements which commences at or about the lower yield strength of the flats themselves. Therefore, the yield strength of laterally unsupported full section specimens is lower than that of similar specimens which are laterally supported. However, for the specimens tested this reduction was not large. The laterally unsupported full section compressive yield strengths were slightly larger than the full section tensile yield strength for all sections tested except one in which the two values were approximately equal. At working load levels, local distortions were not visible in any of the sections tested. ($Q = 1$ for all but the 16 gage channel specimens for which $Q = 0.72$.) The most compact stub columns exhibited stability up to reasonably large values of plastic strain, i.e. had long stable yield plateaus and reached the ultimate load at strains from 16 to 27 x 10^{-3} in./in. Because of local buckling in the flat plate elements the less compact sections exhibited instability at relatively low values of plastic strain, i.e. reached the ultimate load at strains of only 3 to 5 x 10^{-3} in./in. after which the load dropped off rapidly. These stub column findings will be used below in Chapter 6 in connection with column buckling in the inelastic range.

5.2 Prediction of Full Section Yield Strength.

Full section tensile stress-strain characteristics may be established in three ways: (1) by full section tension

tests, (2) by weighted averaging of tension tests of corners and narrow strips from the flat portions of the cross section, and (3) by weighted averaging of standard tensile coupons from the flats of the cold-formed section and calculated corner tensile yield strength using a formula which will be given below. Full section compressive stress-strain charcteristics may also be established in three ways: (4) from laterally supported full section compression tests, (5) from laterally unsupported full section compression (stub column) tests, and (6) by weighted averaging of compression tests of corners and specimens from the flats. These six techniques for obtaining full section stress-strain characteristics are summarized and compared below:

(1) Full section tension tests were accomplished by welding 1/4 in. thick plates to the sections in the neutral plane of the member. Several SR-4 strain gages were applied to each specimen at mid-height. These tests require considerable time for specimen preparation, difficult welding procedures, and reduction of data. The full section tensile yield strength of the member was obtained in every test and the ultimate strength in most tests, with necking down and failure occurring near mid-length of the specimen. Certain cross sectional shapes are extremely difficult to weld adequately, however, and premature failure occurs by tearing at the pull plates.

(2) The full section tensile yield strength may be calculated from the test results of tension specimens of

corners and narrow strips from flats. Special and somewhat difficult machining techniques are required for the preparation of corner specimens. Testing of corner specimens is much the same as for standard tensile coupons. The area of the corner may be determined by weighing a known length of the tested corner specimen. Tension testing of narrow strips from flats is also rather routine. The exact number of flat specimens will depend on the shape of the cross section of the member, i.e. on the number of flats in the cross section. No less than one tension coupon should be taken from each flat, and if only one is taken from each flat it should be taken from the middle of the flat. More coupons may be taken from each flat if desired. This may be of some advantage in roll-formed sections where the yield strength of flats is not as uniform as in press braked sections.

Composite stress-strain curves may be calculated by selecting convenient values of strain and calculating corresponding mean stresses from the stress-strain curves of all component corner and flat specimens as described in Section 5.1d. This is a tedious procedure which would not be practical for design use. If, rather than the full stress-strain curve, only the full section tensile yield strength is desired, it may be computed by simply taking a weighted average of the yield strengths of the corner and flat elements of the cross section. The weighted average flat yield strength σ_{yf} may be obtained from the coupon yield strengths

by summing the product for each flat of tne average yield strength for that flat by the ratio of the area in that flat to the total area of flats in the cross section. With σ_{yf} computed and the corner yield strength σ_{yc} averaged from corner tests, the full section tensile yield strength of the section is given by

$$\sigma_{ys} = C\ \sigma_{yc} + (1 - C)\sigma_{yf} \tag{50}$$

where C is the ratio of corner area to total cross sectional area. This is not an exact procedure, but for sharp yielding materials the error will be practically nil and for gradual yielding materials it will be quite small. This simple computation will be demonstrated for a member made from a sharp yielding material, the HRSK16-37.5 press braked hat of Fig. 24(a):

$$\begin{array}{l} 39.7 \times .92 = 36.5 \\ 65.8 \times .08 = \underline{\ 5.3} \\ \qquad\qquad\ \ 41.8 \text{ ksi.} \end{array}$$

Here .92 and .08 are the ratios of flat and corner areas to total cross section area, respectively. This compares well with the average tensile yield strength, 42.5 ksi., of the two full section tests performed on this member. A similar computation for ultimate strength of this member is:

$$\begin{array}{l} 49.5 \times .92 = 46.0 \\ 69.5 \times .08 = \underline{\ 5.0} \\ \qquad\qquad\ \ 51.0 \text{ ksi.} \end{array}$$

This compares favorably with that of 51.1 ksi. obtained for HRSK16-37.5 press braked hat full section tension test T4.

(3) Calculation of full section tensile yield strength requires a sufficient number of standard tensile coupon tests

of the virgin steel to establish representative yield and ultimate strengths, σ_y and σ_u, for the material. With these material properties established, the corner tensile yield strength σ_{yc} may be found from Eqs. 35, 6, 7, 47, and 48, or more simply from the corner yield strength design chart, Fig. 8(d). Next, the average tensile yield strength of the flats σ_{yf} is established from standard tensile coupon tests. The full section tensile yield strength σ_{ys} may then be computed from Eq. 50. σ_{yf} may be substantially larger than σ_y, particularly in roll-formed sections. However, if it is not considered worthwhile to test to determine σ_{yf}, σ_y may be used in its place in Eq. 50.

(4) Full section compression test specimens require careful machining of the ends to insure trueness and squareness, application of several strain gages and attendant instrumentation, somewhat tedious testing techniques, and considerable reduction of data. To provide lateral support against local buckling, the strain gages must be waterproofed and protected, and the whole specimen must be lubricated and then cast in hydrostone, a time consuming process.

(5) Laterally unsupported full section compression test specimens require less preparation time than laterally supported ones. Since inelastic local buckling may occur in the flats at or about their own yield strength, the yield strengths determined from these tests are somewhat smaller than those of laterally supported full section compression tests.

(6) The full section compressive yield strength may be computed from the test results of compression specimens of corners and flats. Compression specimens of corners require the same special machining techniques necessary for tensile corner specimens. To keep the specimen from buckling, testing may be done in a steel jig or in hydrostone in a pipe sleeve, providing the specimen is greased so that it is free to slide in the longitudinal direction. Measurement of strains is difficult. Strain gages may be applied to the specimens for this purpose. Even the compression testing of flats requires expensive jigs and averaging compressometers if accurate results are desired.

In summary, the easiest method of establishing either tensile or compressive full section properites is by method (3), calculation of the tensile yield strength by Eq. 50 using σ_y and σ_u established from standard tensile coupon tests for virgin steel lots and σ_{yf} established from standard tensile tests of flats from cold-formed members. The laterally supported full section yield strength is generally somewhat larger than the tensile full section yield strengtn. Thus for design purposes the tensile full section yield strength value is the most conservative and the most easily established yield strength value which can be obtained by any of the above six methods.

Predictions of full section tensile yield strength by use of Eq. 50 and the calculated corner yield strength are given in Table 8 for a selection of four cold-formed cross

sections for which the ratio of corner to total cross sectional area varies from 8 to 31%. The sections which have been chosen for illustrative purposes are the sections shown in Figs. 24(a), (b), (c), and (g). Values obtained from full section tests and composite stress-strain curves are available for comparison with the predicted values for all of these sections.

Predicted values along with test values of the tensile full section yield strength for each of the sections are tabulated in Table 8. Column (6) gives the ratio of corner area to the total cross sectional area of the member. The "Calculated Tensile Corner Yield Strength σ_{yc}," Column (7), was computed using Eqs. 35, 47, and 48. The material constants k and n for these equations were calculated from Eqs. 6 and 7. Column (8), the "Average Flat Tensile Yield Strength σ_{yf}," gives the weighted average from tensile test specimens taken from the flats of the cold-formed members. The "Calculated Tensile Full Section Yield Strength σ_{ys}," Column (9), was computed from Eq. 50. The predicted values of Column (9) agree quite well with those obtained from the full section tests shown in Column (10).

No attempt is made to predict full section compressive properties because: (1) the method of predicting the yield strength of corners used above, i.e. by Eq. 35, was based on basic material properties obtained from tensile tests and (2) the full section yield strength in compression is generally above that in tension. The only exceptions which were

found to this in this investigation were for sections cold-formed from the cold reduced killed or "non-aging" steel. (Compare Column (11) with Column (10) in Table 8.) The full section yield strengths for the CRK16-38.3 press braked hats averaged not more than 4.5% lower in compression than in tension. Consequently, it appears that the use of the tensile in lieu of the compressive full section yield strength would be conservative in most cases and very close in those cases where the compressive is smaller than the tensile yield strength.

6. THE EFFECT OF COLD-FORMING ON COLUMN BUCKLING STRENGTH IN THE INELASTIC RANGE

6.1 Review of Inelastic Buckling Theory.

Axially loaded columns buckle inelastically at a critical stress very close to that given by the tangent modulus equation[15]

$$\sigma_{cr} = \pi^2 E_t/(L/r)^2 \qquad (51)$$

where E_t, the tangent modulus, replaces the modulus of elasticity in the Euler equation, L is the effective length of the column, and r is the radius of gyration in the plane of bending. Osgood[16] extended the tangent modulus theory to include cases where,(due to the influence of residual stresses) stress-strain characteristics are not constant throughout the cross sectional area of a column. Yang, Beedle, and Johnston[17] further modified the theory and applied it to steel wide flange columns subject to residual cooling stresses. This investigation was continued and completed in 1954 by Huber and Beedle[14]. The steel had sharp yielding stress-strain curves which were idealized by two straight lines, the first with a slope of E, and the second with zero slope. Even though, as yielding progresses, the residual stresses are eliminated and all of the material finally ends up at the yield stress, the presence of residual stresses lowers the buckling load of compression members in the inelastic range. In this method of analysis an algebraic expression is selected which approximates the residual stress distribution. That portion of the cross section with the highest

compressive residual stress yields first. Theoretical column curves are obtained by considering that only the moment of inertia of the unyielded portion of the cross section is effective. The critical stress σ_{cr} (i.e. the buckling load divided by the total cross sectional area) may be found from

$$\sigma_{cr} = \frac{\pi^2 E I_e / I}{(L/r)^2} \tag{52}$$

where I_e = the moment of inertia of the unyielded portion of the cross section,

I = the moment of inertia of the total cross section, and

E = the modulus of elasticity of the idealized material.

The effects of residual stresses in connection with the tangent modulus theory satisfactorily explained, for the first time, the reasons for the large disparity between tests of axially loaded hot rolled columns and the Euler column theory.

In 1952, Bleich[18] proposed the following parabolic equation as an approximation for the tangent modulus equation (Eq. 51):

$$\sigma_{cr} = \sigma_y - \frac{\sigma_p(\sigma_y - \sigma_p)}{4\pi^2 E} (L/r)^2 \tag{53}$$

If the proportional limit σ_p is taken as half the yield strength σ_y, this equation is reduced to

$$\sigma_{cr} = \sigma_y - \frac{\sigma_y^2}{\pi^2 E} (L/r)^2 \tag{54}$$

Eq. 54 applies for short and intermediate length columns for which the slenderness ratio L/r is less than C_c =

$\sqrt{2\pi^2 E/\sigma_y}$. Of course, for L/r greater than C_c the Euler equation for elastic buckling applies. In 1960, the CRC (Column Research Council) proposed[19] the use of Eq. 54 as a compromise between the strong and weak axis buckling curves obtained in the Lehigh University residual stress study[14]. Eq. 54 is sometimes referred to as the "CRC formula". It was adopted as the basic column design formula for the specification of the AISI (American Iron and Steel Institute) in 1946 and for that of the AISC (American Institute of Steel Construction) in 1961. Allowable design stresses may be obtained by dividing the right hand side of the equation by the safety factor n. The AISI has further modified[12] Eq. 54 to provide for the effects of local buckling by including the form factor Q:

$$\sigma_{allow} = \frac{\sigma_y Q}{n} - \frac{\sigma_y^2 Q^2}{4n\pi^2 E} (L/r)^2 \qquad (55)$$

Peterson and Bergholm[20] applied Osgood's development[16] to bi-symmetric* members (i.e. members having symmetric areas and distributions of materials properties about both major axes) in which the tangent modulus of the material is not constant throughout the cross section. In this case, it is assumed that the effects of residual stresses may be neglected. All of the material does not end up at the same yield stress after complete plastification of the section as in hot rolled shapes with large residual stresses. For bi-symmetric sections the neutral axis is located at the

---

* Osgood's derivation for the location of the neutral axis for mono-symmetric sections appears to be incorrect. See Appendix C for a more rigorous derivation.

geometric center of the cross section. Since the tangent modulus is not constant, it must be retained inside the integral for flexural rigidity, $\int_A E_t\ x^2\ dA$. The buckling stress may be found from

$$\sigma_{cr} = \frac{\pi^2}{AL^2} \int_A E_t\ x^2\ dA \qquad (56)$$

If the cross section were composed of j sub-areas, having constant properties over each sub-area, Eq. 56 could be written as

$$\sigma_{cr} = \frac{\pi^2}{AL^2} \sum_{i=1}^{j} E_{ti}\ I_i \qquad (57)$$

where E_{ti} is the tangent modulus of the i-th sub-area at a particular value of strain, and I_i is the moment of inertia of the i-th sub-area about the neutral axis of the total cross section. By application of a form of Eq. 57, Peterson and Bergholm were able to obtain excellent correlation between experimental critical stresses and analytical column curves for compact bi-symmetric sections fabricated from stainless steel[20].

The method of Eq. 57 used in the stainless steel column investigation is better suited for application to the tests described herein than the method of Eq. 52 used in the residual stress study. This is true because: (1) The effects of residual stresses on the stress-strain curves of the cold-formed full section specimens tested were found to be negli-

gible. (2) The main factor which affects behavior of hot

rolled steel sections is residual stresses, while in stainless steel columns the main factor is changes in materials properties due to cold working. (3) The stress-strain curves of corners from cold-formed members are gradual yielding, rather than sharp yielding as is assumed in the use of Eq. 52.

6.2 Column Tests.

a. Column Test Specimens. Several lengths of each of two types of doubly symmetrical column cross sections were fabricated by connecting singly symmetrical sections back to back. I-sections, Fig. 36(a), were made from roll-formed 10 gage HRSK10-37.0 channel sections. Doubly-flanged sections, Fig. 36(b), were made from roll-formed 9 gage HRSK9-30.7 joist chord sections. After the sections were connected the ends were milled. Six channel columns and three joist chord columns were fabricated by bolting at two in. centers with 3/16 in. diameter mild steel bolts. It was found that the bolted joist chord columns (specimens CT9, CT10, and CT11 of Table 9) buckled at loads significantly smaller than predicted by Eq. 57. Therefore, a new series of four joist chord columns was prepared. These columns were cold-riveted with 3/16 in. diameter rivets at one in. centers in a single row extending the entire length of the column. These columns gave results in good agreement with theoretical column buckling loads. The bolted channel columns buckled at stresses close to analytical values predicted by Eq. 57. However, it was felt advisable to have additional confirming data before

determining whether or not to repeat the channel column test series using cold-riveted specimens. Therefore, channel column specimen CT7 was fabricated with 3/16 in. cold-driven rivets at one in. centers. It was the same length as bolted specimens CT4 and CT5. Channel specimen CT7 buckled at a load of 48,000 lb., which compares favorably with the buckling loads of 48,000 and 49,000 lbs. for bolted companion specimens CT4 and CT5. It was, therefore, considered unnecessary to repeat the bolted channel column test series. Note that both of the column shapes tested had a value of Q = 1.

b. Column Test Procedure. The milled ends of the columns were supported on knife edge fixtures parallel to and in the plane of the weak axis of the specimens. The weak axes of the columns were placed in the plane of the screws of the testing machine. SR-4 strain gages were mounted on each specimen with a total of eight at each quarter point and eight or twelve at the center as shown in Fig. 36. Four dial gages, one at the upper head, at each quarter point, and at the center point, were arranged to measure deflection perpendicular to the weak axis of the columns, Fig. 37.

The columns were centered geometrically before any load was applied. The centering was checked and adjusted in trial runs in which the maximum applied load was approximately 2/3 of the theoretical maximum load. Eccentricity adjustments, made by means of opposing pairs of set screws

in the knife edge fixtures, were made with the dual objectives of minimizing differences in strain readings from the mean strain at each height and of minimizing deflections. If both of these objectives could not be realized because of initial crookedness of the columns, the deflection requirement governed over the equalization of strains. For the longer columns the dial gages were much more sensitive to adjustments than the strain gages. For the shorter columns the reverse was true.

Opposing gages were read in pairs to eliminate possible local bending effects from the strain readings. All of the sets of gages were read up to a load of about 2/3 of the analytical buckling strength, after which only the centerline gages were read. Deflections were measured at stages throughout the loading. Straining was continued in several of the specimens until the stabilized load had decreased to about 2/3 of the maximum load attained. Once the maximum load had been reached, strain and deflection readings were taken only after the load and strains had stabilized.

No correction was necessary for the larger moment of inertia of the end fixtures for these tests of axially loaded pin-ended columns[21].

c. Discussion of Results. Eq. 57 was used to develop analytical curves for comparison with test data obtained for weak axis buckling of the channel and joist chord columns. The procedure was as follows: (1) The area of the cross section was divided into three or more regions. Each area

was considered to have constant stress-strain characteristics. For example, the joist chord was divided into four regions as shown in Fig. 43. (2) Average stress-strain curves (Figs. 38, 39, 43, and 44) were established for each region of the cross section from tensile and compressive corner and flat specimens. Tensile and compressive composite stress-strain curves were computed for the full sections (Figs. 38, 39, 43, and 44). (3) The tangent moduli of the stress-strain curve of each region was determined graphically for a number of convenient values of strain. This was accomplished with a semi-transparent mirror held perpendicular to the page containing the stress-strain curve. When the reflected image coincided with the image transmitted through the mirror, the mirror was considered to be normal to the curve. The slope at this point was easily read by means of a small triangle held at right angles to the mirror. (4) The stress for each of the above mentioned convenient strains was taken from the composite stress-strain curve. Each of these values represents the average stress σ_{cr} on the section at a particular value of strain. (5) The section properties of the full section and of each of the sub-regions were computed. (6) For each value of strain chosen the values of E_t and had now been determined. Values of I and I_i were next computed for the section. The slenderness ratio L/r was calculated from Eq. 57. Theoretical column curves were computed in this manner based separately on the compressive and the tensile stress-strain curves of flat and corner cross

sectional elements. Column curves for weak axis buckling are compared to experimental column buckling stresses in Figs. 40 and 45. Column curves for strong axis buckling are included in Figs. 41 and 46. Curves plotted from the CRC formula, Eq. 54, are included in Figs. 40 and 45. Average values of the 0.2% offset yield strength from tensile and compressive full section tests (values are given in Table 7b) were used for this purpose. The load-deflection curves of all 15 columns tested are included in Figs. 42 and 46.

The theoretical Eq. 57 column curve based on tensile properties is lower than that based on compressive properties for both the channel and the joist chord columns. The difference between the two curves is larger for the channel columns (Fig. 40) than for the joist chord columns (Fig. 45). It can be seen from the Eq. 57 curves for the channel columns (Fig. 40) that the experimental points correlate better with the theoretical curve computed from the tensile rather than from the comressive stress-strain curves. It is reasoned that this is so because of local inelastic buckling which reduced the compressive yield strength 11% from an average of 55.4 ksi. for laterally supported to an average of 49.1 ksi. for laterally unsupported full section compression specimens. (For details on stub column tests see Section 5.1f and Table 7b.) The latter value is close to the average full section tensile yield strength of 47.8 ksi. For the joist chord columns the experimental maximum column stresses appear to correlate better with the theoretical curve based

on the compressive than with the tensile yield strength. However, as was noted above, the difference between these two curves is quite small for the joist chord columns. Also note that for the joist chords the reduction in compressive yield strength was only 4% from 53.8 ksi. for laterally supported to an average of 51.6 ksi. for laterally unsupported full section compression specimens (Table 7b). For both channel and joist chord columns there is very little difference between the column curves for strong and weak axis buckling.

Direct application of the tangent modulus theory (Eq. 51) to cold-formed members utilizing stress-strain curves from stub column tests, is not a completely rigorous procedure. However, column curves so obtained are shown in Figs. 41 and 46. The Eq. 51 curve in Fig. 41 is based on tangent moduli from the stress-strain curve of HRSK10-37.0 roll-formed channel specimen C9 (Fig. 33). It is considerably lower than the more rigorous Eq. 57 curves for L/r ratios from 65 to 100. For L/r ratios less than 60, the Eq. 51 curve falls between the two Eq. 57 curves. In fact, in this range it falls closer to the experimental points than either of the Eq. 57 curves. The Eq. 51 curve in Fig. 46 is based on HRSK9-30.7 roll-formed joist chord specimen C21 (Fig. 34). It is slightly lower than the Eq. 57 curves for L/r ratios from 80 to 100. For L/r ratios less than 80, the Eq. 51 curve falls slightly above the Eq. 57 curves. In general, the Eq. 51 curves are either on the conservative side of or close to the Eq. 57

curves based on tensile stress-strain curves.

For both kinds of columns the upper CRC curve (Eq. 54), based on the average laterally supported compressive full section yield strength, gives conservative predictions for critical stress only for L/r values greater than 65. The lower CRC curve, based on the average full section tensile yield strength, gives conservative and reasonable results over the entire inelastic range. Furthermore, it forms a lower bound to all of the other column curves in both channel and joist chord columns.

In summary, the following conclusions may be drawn from the results of tests of axially loaded pin-ended columns. Tests have been conducted on six bolted and two cold-riveted I-shaped channel specimens and on four cold-riveted joist chord specimens. Q = 1 for both kinds of columns. Analysis of these two cold-formed column shapes by means of a modified tangent modulus equation (Eq. 57) gives column curves in good agreement with test results. Exact agreement cannot be expected for three reasons: (1) There is a variation in the yield strength of the steel within even a modest size sheet. (2) There is undoubtedly some error involved in obtaining stress-strain curves and in determining tangent moduli from them. (3) There are unavoidable imperfections in cold-formed column specimens.

In spite of these minor sources of error the analytical method used gives good correlations with test data. Column curves obtained by direct application of the tangent

modulus equation (Eq. 51), using stress-strain curves from stub column tests, were either on the conservative side of or close to experimental values. It was found that the CRC column curve gives conservative and reasonable results when based on the full section tensile yield strength. It would be reasonable to use the laterally unsupported full section compressive yield strength for this purpose, but it would not be conservative to use the laterally supported full section compressive yield strength in this way. It should be noted that both materials in these two cold-formed shapes were hot rolled semi-killed, or aging, steels with the proportional limit equal to or greater than one half of the yield strength.

If a cold reduced non-aging steel (such as the CRK16-38.3 sheet steel) with a gradual yielding stress-strain curve having a proportional limit less than half of the yield strength were used, Eq. 54 would not be applicable.

6.2 Safety Factors in Column Design.

Some of the test results of this investigation have direct bearing on the choice of safety factors to be used in column design. For this reason a discussion of safety factors is pertinent.

The question might be raised whether any compression member of practical length should have the same factor of safety as a tension member. It may be argued that tension specimens have long stable yield zones and a reserve strength in the ability to strain harden, which most com-

pression members do not. However, results of the stub column tests on cold-formed members show that the more compact sections are in fact quite stable for low L/r ratios. The 10 gage roll-formed channel and the 9 gage roll-formed joist chord specimens for which Q = 1 showed a long yield plateau and reached the ultimate load at high values of strain, i.e. 16 to 27 x 10^{-3} in./in. (For example, see the stress-strain curve for HRSK10-37.0 roll-formed channel specimen C16 in Fig. 35.) The behavior of these more compact roll-formed sections in stub column tests is quite like that of compact hot rolled sections in such tests[22]. However, there are less compact cold-formed and hot rolled[22] sections which reach the maximum stub column load at low values of plastic strain, followed by rapid collapse. The stub column tests for which Q is less than 1 and the 16 gage press braked lipped angle and hat sections for which Q = 1 reached the ultimate compressive load at strains in the range from 3 to 5 x 10^{-3} in./in., after which the load dropped off sharply. (See, for example, the stress-strain curve for CRK16-38.3 press braked hat specimen C15 in Fig. 35.)

It seems reasonable that the safety factor used for the short compact compression members described above be the same as that used for tensile members. (For the purpose of this discussion a compact section is defined as one which has a long stable yield zone when tested as a stub column.) The compression member may or may not have the capability to strain harden; the important factor is the long stable yield

plateau before reaching the maximum load. The presence of the stable yield zone would permit plastic redistribution of loads and thus provide warning of failure without premature and sudden collapse.

A variable factor of safety could be provided for use with such compact members. (The AISC[23] factor of safety for compression members varies approximately as a sine curve from 1.65 at L/r = 0 to 1.92 for L/r = $\sqrt{2\pi^2 E/\sigma_y}$.) Such a variable factor of safety would provide a transition between the stable behavior of short compact columns and the less stable behavior of longer columns. For the less compact shapes which showed a sudden drop in load at low values of plastic strain, a larger and constant safety factor (say 1.92 or 1.95) seems definitely in order.

This would be in line with the generally recognized practice of applying higher safety factors to members which fail suddenly and without warning, e.g. for members made from brittle materials.

For design by the allowable stress concept, it has in the past been considered sufficient to reach the yield point without local buckling. However, in plastic design it is necessary that failure by local buckling not occur at low values of plastic strain. Haaijer and Thurlimann[22] proposed limitations on width to thickness ratios for flanges and webs of hot rolled wide flange sections. Compact members with width to thickness ratios not exceeding these restrictions are suitable for plastic hinge action and moment

redistribution. These recommendations were based on results of a theoretical and experimental investigation of plate buckling in the inelastic range. The recommendations for uniform compression were:

(1) for flanges,

> "The ratio of the outstanding width of flanges, b/t, shall not exceed the following values depending on the value of the yield stress, σ_o:
>
> for σ_o = 33 ksi: b/t = 8.7 and
>
> for σ_o = 36 ksi: b/t = 8.3."

and (2) for webs,

> "If a section is subject to axial load only, the ratio of the distance between the center planes of the flanges over the thickness of the web, d/t, shall not exceed the following values depending on the magnitude of the yield stress σ_o:
>
> for σ_o = 33: d/t = 44, and
>
> for σ_o = 36: d/t = 42."

It was noted[22] that hot rolled wide flange stub column specimen D6 (d/t = 41) failed by local buckling after just reaching the yield point, but that D2 (d/t = 33) failed in the strain hardening range. (Thus it is seen that the behavior of compact and non-compact cold-formed sections parallels the behavior of hot rolled shapes.) It was also noted[22] that the second recommendation above was based on the following concept: "For a section subjected to an axial load only, the first attainment of the yield stress is generally a sufficient requirement." This is a different philosophy than that being offerred herein, i.e. that to qualify as a compact section proportions must be such that local failure

will not take place at low values of plastic strain. Therefore, for webs of wide flange sections, a limiting w/t ratio smaller than 42 would be necessary. It may also be necessary to establish entirely separate limiting w/t ratios for webs of other shapes. At any rate, criteria such as those of Haaijer and Thurlimann could be extended, or similar criteria developed, which would be used to determine whether or not to apply a variable safety factor or a constant, but higher one. Presumably such w/t restrictions would be dependent on the level of the design stress. The resulting provisions would be applicable to hot rolled, cold-formed, and built-up sections alike.

There are two minor points which favor a higher safety factor for cold-formed than for hot rolled members: (1) the fact that larger out-of-planeness imperfections are found in cold-formed sections is one of these. (2) Differences in rigidity of connections is the other. The first of these is mainly of concern in short columns, and should be provided for in the selection of limiting w/t ratios. The second is of concern in longer columns and should be provided for by a consideration of effective lengths rather than by a higher factor of safety. Therefore, it appears that it would be feasable and desirable to combine the design of hot rolled and light-gage cold-formed compression members under one specification. Additional provisions would be required for classification of compact and non-compact sections. Special provisions would be required for determining the yield

strength of cold-formed members. A provision such as the AISI form factor Q or other local buckling criterion should be included in the CRC column curve as in Eq. 55. Provisions for torsional-flexural buckling would be needed for open shapes with only one or no axis of symmetry. If a section with a gradual yielding stress-strain curve having a proportional limit less than half of the yield strength were used, Eq. 54 would not be applicable. An alternate empirical column equation needs to be provided for such gradual yielding materials.

7. SUMMARY AND CONCLUSIONS

1. Gains in both the compressive and tensile yield strengths caused by the cold work of forming in light gage steel members may be as large as 70%. The largest increases occur in the corners of the cross section. The yield strength after cold working may be considerably higher than the original ultimate strength of the material for corners with small a/t ratios. Though much smaller than in corners, the increase in yield strength of flats may also be significant. The largest tensile yield strength increase found in this investigation was 52% for the flats of a roll-formed HRSK9-30.7 joist chord section. The smallest change in yield strength in flats was a decrease of 1% in a press braked CRK16-38.3 hat section.

2. Three methods of cold-forming were utilized in this investigation: air press braking, coin press braking, and roll-forming. Nine different sheet steel materials of varying gages and chemical composition were used (see Table 1). Only one of these, the CRK16-38.3 material, was a gradual yielding, non-aging material. The rest were sharp yielding, aging materials.

3. By plotting the logarithm of the true yield strength versus the logarithm of true plastic strain it was found that a straight line could be fitted to the stress-strain data, establishing the power relationship of Eq. 5 for each of the nine materials used in the investigation. (This relationship

was observed to be valid in tensile specimens for plastic strains from approximately 15 to 200 x 10^{-3} in./in. and is presumably valid until fracture of the material occurs.) Values of k, the strength coefficient, and n, the strain hardening exponent, were established from virgin tensile specimens tested in the plastic range. Values of n varied from 0.13 to 0.28 and values of k varied from 70 to 114 ksi. Empirical equations (Eqs. 6 and 7) were established which enable k and n to be computed directly from the yield strength σ_y and the ultimate strength σ_u of virgin tensile specimens rather than from log log plots of true stress and true strain. Values of σ_y and σ_u which are representative of the virgin sheet are necessary for this purpose.

4. Two analytical corner models are used in studying the changes which cold-forming causes in corners. The first consists of a wide flat plate subjected to pure flexure as shown in Fig. 5. The second includes the effect of radial pressure during plastic bending. Consideration of the mechanics of the cold-forming operations used in the investigation indicates that there is an inside radial pressure present in all of the three methods of cold-forming studied.

5. In order to study the plastic distortions occurring during the various kinds of cold-forming operations, photogrids of 200 lines per inch were applied to the surfaces of sheets before cold-forming them into corners. From this study it was found that: (1) Plane sections (in the radial direction) before bending do appear to remain plane.

(2) Circumferential plastic strains on the outside of a corner are somewhat larger than predicted by the first corner model (see Fig. 7). The second corner model was so chosen that better agreement with photogrid strains was obtained.

6. Equations for theoretical tensile yield strengths were derived for both analytical corner models. In the derivations several assumptions were necessary: (1) It was assumed that a condition of plane strain exists, i.e. that the strain in the longitudinal direction is negligible because of the restraint imposed on the corner by the adjacent undeformed flats. (2) It was further assumed, using the plane strain condition and the volume constancy concept for large plastic deformations, that the natural strain in the circumferential direction is equal in magnitude and opposite in sign to the natural strain in the radial direction. (3) From assumption (2) it was concluded that there will be no Bauschinger effect in volume elements taken from such a corner and tested in the longitudinal direction. This conclusion is verified by test results. (4) Using the concepts of "effective stress" and "effective strain" given by Eqs. 2 and 3, the power function, Eq. 5, was applied to a volume element and integrated over the area of a corner to obtain Eq. 33. Eq. 35 is a simple, but accurate, empirical approximation of Eq. 33.

7. For a/t ratios greater than about 5 there is very little difference in the values of the tensile yield strength obtained by the two corner models. However, for small a/t

ratios, the yield strengths predicted by the second model are about 10% larger than those predicted by the first model. Both the experimentally observed strains and the experimentally obtained corner yield strengths agree better with the second model, than the first. The tensile corner yield strength can, therefore, be conservatively and adequately predicted from Eqs. 35, 47, and 48. The virgin material constants k and n which are used in these equations may be obtained most readily by means of Eqs. 6 and 7. (No correlation was achieved by using values of k and n obtained from the data from uniaxially prestrained and aged specimens of a previous investigation. It would be somewhat surprising if such a correlation had been obtained, since uniaxially prestrained specimens did exhibit Bauschinger effects and specimens from corners have been demonstrated to be free of the Bauschinger effect.[5])

8. The percentage increase in ultimate strength in the corners is considerably smaller than the increase in yield strength, with a consequent marked reduction in the spread between yield and ultimate strength. Also the percent elongation drops rapidly with increasing amounts of cold work in the corner, indicating a loss of ductility with increasing strength. The reduction in percent elongation as compared to that of the virgin material varies from 20 to as much as 90% in CRK16-38.3 corners.

9. The increases in yield strengths in the flats of cold-formed members may be attributed mainly to: (1) the

strain hardening and aging resulting from stretcher-straightening of sheets stored as coils and (2) the normal pressures present in the coin press braking and roll-forming operations. The first factor is the only one which contributes significantly to the increase in yield strength of the flats of either air or coin press braked members. It was found that the increase in yield strength of flats next to coin press braked corners due to the second factor drops off very close to the corner, i.e. within less than a thickness on each side of the corner. No increase in yield strength due to the second factor was observed in the flats next to air press braked corners. Both factors contribute to the increase in yield strength of flats of roll-formed members.

10. The largest average tensile yield strength percentage increase for flats found in this investigation was 52% for the roll-formed HRSK9-30.7 joist chord section. The smallest increase in the tensile yield strength of flats of a hot rolled material was 6% for the press braked HRSK16-37.5 hat section. The tensile yield strength in the flats of the press braked CRK16-38.3 hat section was 1% below the virgin value. (Percentage increases in compressive yield strengths were approximately the same as for tensile yield strengths.) It follows that roll-forming produces larger increases in yield strength in the flats than brake forming, and that larger increases are found in flats made from aging than from non-aging materials. For practical purposes, the yield strength in flats of press braked material may be taken

as the virgin value. If it is desired to utilize the increases in yield strength in the flats of roll-formed members, the uncertainties connected with predicting such increases dictate that they be determined experimentally by coupons taken from the cold-formed members.

11. Percentage increases in tensile ultimate strength of flats due to the cold work of forming were much smaller than the increases in yield strength. The maximum percentage increase in ultimate strength was 10% for the flats of the 9 gage HRSK9-30.7 roll-formed joist chord. The change in ductility of cold-formed flats is generally quite small. The largest reduction in percent elongation (as compared to that of the virgin material) was 26% in the HRSK9-30.7 roll-formed joist chord.

12. Full section tensile stress-strain characteristics have been established in three ways: (1) by full section tension tests, (2) by weighted averaging of tension tests of corners and narrow strips from the flat portions of the cross section, and (3) by weighted averaging of standard tensile coupons from the flats of the cold-formed section and of calculated corner tensile yield strength, using Eqs. 35, 47, 48, and 50. Full section compressive stress-strain characteristics have also been established in three ways: (4) from laterally supported full section compression tests, (5) from laterally unsupported full section compression (stub column) tests, and (6) by weighted averaging of compression tests of corners and of flats. None of these methods is particularly

easy. Of the six methods, those three which would be most useful are (3), (5), and (1). These are listed in the order of increasing difficulty. Method (3) is discussed in detail below in conclusion 14. Full section tension tests were conducted on all of the sections shown in Fig. 16. Laterally supported full section compression tests were conducted on all but the press braked 16 gage channel of Fig. 24(e). Laterally unsupported full section compression (stub column) tests were performed for all of the shapes in Fig. 24 except the first two.

13. The following conclusions and trends may be seen from studying the full section tests results: (1) Composite stress-strain curves calculated from the stress-strain curves of strip specimens from the flats plus those of corner specimens match the stress-strain curves for both tensile and laterally supported compressive full section test specimens quite well. This implies that the longitudinal residual shearing stresses which are released by the cutting of strip specimens are not of sufficient value to have a significant direct effect on the mechanical properties of the full section. This is an important factor with regard to inelastic column buckling. (2) Increases above virgin values in both the full section tensile and full section compressive yield strengths were higher for the roll-formed sections than for the press braked sections tested. (3) Laterally supported full section compressive yield strengths were higher than the full section tensile yield strengths for all the sections except the press

braked CRK16-38.3 hat section. (4) Laterally supported full section compression yield strengths were higher than unsupported stub column yield strengths for all of the sections except for a press braked CRK16-38.3 hat section. It was found that local buckling of the flat plate elements at or slightly above the compressive yield strength of the flats did not allow the higher yield strength of the corner to become fully effective. However, the maximum stub column stress was slightly above the full section tensile yield strength for all sections except for a press braked CRK16-38.3 hat section. (5) Local buckling of flats did not become noticeable in the most compact stub column sections having Q equal to one until the maximum stub column load was reached. For the less compact sections with Q varying from 0.72 to 1.00, local buckling of flats became visible at loads only about 10 to 20% less than the maximum stub column loads. Therefore, it is assumed that distortions at working loads would probably not be serious in these sections. (6) The 16 gage press braked channel stub column specimens for which Q = 0.72 (Fig. 24(e))and the 16 gage press braked lipped angle and hat sections (Fig. 24(d) and (f)) for which Q = 1 reached the ultimate compressive load at strains in the range of from 3 to 5 x 10^{-3} in./in. after which the load dropped off suddenly. The 10 gage roll-formed channel and the 9 gage roll-formed joist chord specimens for which Q = 1 (Figs. 24(c) and (g)) showed long stable yield plateaus and reached the ultimate load at much higher values of strain, i.e. 16 to 27 x 10^{-3}

in./in. The behavior of these more compact roll-formed shapes has significance with regard to the safety factors for column design; i.e. a higher safety factor is indicated for the less compact sections as is discussed below in conclusion 16. (7) Welding decreased the full section compressive yield strength of specimen C9A from 55.4 to 51.7 ksi, 8% below the average yield strength of specimens C7 and C8 on which no welding was done. (8) Percentage increases in the full section ultimate strength values were much smaller than in either the tensile or the compressive yield strengths. (9) For the CRK16-38.3 press braked hat the percent elongation was 50%, and for the HRSK10-37.0 roll-formed channel it was 26%, showing that sections having large increases in yield strength still have ample ductility.

14. Calculation of the full section tensile yield strength requires a sufficient number of standard tensile coupon tests of the virgin steel to establish representative yield and ultimate strengths, σ_y and σ_u, for the material. With these material properties established, the corner tensile yield strength σ_{yc} may be found from Eq. 35 with k and n given by Eqs. 6 and 7 and with b and m given by Eqs. 47 and 48 or, more easily, from Fig. 8(d). (k and n are called the "strength coefficient" and the "strain hardening exponent".) Next, the average tensile yield strength of the flats σ_{yf} is established from standard tensile coupon tests. The full section tensile yield strength σ_{ys} may then be computed from Eq. 50. Once representative values of σ_y and σ_u are avail-

able for a given lot of steel, k, n, b, and m are also fixed for that lot and a curve for σ_{yc} versus the a/t ratio may easily be established. This leaves only the value of σ_{yf} to be determined experimentally for fabricated sections. σ_{yf} may be substantially larger than σ_y, particularly in roll-formed sections. However, if it is not considered worthwhile to test to determine σ_{yf}, σ_y may be used conservatively in its place in Eq. 50.

15. Tests of axially loaded pin-ended columns were made on eight I-shaped sections, fabricated by connecting, (i.e. by bolting or cold-riveting) two roll-formed 10 gage channels back to back, and on four sections fabricated by cold-riveting 9 gage roll-formed joist chord sections back to back. These compact shapes both had a value of Q = 1, where Q is defined in Section 3.6.1 of Reference 12. Direct application of the tangent modulus theory by using the stress-strain curve from a stub column or other full section test is not a completely rigorous procedure. Therefore, analytical column curves for these two column shapes were computed from stress-strain curves of flats and corner coupons taken from the cold-formed sections. An extended form (Eq. 57) of the tangent modulus equation for column buckling (Eq. 51) was used for this purpose. Column test results were found to be in good agreement with these analytical column curves.

16. It appears that it would be feasible to treat the design of hot rolled, built-up, and cold-formed axially loaded compression members in one unified specification. It

is recommended that the form factor Q or a similar local buckling criterion be used in the CRC column formula (as in Eq. 55). An alternate semi-empirical equation should be provided for columns which have ratios of σ_p/σ_y less than 0.5. A constant safety factor should be used for all but the most compact sections. Maximum ratios of width to thickness of flat plate elements of various shapes need to be established to distinguish between compact and non-compact sections. (A compact section is defined as one which has a long stable yield zone when tested as a stub column.) These w/t restrictions could be quite similar to those recommended by Haaijer and Thurlimann[20] for selection of compact sections suitable for plastic design. Such restrictions would apply to hot rolled sections, built-up sections, and cold-formed sections alike. A variable safety factor (such as is now used in the American Institute of Steel Construction specification[21]) would be used in compact sections meeting such limitations. Provisions on torsional-flexural buckling should be included. For cold-formed compression members with Q = 1, the full section yield strength for use in the column design formula, Eq. 55, may be established by calculation as outlined in conclusion 14, or from stub column tests, or from full section tension tests. The laterally supported full section compression yield strength may not be used for this purpose. For cold-formed compression members with Q less than 1, either σ_y or σ_{yf} may be used in Eq. 50. The yield strength for flats may be either tensile or compressive.

APPENDIX A-NOTATION

A = instantaneous cross sectional area

A_o = original area

ℓ = instantaneous length of a fiber

ℓ_o = original length

t = thickness of sheet, element, or corner

w = width of a plate element

r = radius to a point in a cold-formed corner

a = inside corner radius

b = outside corner radius

r_o = radius to surface of zero strain

r_n = radius to neutral surface, surface of zero circumferential stress

ε = engineering strain = $(\ell - \ell_o)/\ell_o$

ε' = natural or logarithmic strain = $\ln (1 + \varepsilon)$

σ = engineering stress = load/ A_o

σ' = true stress = load/A

Δ = volume strain = $\varepsilon_1 + \varepsilon_2 + \varepsilon_3$

Δ' = logarithmic volume strain = $\varepsilon_1' + \varepsilon_2' + \varepsilon_3'$

ε_1, ε_2, ε_3, and ε_θ, σ_r, σ_z are principal strains

σ_1, σ_2, σ_3, and σ_θ, σ_r, σ_z are principal stresses

σ_p = proportional limit determined by 0.02% offset method

σ_y = yield strength determined by 0.2% offset method

σ_u = ultimate strength

σ_{yc} = yield strength of corner

σ_{yf} = yield strength of flats of cold formed member

σ_{ys} = yield strength of full section

S' = deviator stress tensor

dE = strain increment tensor

$d\lambda$ = a scalar factor of proportionality

K = constant = $\sigma_y / \sqrt{3}$

x = a variable of integration or of distance

y = vertical distance of a point from mid-surface of undeformed sheet (except where defined otherwise.)

b and m are empirical constants

e = base of natural logarithms

k = strain hardening coefficient having same units as stress

n = strain hardening exponent-non-dimensional

C = ratio of corner area to total cross sectional area

p = uniform inside radial pressure on second corner model

Q = "form factor", Q, which is used in the design of sections containing one or more flat plate elements with large w/t ratios. Its purpose is to provide safety against local buckling. See Section 3.6.1 of Reference 12.

σ_{cr} = stress at the critical buckling load of a member

σ_{allow} = allowable column design stress

L = effective length of a column

r = radius of gyration in the plane of bending

E = initial modulus of elasticity of a material

E_t = tangent modulus of a stress-strain curve at a point above the proportional limit

E_{ti} = tangent modulus of the i-th element of a cross section

I = moment of inertia of a complete cross section

I_i = moment of inertia of the i-th element of a cross section about the neutral axis of the total cross section

I_e = moment of inertia of the unyielded portion of a partially yielded cross section

APPENDIX B.

YIELD STRENGTH VERSUS PLASTIC STRAIN RELATIONSHIPS OF UNIDIRECTIONALLY PRESTRAINED FLAT SHEETS

The purpose of this appendix is twofold: (1) to present data from the first phase[1] of this continuing investigation in a more usable form and (2) to evaluate the applicability of this data to the analysis of corner yield strengths presented above. The yield strengths on reloading of these permanently prestretched flat specimens are expressed as a function of the prior strain by means of Eq. 5. Values for the material constants k and n are tabulated (Table 10) for each of the first five materials listed in Table 1.

In the first phase of the investigation sheets were uniaxially stretched to permanent prestrains of 10, 25, 50 and 100 mils and allowed to age. After aging, specimens taken parallel and perpendicular to the direction of prestretching were tested in both tension and compression. The yield strengths of these specimens were based on the area of the specimens after prestraining.[1] Consequently, they may be considered as an approximation of the true yield strengths. True yield strengths versus true strains were plotted on log log paper for each of the five materials. Above strains of about 15 mils these experimental points approximate straight lines as shown in Fig. 48, which is typical. (No correction was made for elastic recovery since such corrections would be quite small compared to the plastic strains occurring.)

Using Eq. 5 in this way automatically includes the influences of aging and of the Bauschinger effect.

Values for k and n are given in Table 10 for four cases for each of the first five materials as determined from these plots. The four cases are for specimens tested in (1) tension in the direction of tensile prestrain, (2) tension transverse to the direction of tensile prestrain, (3) compression in the direction of tensile prestrain, and (4) compression transverse to the direction of tensile prestrain.

Curves of tensile σ_{yc} versus a/t ratio for corners determined by using these k and n values from uniaxially prestretched specimens did not correlate at all well with experimental values and are not shown on the curves of Figs. 9-17. This is not surprising since uniaxially prestrained specimens exhibited Bauschinger effects[1] and specimens from corners have been demonstrated to be free of the Bauschinger effect.[5] Note that the presence of the Bauschinger effect violates the seventh assumption, listed as requisite to the validity of the general strain hardening equation (Eq. 1) and, consequently, to the validity of Eq. 5. Thus it is seen that the yield strength versus permanent prestrain curves of prestretched and aged specimens given by Chajes, Britvec, and Winter[1] are not directly applicable to other states of plastic strain.

APPENDIX C

LOCATION OF THE NEUTRAL AXIS IN MONO-OR NON-SYMMETRIC CROSS SECTIONS WITH NON-UNIFORM MATERIALS PROPERTIES

Consider a mono- or non-symmetric column section such as that shown in Fig. 49(a). Assume that the section is constrained to buckle about the y-y axis. Also assume that the stress-strain characteristics of the material are distributed symmetrically with respect to the x-x but not to the y-y axis. The column is considered to be axially loaded and perfectly straight as in Fig. 49(b). It is further assumed that the column has been compressed beyond the proportional limit. The minimum load at which such an ideal column can, and generally will, begin bending is the tangent modulus load.[15] Therefore, at a load infinitesimally smaller than the tangent modulus load the column will have uniform compressive strains. However, since the column is stressed beyond the proportional limit, the compressive stress is not uniform in the cross section. Let $\bar{x}$ be the distance from an arbitrary reference line to the neutral axis y-y. $\bar{x}$ must be such that

$$M = \int_A \sigma x \, dA = 0 \qquad \text{(C1)}$$

where x is the distance from the neutral axis y-y to an element of area dA as shown in Fig. 49(a).

A procedure for establishing a column curve for such a section is outlined as follows: (1) Assume a value of strain ε above the proportional limit. (2) Establish the stress

distribution in the cross section from known stress-strain relationships for the elements of the cross section. (For example, see the stress-strain curves in Figs. 43 and 44.) (3) The average tangent modulus stress corresponding to ε may be obtained from

$$\sigma_{cr} = \frac{1}{A} \int_A \sigma dA \qquad (C2)$$

(4) Establish the location of the neutral axis for this stress by trial from Eq. C1. (5) Solve for the column length L corresponding to σ_{cr} from Eq. 56. Divide L by the radius of gyration r to obtain the slenderness ratio. (For design purposes it is convenient to use the radius of gyration r computed without regard to the distribution of materials properties. Therefore, it seems appropriate to express the slenderness ratio L/r in terms of the constant r rather than a variable r depending on materials properties.) (6) Repeat steps (1)-(5) for various assumed values of ε and plot the column curve.

REFERENCES

1. Chajes, A.; Britvec, S. J.; and Winter, G., "Effect of Cold-Straining on Structural Sheet Steels", Journal of the Structural Division, ASCE, Vol. 89, No. ST2, Proc. Paper 3477, April, 1963, pp. 1-32.

2. Sangdahl, G. S.; Aul, E. L.; and Sachs, G., "An Investigation of the Stress and Strain States Occurring in Rectangular Bars", Proceedings of the Society for Experimental Stress Analysis, 6, I.1. 1948.

3. Hill, R., The Mathematical Theory of Plasticity, Oxford University Press, London, 1950.

4. Nadai, A., Theory of Flow and Fracture of Solids, Vol. I, McGraw-Hill, New York, 1950.

5. Rolfe, S. T., "Effects of Cold-Straining on Structural Sheet Steels", Discussion, Journal of the Structural Division, ASCE, Vol. 89, No. ST5, October, 1963.

6. Holloman, J. H., "Tensile Deformation", Trans. A.I.M.E., Iron and Steel Div., Vol. 162, 1945, pp. 268-290.

7. Low, J. and Garafalo, F., "Precision Determination of Stress-Strain Curves in the Plastic Range", Proc. S.E.S.A., Vol. 4, No. 2, pp. 16-25.

8. Hoffman, O. and Sachs, G., Plasticity, McGraw-Hill, New York, 1953.

9. Lubahn, J. D., and Sachs, G., "Bending of an Ideal Plastic Metal", ASME Trans., Vol. 72, 1950, pp. 201-208.

10. Chajes, A. and Winter, G., "First Progress Report on Investigation of Effects of Cold-Forming on Mechanical Properties", unpublished progress report to American Iron and Steel Institute, New York, N.Y., Dept. of Civil Engineering, Cornell University, Ithaca, N.Y., October 10, 1961, (see Fig. 22).

11. Lenzen, K. H. and Dixon, J. H., "Preliminary Tests of Cold Roll-Formed Steel Joist Chord Sections", unpublished report for Sheffield Division, Armco Steel Corp., Kansas City, Missouri, July 11, 1960.

12. "Specification for the Design of Light Gage Cold-Formed Steel Structural Members", American Iron and Steel Institute, New York, N.Y., 1962 Edition.

13. Wolford, Don. S. and Rebholz, M. J., "Beam and Column Tests of Welded Steel Tubing with Design Recommendations", ASTM Bulletin, (TP 227), Oct. 1958.

14. Huber, A. W. and Beedle, L. S., "Residual Stress and the Compressive Strength of Steel", The Welding Journal, 33, Research Suppl., 1954, pp. 589s-614s.

15. Shanley, F. R., "Inelastic Column Theory". The Journal of the Aeronautical Sciences, Vol. 14, No. 5, May, 1947, p. 261.

16. Osgood, W. R., "The Effect of Residual Stresses on Column Strength", Proceedings of the First National Congress of Applied Mechanics, June, 1951.

17. Yang, C. H., Beedle, L. S., and Johnston, B. G., "Residual Stress and the Yield Strength of Steel Beams", The Welding Journal, 31 (4), Research Suppl., 1952, pp. 205s-229s.

18. Bleich, Friedrich, Buckling Strength of Metal Structures, McGraw-Hill Book Co., Inc., New York, N.Y., 1952.

19. Column Research Council: "Guide to Design Criteria for Metal Compression Members", 1960.

20. Peterson, Robert E. and Berghom, Axel O., "Effect of Forming and Welding on Stainless Steel Columns", Aerospace Engineering, V. 20, No. 4, April, 1961.

21. Osgood, W. R., "Column Strength of Tubes Elastically Restrained Against Rotation at the Ends", National Advisory Committee for Aeronautics, Report No. 615, 1938.

22. Haaijer, B. and Thurlimann, B., "On Inelastic Buckling in Steel", Journal of the Engineering Mechanics Division, ASCE, Vol. 84, No. EM2, Proc. Paper 1581, April, 1958.

23. "Specification for the Design, Fabrication, and Erection of Structural Steel for Buildings", American Institute of Steel Construction, New York, N.Y., 1963 Edition.

TABLE 1 - MATERIAL PROPERTIES

Material	Gage	Chemical Composition by Random Check Analysis				Compr. Yield Strength ksi	Tensile Properties			
		C	M_n	S	P		Yield Strength ksi	Ultimate Strength ksi	% Elong in 2" gage length	$\frac{\sigma_u}{\sigma_y}$
1. Cold Reduced Annealed, Temper-Rolled Killed, Sheet Coil	16	.15	.40	.024	.008	34.6	38.3	51.1	40	1.34
2. Cold Reduced Annealed, Temper-Rolled Rimmed, Sheet Coil	16	.09	.39	.028	.008	33.0	36.4	50.7	35	1.39
3. Hot Rolled Semi-killed Sheet Coil	16	.04	.32	.025	.008	40.5	37.5	49.0	37	1.31
4. Hot Rolled Rimmed Sheet Coil	16	.08	.32	.045	.008	40.3	40.5	50.7	35	1.25
5. Hot Rolled Semi-Killed Sheet Coil	10	.18	.50	.029	.008	38.5	37.0	57.5	36	1.55
6. Hot Rolled Semi-Killed Sheet Coil	16	.16	.46	.024	.009	37.6	39.7	55.9	35	1.41
7. Hot Rolled Semi-Killed Sheet Coil	10	.22	.43	.024	.008	43.2	42.8	66.6	31	1.55
8. Hot Rolled Semi-Killed Sheet Coil	16	.23	.45	.025	.012	39.1	40.7	61.4	31	1.51
9. Hot Rolled Semi-Killed Sheet Coil	9	.09	.52	.033	.010	32.0	30.7	52.9	35	1.72

TABLE 2

VALUES FOR THE STRENGTH COEFFICIENT k AND STRAIN HARDENING EXPONENT n FROM VIRGIN TENSILE SPECIMENS

Material	Tensile Properties		σ_u/σ_y	n	k
	Yield Strength σ_y ksi	Ultimate Strength σ_u ksi			ksi
1. CRK16-38.3	40.1	50.7	1.27	.149	77.7
	40.7	51.0	1.25	.143	77.2
	40.2	50.8	1.27	.155	78.8
	37.0	45.7	1.24	.149	69.6*
2. CRR16-36.4	38.2	49.8	1.30	.149	76.3
	38.9	50.3	1.29	.155	78.8
	38.6	50.3	1.30	.143	76.2
	37.8	51.4	1.36	.137	76.5*
3. HRSK16-37.5	40.3	49.8	1.23	.161	77.4
	40.5	49.3	1.22	.161	76.8
	40.5	49.3	1.22	.158	76.8
	41.0	50.8	1.24	.198	85.2*
4. HRR16-40.5	34.7	45.5	1.31	.195	75.2
	33.7	45.3	1.34	.203	76.1
	38.7	46.8	1.21	.152	71.7
	41.5	51.5	1.24	.198	87.0*
5. HRSK10-37.0	39.1	58.1	1.49	.208	99.2
	42.5	60.5	1.42	.197	101 5
	42.7	60.2	1.41	.236	109.0
	37.5	58.0	1.55	.228	101.7*
6. HRSK16-39.7	35.8	52.3	1.46	.210	90.1
	35.8	52.0	1.45	.212	90.4
	36.0	51.3	1.43	.201	86.7
7. HRSK10-42.8	41.4	65.0	1.57	.215	114.0
	40.8	64.0	1.57	.212	111.0
	45.2	66.1	1.46	.208	114.0
8. HRSK16-40.7	44.8	64.8	1.45	.208	111.2
	45.3	65.5	1.45	.204	112.8
	45.7	66.0	1.45	.199	110.9
9. HRSK9-30.7	30.9	52.0	1.68	.262	99.2
	29.5	52.2	1.77	.276	99.6
	31.1	50.6	1.63	.281	103.7

* Computed from data from tests conducted more than two years prior to those for other data shown in this table.

TABLE 3

NUMERICALLY INTEGRATED VALUES OF σ_{yc}/k

SECOND CORNER MODEL

n \ a/t	1	2	3	4	5	6	7	8	9	10
.10	.875	.796	.760	.738	.721	.708	.698	.689	.681	.674
.12	.846	.760	.721	.696	.678	.664	.652	.642	.633	.625
.14	.817	.726	.684	.657	.637	.622	.609	.598	.589	.581
.16	.790	.694	.649	.621	.599	.583	.569	.557	.547	.538
.18	.764	.663	.616	.586	.564	.546	.532	.520	.509	.500
.20	.738	.634	.585	.554	.530	.512	.497	.485	.474	.464
.22	.714	.607	.556	.523	.499	.480	.465	.452	.441	.431
.24	.691	.580	.528	.494	.470	.450	.435	.422	.410	.400
.26	.668	.555	.501	.467	.442	.423	.407	.393	.382	.372
.28	.647	.531	.477	.442	.416	.397	.381	.367	.356	.346
.30	.626	.508	.453	.418	.392	.372	.356	.343	.331	.321

FIRST CORNER MODEL

n \ a/t	1	2	3	4	5	6	7	8	9	10
.10	.817	.777	.751	.732	.718	.706	.696	.687	.680	.673
.12	.788	.741	.712	.691	.675	.661	.650	.640	.632	.624
.14	.760	.708	.675	.652	.634	.620	.607	.600	.587	.579
.16	.733	.676	.641	.616	.596	.581	.567	.556	.546	.538
.18	.707	.646	.608	.581	.561	.544	.530	.518	.508	.499
.20	.682	.617	.577	.549	.527	.510	.496	.483	.473	.463
.22	.659	.590	.548	.518	.496	.478	.463	.451	.440	.430
.24	.636	.564	.520	.490	.467	.449	.433	.421	.410	.400
.26	.614	.539	.494	.463	.439	.421	.405	.392	.381	.371
.28	.593	.515	.469	.438	.414	.395	.379	.366	.355	.345
.30	.573	.493	.446	.414	.390	.371	.355	.342	.331	.321

TABLE 4

CORNER SPECIMENS

Material and Forming Method	Compression Tests a/t	σ_p (ksi)	σ_y (ksi)	$\frac{\sigma_p}{\sigma_y}$	Tension Tests a/t	σ_p (ksi)	σ_y (ksi)	σ_u (ksi)	$\frac{\sigma_p}{\sigma_y}$	% Elong. in 2"
CRK16-38.3 Roll Formed	1.59	44.0	60.0	.73	1.59	49.3	61.1	65.3	.80	8
	1.59	36.0	54.5	.66	1.59	45.7	57.5	57.5	.79	
	1.59	37.0	54.5	.67	1.59	43.0	57.7	59.0	.74	8
	1.59	46.0	59.0	.77	3.02	32.2	49.2	52.0	.65	31
	3.02	51.0	58.5	.87						
	3.02	43.0	53.0	.81						
	3.03	38.0	51.5	.73						
	3.03	37.0	51.5	.71						
	3.03	36.0	50.0	.72						
CRK16-38.3 Coin Press Braked	1.00	41.5	62.5	.66	1.06	44.8	64.7	67.0	.69	5
	1.62	43.0	63.0	.68	1.05	42.0	58.0	62.0	.72	6
	2.29	30.0	53.0	.56	1.06	51.7	65.6	66.2	.78	9
	2.16	39.0	51.0	.76	2.43	42.0	58.6	60.0	.71	7
	4.32	36.0	48.5	.74	4.58	40.3	48.2	50.3	.83	26
	4.50	39.0	53.0	.73						
CRK16-38.3 Air Press Braked	1.62	44.6	61.5	.72	1.61	38.3	57.5	57.5	.66	5
	2.04	44.0	55.0	.80	2.12	41.7	57.5	58.2	.72	8
	2.38	39.0	57.6	.67	4.23	36.9	50.3	52.3	.73	32
	3.98	36.0	46.5	.77						
	4.32	33.0	52.0	.63						
CRR16-36.4 Roll Formed	1.54	50.0	63.0	.79	1.54	52.8	61.0	71.0	.86	
	1.54	44.0	59.0	.74	1.54	50.0	61.7	64.8	.81	10
	1.54	46.0	61.5	.74	3.23	44.0	52.0	58.7	.84	
	3.23	50.0	59.0	.84	3.23	45.7	53.7	60.4	.85	14
	3.23	38.0	53.0	.71						
	3.23	49.0	56.0	.87						
	3.23	46.5	55.5	.83						
	3.23	44.0	54.0	.81						
CRR16-36.4 Coin Press Braked	1.02	54.0	68.2	.79	1.06	49.0	67.6	67.6	.72	
	1.54	54.0	65.8	.82	1.06	41.3	62.3	70.0	.66	5
	2.18	42.0	60.5	.69	1.30	49.6	64.1	68.1	.77	10
	4.10	39.5	54.0	.73	2.34	46.3	60.8	65.2	.76	8
	4.56	41.0	52.0	.78	4.62	34.2	48.8	55.2	.70	18
CRR16-36.4 Air Press Braked	1.89	50.0	63.8	.78	1.89	42.3	58.7	61.7	.72	4
	2.05	44.0	64.0	.68	2.08	43.8	59.1	62.8	.74	7
	4.10	41.5	53.0	.78	4.36	33.7	47.5	54.5	.70	24
	4.36	42.5	53.0	.80						

TABLE 4

CORNER SPECIMENS

Material and Forming Method	Compression Tests a/t	σ_p (ksi)	σ_y (ksi)	$\frac{\sigma_p}{\sigma_y}$	Tension Tests a/t	σ_p (ksi)	σ_y (ksi)	σ_u (ksi)	$\frac{\sigma_p}{\sigma_y}$	% Elong. in 2"
HRSK16-37.5	1.49	56.0	62.5	.89	1.42	53.0	60.0	67.0	.88	
Roll	1.49	58.5	62.5	.93	1.49	54.3	58.7	65.0	.92	10
Formed	3.02	54.5	54.5	1.00	3.02		53.3	57.0		
	3.03	52.8	54.1	.97	3.02	50.0	52.7	59.0	.94	18
	3.03	54.5	56.0	.97						
	3.03	53.0	55.0	.96						
HRSK16-37.5	1.05	67.5	69.0	.97	1.00	67.0	67.0	69.0	1.00	
Coin	1.51	54.1	63.8	.84	1.00	55.3	64.5	70.0	.85	6
Press	2.11	53.5	56.5	.94	1.76	55.2	61.9	67.0	.89	6
Braked	2.14	47.5	56.0	.84	1.24	48.2	56.9	61.3	.84	7
	3.72	51.0	53.0	.96	2.23	49.8	54.2	58.3	.91	10
	4.03	48.0	54.5	.88	2.24	51.0	59.0	64.3	.86	8
					4.22	47.1	47.4	55.2	.99	16
HRSK16-37.5	1.76	56.7	62.2	.91	1.49	54.8	61.5	67.4	.89	8
Air	2.02	46.0	58.0	.79	1.98	52.8	57.3	63.8	.92	10
Press	3.97	47.5	49.0	.96	3.78	47.6	49.8	57.3	.95	20
Braked	3.72	50.0	53.5	.93						
HRR16-40.5	1.75	54.0	64.0	.84	1.75	58.0	64.5	70.5	.89	
Roll	1.75	46.5	66.0	.70	1.75	55.7	62.0	68.0	.89	9
Formed	1.75	58.0	65.7	.88	3.02		54.0	62.5		
	1.75	58.0	67.0	.86	3.02	53.2	56.0	64.0	.95	19
	3.02	55.0	59.0	.93						
	3.03	54.5	55.5	.98						
	3.03	43.0	56.5	.76						
HRR16-40.5	1.06	68.3	72.6	.94	1.02	59.7	71.2	76.6	.83	10
Coin	2.02	53.0	61.0	.86	1.02	60.7	69.0	74.8	.87	7
Press	2.02	49.0	55.0	.89	1.24	51.0	60.0	67.0	.85	10
Braked	3.97	45.0	55.0	.81	1.24	64.5	66.4	69.6	.97	11
	3.97	45.0	50.0	.90	2.27	47.0	56.0	63.0	.83	9
					4.22	48.0	50.0	57.0	.96	17
HRR16-40.5	1.74	53.5	64.0	.83	1.74	48.0	56.0	61.0	.85	10
Air	1.98	57.0	62.0	.91	1.74	47.6	59.0	64.5	.80	6
Press	1.88	53.0	59.0	.89	1.98	50.0	56.0	62.0	.89	9
Braked	3.72	52.0	53.0	.98	3.72	48.0	51.0	58.0	.94	19

TABLE 4

CORNER SPECIMENS

Material and Forming Method	Compression Tests a/t	σ_p (ksi)	σ_y (ksi)	$\frac{\sigma_p}{\sigma_y}$	Tension Tests a/t	σ_p (ksi)	σ_y (ksi)	σ_u (ksi)	$\frac{\sigma_p}{\sigma_y}$	% Elong. in 2"
HRSK16-39.7	.96	55.0	69.0	.80	.97	52.0	65.5	70.5	.79	6
Air	.96	52.6	70.0	.75	.96	50.6	64.7	69.5	.78	5
Press	.96	52.0	68.0	.76	.96	54.5	66.4	70.3	.82	6
Braked	1.97	44.0	64.2	.69	1.74	43.3	59.8	68.8	.72	7
	1.97	51.2	65.2	.79	1.75	46.8	59.7	68.0	.78	8
	1.97	42.3	62.4	.68	1.73	47.2	59.6	68.4	.79	8
	4.97	39.3	53.6	.73	4.52	39.9	48.3	60.1	.82	25
	4.97	43.3	53.0	.82	4.53	39.5	47.9	59.1	.82	24
	4.47	40.3	53.5	.76	4.51	42.7	49.4	60.7	.86	22
	5.83	45.2	47.2	.96	5.93	40.4	47.2	59.0	.86	30
	5.83	43.2	47.3	.91	5.94	41.1	48.7	61.1	.85	29
	6.32	37.9	46.4	.82	5.92	41.4	47.7	59.2	.87	33
HRSK10-42.8	.71	66.5	87.0	.76	.96	67.3	79.7	88.2	.85	10
Air	.71	64.5	82.0	.79	.96	58.2	76.3	87.0	.76	11
Press	.71	62.8	81.0	.78	.96	58.2	75.0	86.3	.78	10
Braked	1.78	57.5	75.4	.76	1.92	49.1	69.0	80.2	.71	17
	1.78	55.7	75.5	.76	1.92	51.3	69.3	80.8	.74	15
	1.78	57.0	74.6	.76	1.92	50.8	69.2	80.1	.74	14
	2.85	53.7	64.2	.84	2.99	45.8	57.0	71.5	.80	26
	2.85	51.2	57.8	.89	2.99	46.7	57.9	72.4	.81	25
	2.85	57.7	65.6	.88	2.99	46.7	58.0	72.0	.80	25
	5.71	48.2	56.9	.85	5.73	39.1	53.3	70.0	.73	32
	5.71	48.4	54.8	.88	5.73	42.2	53.7	69.5	.67	32
	5.71	51.1	57.3	.89	5.73	44.8	54.7	70.5	.82	32
HRSK16-40.7	1.03	68.3	77.9	.88	1.06		67.2	75.3		8
Air	1.03	52.9	68.8	.73	1.06	50.5	66.3	73.5	.76	8
Press	1.03	58.8	72.7	.81	1.04	45.1	65.7	74.0	.69	8
Braked	2.10	53.5	67.5	.79	1.83	48.8	61.3	68.6	.80	14
	2.10	47.5	67.5	.70	1.83	52.6	62.3	69.2	.84	14
	2.10	45.5	66.2	.69	1.84	44.7	61.8	69.8	.72	12
	4.21	40.5	60.1	.67	4.18	38.2	53.9	65.3	.71	28
	4.21	46.0	62.3	.74	4.18	38.5	54.5	65.6	.70	27
	4.21	40.7	58.0	.70	4.21	39.7	55.2	65.7	.72	32
	6.30	30.5	48.3	.63	6.33	39.3	50.4	63.7	.78	30
	6.30	37.2	45.4	.82	6.33	38.3	49.3	62.8	.78	30
	6.30	37.7	47.7	.79	6.32	37.9	49.7	63.7	.76	31
HRSK9-30.7	1.34	61.5	68.8	1.12	1.45	50.6	59.6	69.3	.83	12
Roll-formed	1.55	60.2	67.4	1.12	1.45	50.0	65.5	73.5	.76	10
	1.55	55.0	66.1	1.20	1.55	52.0	62.9	71.8	.82	13
	1.45	54.0	67.7	1.25	1.45	52.7	65.4	74.0	.80	11

TABLE 4

CORNER SPECIMENS

Material and Forming Method	Compression Tests a/t	σ_p (ksi)	σ_y (ksi)	$\frac{\sigma_p}{\sigma_y}$	Tension Tests a/t	σ_p (ksi)	σ_y (ksi)	σ_u (ksi)	$\frac{\sigma_p}{\sigma_y}$	% Elong. in 2"
HRSK10-37.0	.89	66.0	74.0	.89	.89	59.0	66.4	72.9	.88	9
Roll Formed	.89	65.0	74.0	.87	.89	62.0	68.8	76.0	.90	10
HRSK10-37.0	.78	64.0	75.0	.85	.78	47.8	71.0	79.2	.67	9
Coin	.78	43.5	73.0	.59	1.90	57.3	63.2	73.2	.90	14
Press	1.90	54.0	63.5	.85	3.10	42.0	55.0	68.2	.76	22
Braked	1.90	50.5	63.0	.80						
	3.10	46.0	56.0	.82						
	3.10	41.0	55.0	.74						
HRSK10-37.0	1.00	52.0	72.0	.72	.78	57.0	70.3	80.0	.81	9
Air	.78	71.0	86.5	.82	1.89	52.2	61.5	72.1	.84	14
Press	1.90	50.5	63.0	.80	1.90	54.3	60.7	70.8	.89	14
Braked	1.90	48.0	62.0	.77	3.12	46.5	54.6	68.7	.85	26
	3.10	43.0	57.0	.75	3.12	49.7	58.3	70.0	.85	15
	3.10	43.0	55.0	.78	3.10	52.0	58.4	68.7	.89	22

TABLE 5

(SERIES 1 FLATS)

FLAT SPECIMENS FROM LOCATIONS ADJACENT TO CORNERS

Material and Forming Method	Compression Tests a/t	σ_p (ksi)	σ_y (ksi)	$\frac{\sigma_p}{\sigma_y}$	Tension Tests a/t	σ_p (ksi)	σ_y (ksi)	σ_u (ksi)	$\frac{\sigma_p}{\sigma_y}$	% Elong. in 2"
CRK16-38.3	1.59	26.9	38.2	.70	1.59	32.3	39.7	52.0	.81	
Roll Formed	3.18	30.0	39.0	.76	1.59	29.4	41.3	51.6	.71	41
					3.02	30.5	40.6	51.5	.75	
					3.02	32.9	42.4	53.7	.77	37
CRK16-38.3	1.09	26.3	34.5	.76	1.08	30.6	39.5	53.0	.77	39
Coin	2.37	24.1	36.0	.66	2.42	31.4	39.6	51.6	.79	39
Press	2.29	24.3	34.8	.69	2.29	23.0	38.4	51.6	.74	38
Braked	4.32	29.8	37.1	.80	4.32	29.7	38.6	50.7	.76	39
CRK16-38.3	2.18	27.0	34.7	.77	2.12	30.6	38.7	49.8	.79	44
Air Press	2.04	21.8	32.8	.66	2.04	23.3	35.6	47.3	.75	39
Braked	3.98	22.8	33.0	.69	3.98	24.2	34.5	46.1	.70	40
CRR16-36.4	1.56	36.4	38.2	.95	1.54	31.8	43.3	52.0	.73	
Roll Formed	3.18	38.4	40.7	.94	1.54	36.9	40.9	51.8	.90	35
					3.23	40.0	40.0	51.3	1.00	
					3.23	39.2	40.9	50.2	.95	34
CRR16-36.4	1.06	36.6	36.6	1.00	1.08	40.0	40.0	53.2	1.00	35
Coin	2.45	34.0	34.0	1.00	2.31	36.8	36.8	50.3	1.00	35
Press	2.18	35.6	38.7	.91	2.18	38.5	38.8	51.3	.99	32
Braked	4.10	35.0	39.5	.88	4.10	39.3	39.3	51.7	1.00	32
CRR16-36.4	2.21	35.5	35.5	1.00	2.19	37.1	37.3	49.8	.99	34
Air Press	2.05	35.9	36.4	.98	2.05	39.2	39.2	51.2	1.00	34
Braked	4.10	36.5	39.3	.92	4.10	39.1	39.1	51.2	1.00	29
HRSK16-37.5	1.49	41.0	46.0	.89	1.49	41.3	41.3	51.0	1.00	
Roll Formed	3.07	41.2	41.2	1.00	1.49	45.3	45.2	54.1	1.00	25
					3.02	43.0	43.0	51.3	1.00	
					3.02	40.8	40.8	50.8	1.00	30
HRSK16-37.5	1.02	45.2	45.3	.99	1.01	40.6	40.6	52.5	1.00	33
Coin	2.26	42.7	42.7	1.00	2.27	39.8	39.8	49.2	1.00	31
Press	2.11	36.2	41.7	.86	2.11	40.8	40.8	50.3	1.00	36
Braked	3.72	42.0	42.0	1.00	3.72	40.2	40.2	50.2	1.00	33
HRSK16-37.5	1.74	41.2	41.2	1.00	1.76	39.1	39.1	49.2	1.00	28
Air Press	2.02	42.2	42.2	1.00	2.02	40.0	40.0	50.3	1.00	34
Braked	3.97	43.6	43.6	1.00	3.97	40.8	40.8	50.1	1.00	28

TABLE 5

(SERIES 1 FLATS)

FLAT SPECIMENS FROM LOCATIONS ADJACENT TO CORNERS

Material and Forming Method	Compression Tests a/t	σ_p (ksi)	σ_y (ksi)	$\frac{\sigma_p}{\sigma_y}$	Tension Tests a/t	σ_p (ksi)	σ_y (ksi)	σ_u (ksi)	$\frac{\sigma_p}{\sigma_y}$	% Elong. in 2"
HRR16-40.5	1.75	47.0	47.0	1.00	1.75	45.2	45.2	55.5	1.00	
Roll Formed	3.07	45.0	45.0	1.00	1.75	43.4	49.2	57.6	.88	25
					3.02	43.5	43.5	55.5	1.00	
					3.02	43.3	43.3	55.4	1.00	27
HRR16-40.5	1.02	44.2	44.2	1.00	1.02	42.3	42.3	56.1	1.00	32
Coin Press	2.02	42.0	42.0	1.00	2.02	38.3	38.3	47.0	1.00	37
Braked	3.97	39.7	40.3	.98	3.97	38.8	38.8	42.7	1.00	30
HRR16-40.5	1.88	35.3	42.5	.83	1.88	40.4	40.4	49.8	1.00	33
Air Press	3.72	41.7	43.7	.95	3.72	39.5	39.5	49.8	1.00	34
Braked										
HRSK10-37.0	.89	43.6	44.1	.98	.89	43.2	43.2	59.6	1.00	34
Roll Formed	.89	45.8	46.1	.99	.89	42.5	45.6	59.1	.93	32
HRSK10-37.0	.78	41.2	41.2	1.00	.78	41.0	41.2	60.8	.99	36
Coin Press	1.90	37.8	37.8	1.00	1.90	38.6	38.6	58.9	1.00	34
Braked	3.10	37.9	37.9	1.00	3.10	37.3	38.5	59.5	.96	33
HRSK10-37.0	1.00	39.1	39.7	.98	1.00			60.5		31
Air Press	1.90	35.3	38.2	.92	1.90	39.3	39.7	59.0	.98	35
Braked	3.10	41.7	42.1	.99	3.10	37.3	37.3	59.3	1.00	36

TABLE 6

AVERAGE TEST RESULTS IN FLAT PORTIONS OF SECTIONS

Section				0.2% offset Yield Strength						Tensile Strength		
				Compressive			Tensile					
Gage	Mat'l	Forming Method	Shape	Virgin (ksi)	Ave Flats (ksi)	% Incr	Virgin (ksi)	Ave Flats (ksi)	% Incr	Virgin (ksi)	Ave Flats (ksi)	% Incr
16	CRK	Press Braked	Hat	34.6	36.0	4	38.3	37.9	-1	51.1	50.5	-1
16	HRSK	Press Braked	Hat	40.5	42.2	4	37.5	39.7	6	49.0	49.5	1
16	HRSK	Roll-Formed	Track	40.5	47.3	17	37.5	43.8	17	49.0	52.7	6
10	HRSK	Roll-Formed	Channel	38.5	49.8	29	37.0	45.6	23	57.5	60.1	5
9	HRSK	Roll-Formed	Joist Chord	32.0	48.1	50	30.7	46.8	52	52.9	58.0	10

TABLE 7a - FULL SECTION TEST RESULTS

Section Type	Spec. No.	Length (in.)	Laterally Supported Compress. Yield Str. (ksi)	Tensile Yield Strength (ksi)	Tensile Ultimate Strength (ksi)
CRK16-38.3	Strips			39.6	51.8
Press	T1*	30		39.6	49.0
Braked	T2*	30		39.3	48.7
Hat	Strips		38.0		
	C1	8	36.8		
	C2	8	38.7		
HRSK16-37.5	Strips			42.5	51.0
Press	T3**	30		42.5	
Braked	T4*	30		41.3	51.1
Hat	Strips		45.1		
	C3A	4 3/4	44.0		
	C3B	4	45.4		
	C3	8	44.9		
	C4	8	45.2		
HRSK16-37.5	Strips			46.0	54.9
Roll-Formed	T5**	30		45.3	
Track	T6**	30		48.5	
	T10	30		46.0	
	Strips		50.8		
	C5	8	50.9		
	C6	8	51.2		

Note: "Strips" indicates values obtained from stress-strain curves calculated from data from narrow strip specimens.

* Achieved failure in central portion of specimen.

** Specimen tore at end weld.

TABLE 7b

FULL SECTION TEST RESULTS FOR LATERALLY UNSUPPORTED COMPARED TO LATERALLY SUPPORTED AND TO FULL SECTION TENSION SPECIMENS

Section Type	Section No.	Compressive Yield Strength of Flats (ksi)	Laterally Supported Compress. Yield Str. (ksi)	Laterally Unsupported Compress. Yield Str. (ksi)	Laterally Unsupported Ultimate Compress. Strength (ksi)	Average Strain at Lat. Unsup. Ult. Compr. Strength (in/inx 10^{-3})	Local Buckling First Noted at Stress (ksi)	Tensile Yield Str. (ksi)	Tensile Ultimate Strength (ksi)
HRSK	C9			49.1	a	a	50.2		
10-37.0	C16			49.1	55.8	27.1	52.2		
Roll-	Strips	49.8	53.0						
formed	C7		56.3						
channel	C8		54.6						
	C9A		52.3						
	Strips							48.9	61.8
	T7*							47.9	59.4
	T8*							47.7	59.0
	T9*							47.8	60.0
HRSK	C21			52.0	55.4	16.3	52.8		
9-30.7	C22			51.2	a	a	53.8		
Roll-	Strips	48.1	54.0						
formed	C23		53.5						
joist	Strips							52.3	62.3
chord	T14*							50.0	61.7

* Achieved failure in central portion of specimen.

a Test not carried to ultimate compressive load.

Note: "Strips" indicates values obtained from stress - strain curves calculated from data from narrow strip specimens.

TABLE 7b (cont.)

Section Type	Section No.	Compressive Yield Strength of Flats (ksi)	Laterally Supported Compress. Yield Str. (ksi)	Laterally Unsupported Compress. Yield Str. (ksi)	Laterally Unsupported Ultimate Compress. Strength (ksi)	Average Strain at Lat. Unsup. Ult. Compr. Strength (in/in x 10^{-3})	Local Buckling First Noted at Stress (ksi)	Tensile Yield Str. (ksi)	Tensile Ultimate Strength (ksi)
16 gage	C10	42.2		44.7	44.7	3.4	b		
HR	C11	42.2		44.7	44.7	3.6	b		
press	C19	42.2	48.1						
braked	C20	42.2	47.1						
lipped angle	T13*							42.8	49.8
16 gage	C12	42.2	44.3[c]	41.7	42.5	4.9	42.0		
HR	C13	42.2	44.3[c]	42.7	42.7	> 2.6	42.0		
press braked channel	T11*							40.9	49.6
16 gage	C14	36.0		41.3	41.7	4.0	34.4[d]	38.9[e]	
CRK-	C15	36.0		39.3	41.6	4.1	32.8[d]	37.2[e]	
16-38.3	C17	36.0	41.7						
press	C18	36.0	41.6						
braked hat	T12*							42.4	50.2

* Achieved failure in central portion of specimen.
b Torsional buckling. Buckling became visible after maximum load.
c Estimated - no laterally unsupported full section test made for this section.
d Slight waving noticeable in simple lips.
e Simple lips and corners buckled outward.

TABLE 7c

PROPERTIES OF STUB COLUMN SPECIMENS

Section Type	Area (in.^{2})	I_x (in.^{4})	I_y (in.^{4})	L/r_y	Maximum Width to thickness ratios for Stiffened Elements	Maximum Width to thickness ratios for Unstiffened Elements	Q
HRSK 10-37.0 Roll-formed Channel	.58	.395	.082	5.6	11.3	6.8	1.00
HRSK 9-30.7 Roll-formed Joist Chord	.702	.646	.117	8.8	4.2	5.8	1.00
16 gage HR Press Braked Lipped Angle	.234	.100	.034	6.9	19.4	5.7	1.00
16 gage HR Press Braked Channel	.227	.057	.039	5.5	15.5	18.7	0.72
CRK16-38.3 Press Braked Hat	.337	.159	.126	6.7	28.7	8.0	1.00

Notes:

1. The effective length L is taken as 0.6 x the total length of specimens, assuming that the milled ends were nearly fixed.
2. Dimensions averaged from tensile and compressive full section specimens are shown in Figures 24 (c), (d), (e), (f), and (g).
3. I_x and I_y are the principal moments of inertia of the sections.

TABLE 8

CALCULATED TENSILE FULL SECTION YIELD STRENGTH

(1)	(2)	(3)	(4)	(5)	(6)	(7)	(8)	(9)	(10)	(11)	(12)
Specimen Description	Virgin Yield Strength Tens.	Compr.	Virgin Ult. Str.	Inside Radius Div. by Thick.	Ratio of Corner Area	Calc. Tensile Corner Yield Str.	Average Flat Tensile Yield Str.	Calc. Tensile Full Section Yield Str.	Full Section Tests Tensile Yield Str.	Compr. Yield Str.	Ult. Str.
	σ_y (ksi)	(ksi)	σ_u (ksi)	a/t	C	σ_{yc} (ksi)	σ_{yf} (ksi)	σ_{ys} (ksi)	(ksi)	(ksi)	(ksi)
CRK16-38.3 Press Braked Hat.	38.3	34.6	51.1	1.05	.082	63.5	37.9	40.0	39.4	37.8	48.8
HRSK16-37.5 Press Braked Hat.	37.5	40.5	49.0	1.00	.082	61.2	39.7	41.5	42.5	44.9	51.1
HRSK16-37.5 Roll-formed Track.	37.5	40.5	49.0	1.49	.17	56.9	43.8	46.0	45.6	51.0	
HRSK10-37.0 Roll-formed Channel.	37.0	38.5	57.5	.89	.148	74.7	45.6	49.9	47.8	55.4	59.5
HRSK9-30.7 Roll-formed Joist Chord.	30.7	32.0	52.9	1.48	.307	59.1	46.8	50.6	50.0	53.5	61.7

TABLE 9

AXIALLY LOADED, PIN-ENDED COLUMN
BUCKLING STRESSES

Column Cross Section	Spec No.	Buckling Stress (ksi)	L/r	Bolted or Riveted
Double HRSK10-37.0 Channels	CT1	47.8	36.8	B
	CT2	46.4	46.0	B
	CT3	45.9	55.2	B
	CT4	43.2	64.4	B
	CT5	43.8	64.4	B
	CT6	43.8	73.7	B
	CT7	43.1	64.4	R
	CT8	39.3	88.5	R
Double HRSK9-30.7 Joist Chords	CT9	47.5	42.0	B
	CT10	42.8	59.8	B
	CT11	34.0	76.3	B
	CT12	34.2	91.5	R
	CT13	41.2	77.3	R
	CT14	45.3	58.3	R
	CT15	47.6	39.3	R

TABLE 10

VALUES FOR THE STRENGTH COEFFICIENT k AND STRAIN HARDENING EXPONENT n FROM UNIAXIALLY PRESTRAINED TENSILE SPECIMENS

Material	k ksi.	n	Type of Specimens*
1. CRK16-38.3	68.6	.121	LT
	55.2	.100	TT
	42.7	.085	LC
	84.5	.163	TC
2. CRR16-36.4	81.9	.133	LT
	85.6	.173	TT
	75.8	.164	LC
	98.5	.192	TC
3. HRSK16-37.5	86.1	.152	LT
	77.6	.135	TT
	66.5	.102	LC
	98.0	.198	TC
4. HRR16-40.5	64.8	.121	LT
	79.5	.145	TT
	71.6	.148	LC
	88.1	.160	TC
5. HRSK10-37.0	127.5	.257	LT
	93.1	.220	TT
	73.7	.161	LC
	109.5	.203	TC

* LT = tested in tension in direction of prestrain,
TT = transverse tension,
LC = longitudinal compression, and
TC = transverse compression.

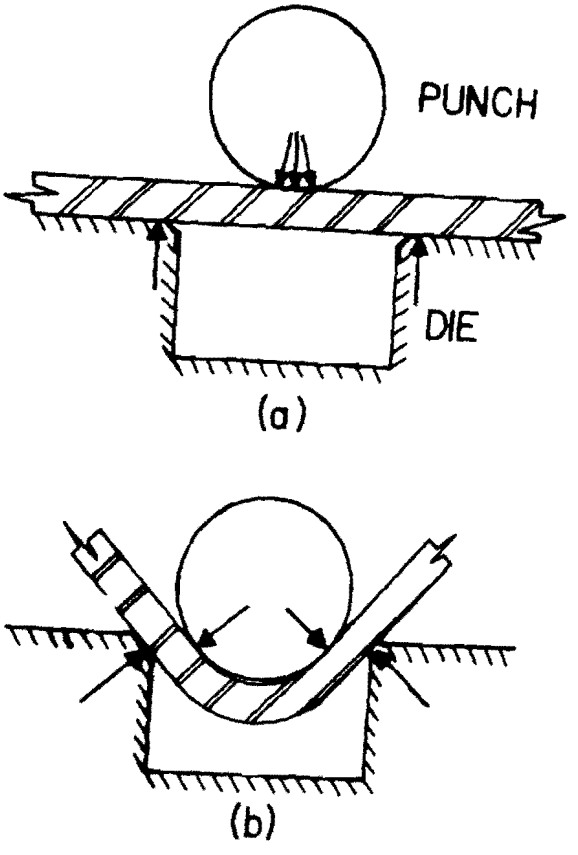

FIG. 1. AIR PRESS BRAKING

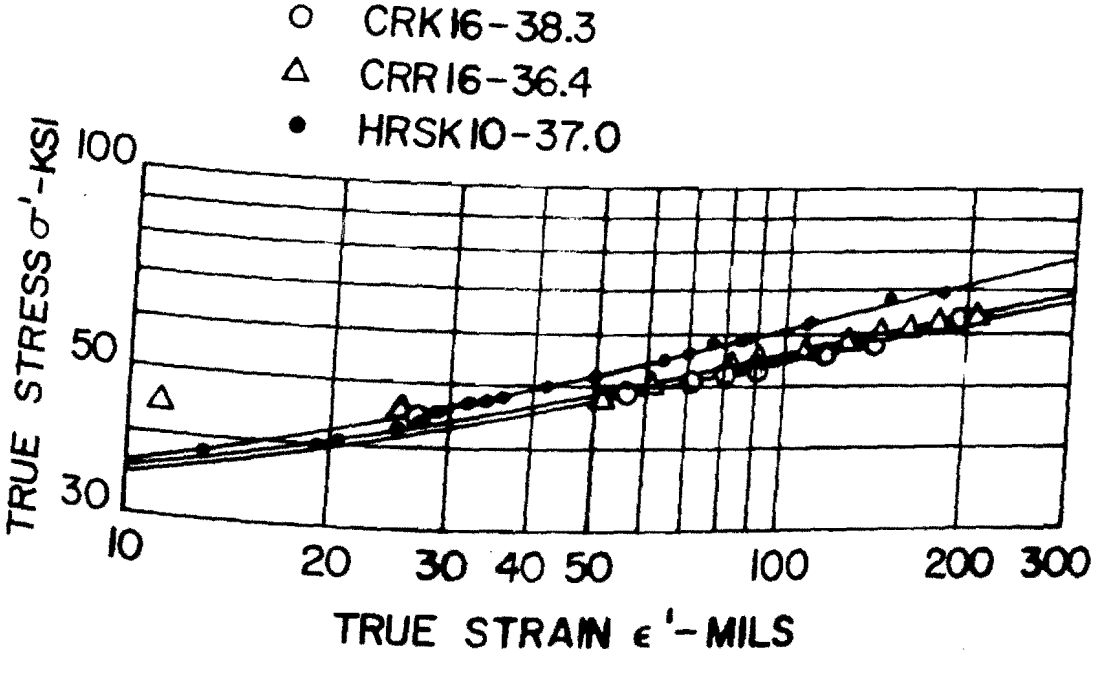

FIG. 2. TENSILE STRESS-STRAIN CURVES OF VIRGIN MATERIALS IN TERMS OF TRUE STRESS AND TRUE STRAIN.

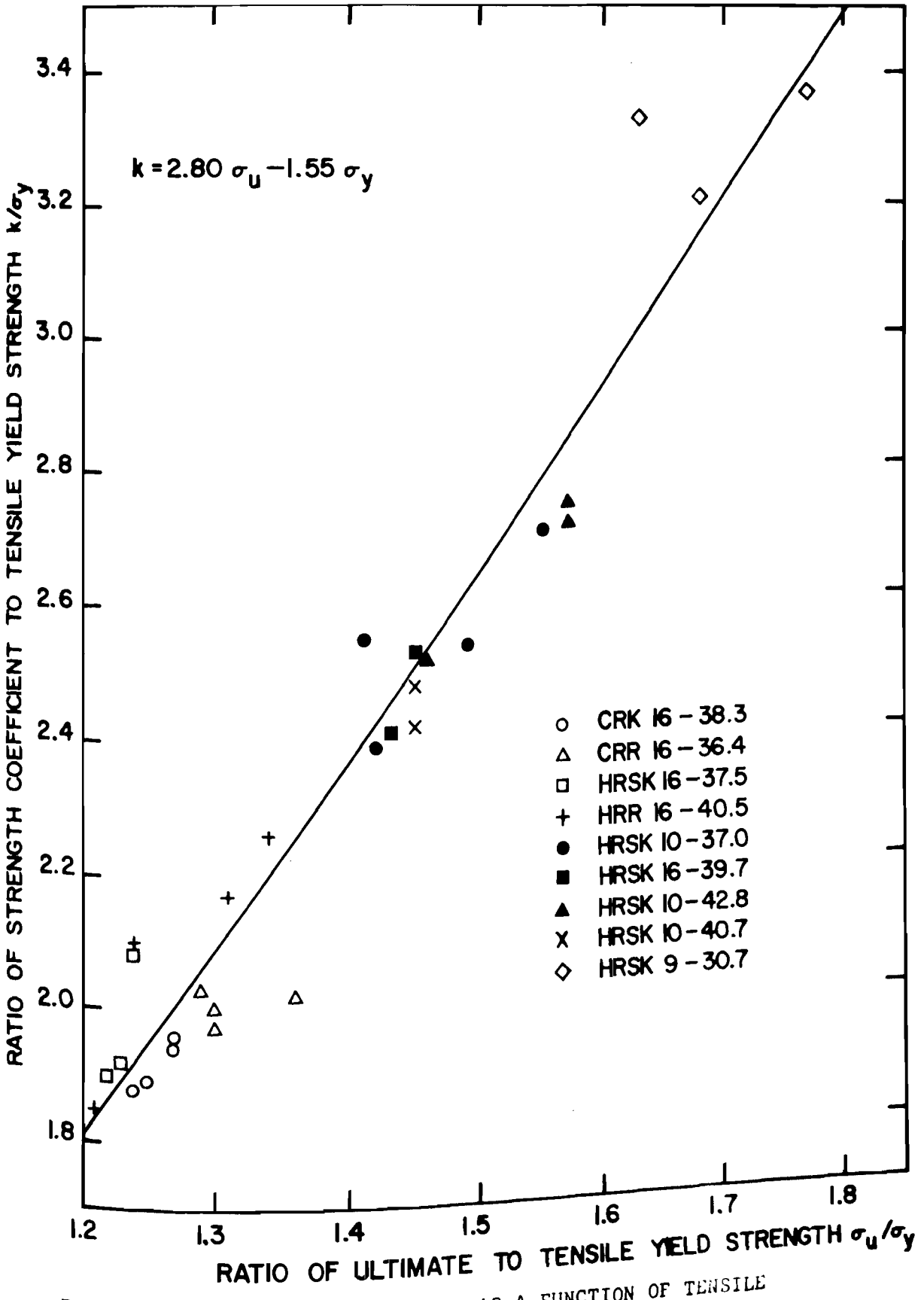

FIG. 3. STRENGTH COEFFICIENT k AS A FUNCTION OF TENSILE YIELD AND ULTIMATE STRENGTHS.

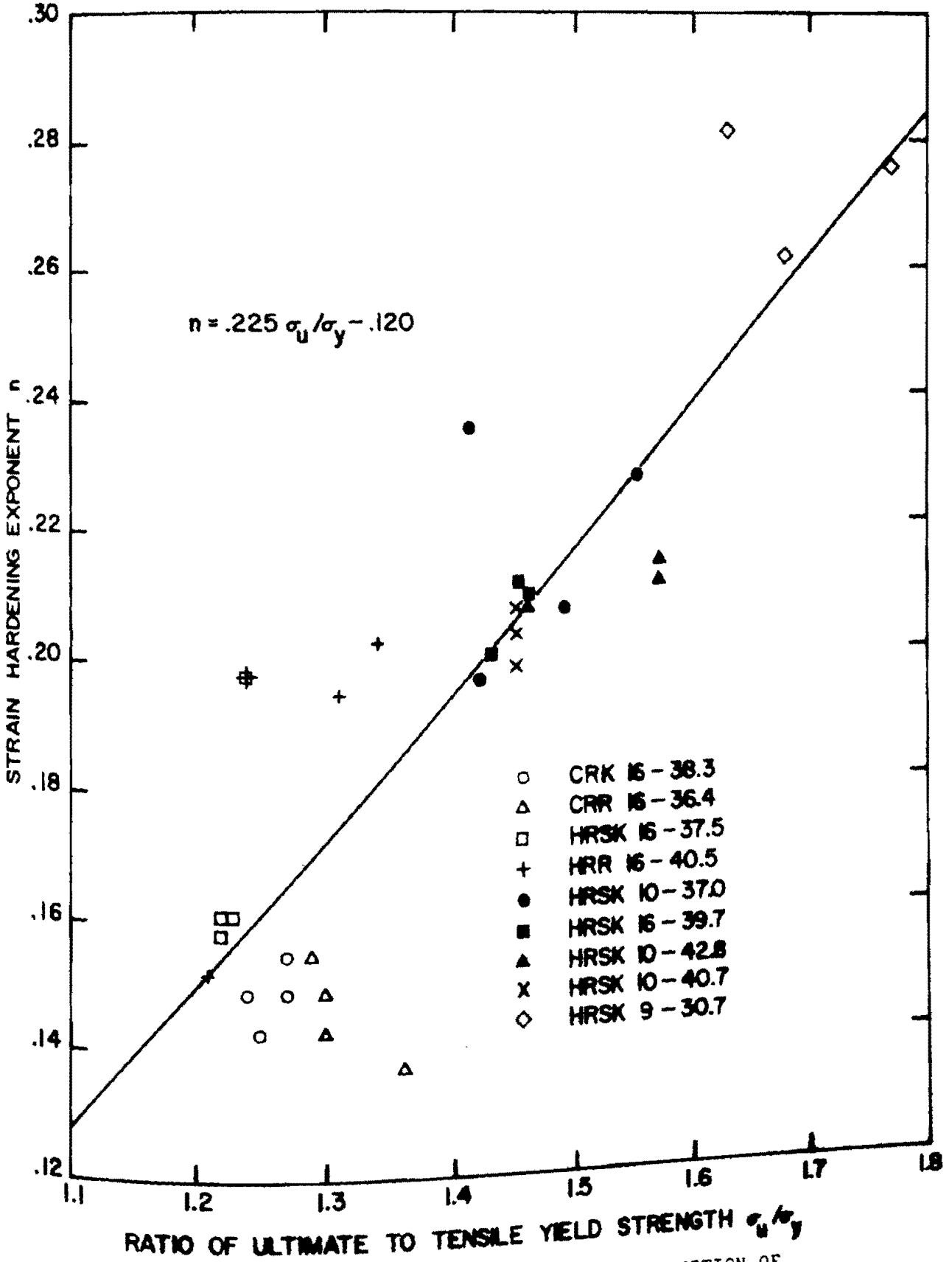

FIG. 4. STRAIN HARDENING EXPONENT n AS A FUNCTION OF TENSILE YIELD AND ULTIMATE STRENGTHS.

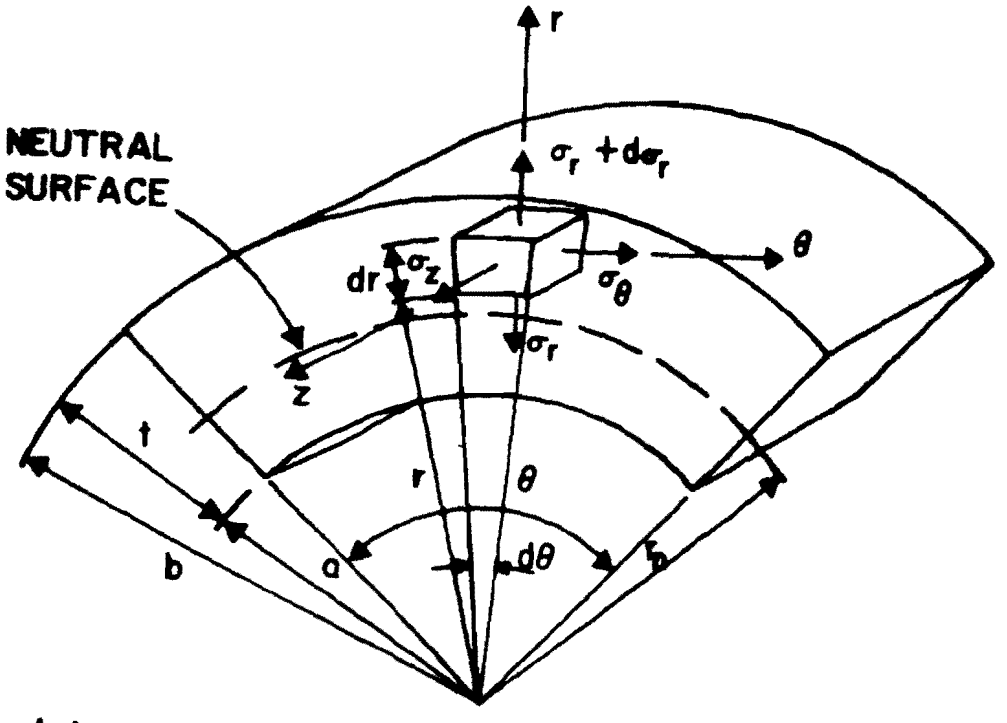

(a) STRESSES ON VOLUME ELEMENT OF PLASTICALLY DEFORMED PLATE

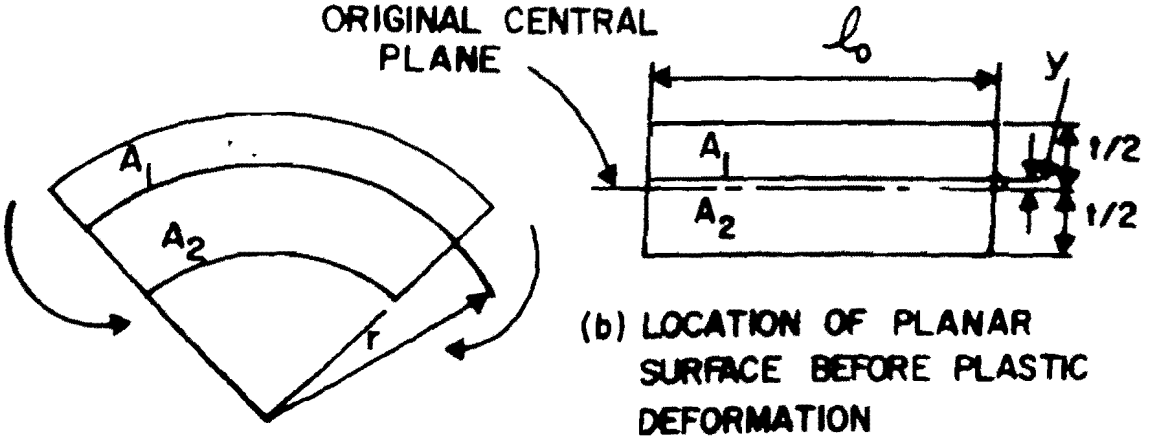

(b) LOCATION OF PLANAR SURFACE BEFORE PLASTIC DEFORMATION

(c) RADIUS TO SURFACE AFTER DEFORMATION

FIG. 5. WIDE PLATE PLASTICALLY DEFORMED BY PURE FLEXURAL LOADING.

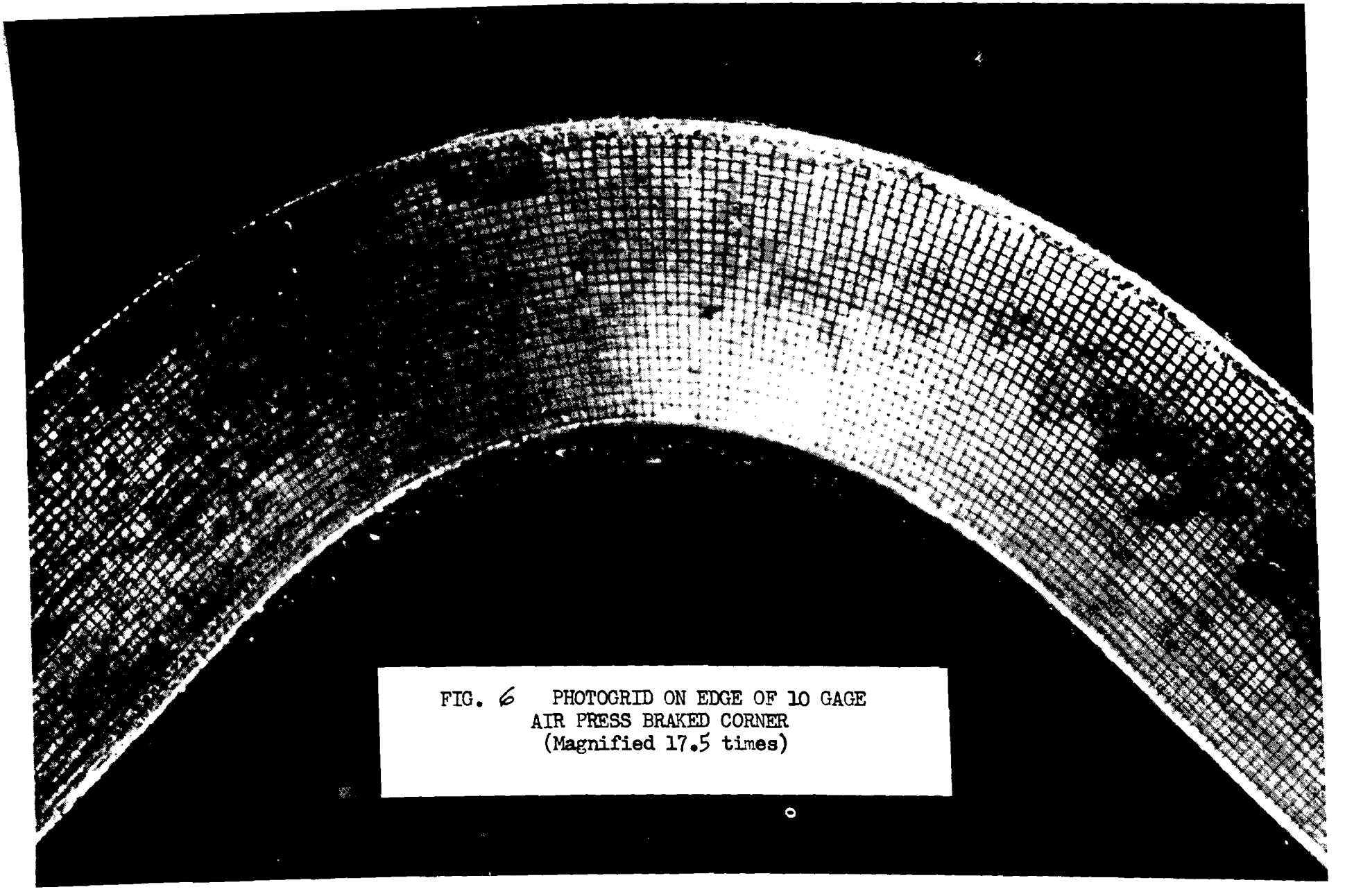

FIG. 6 PHOTOGRID ON EDGE OF 10 GAGE
AIR PRESS BRAKED CORNER
(Magnified 17.5 times)

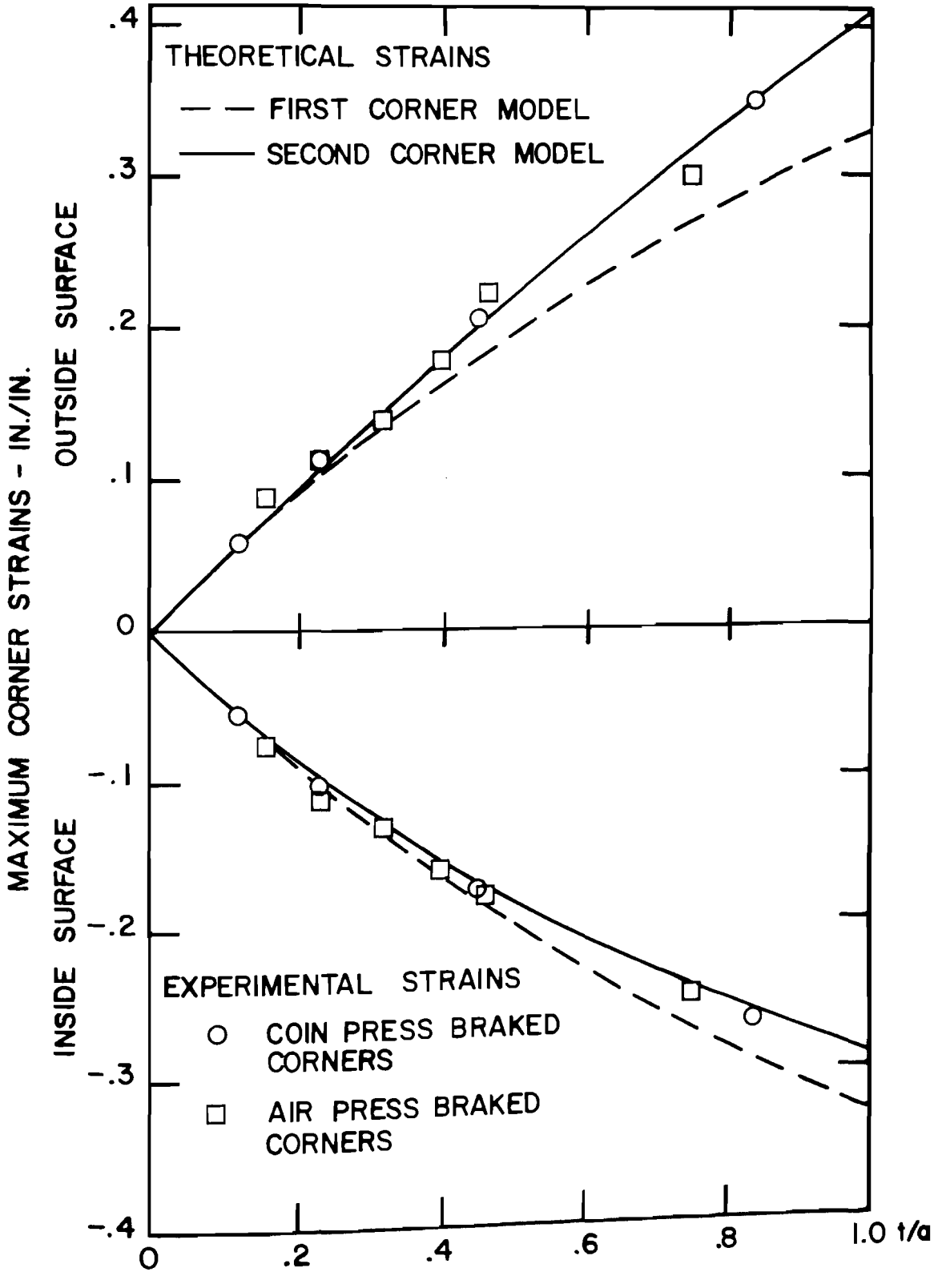

FIGURE 7 – MAXIMUM CORNER STRAINS BY THE PHOTOGRID METHOD

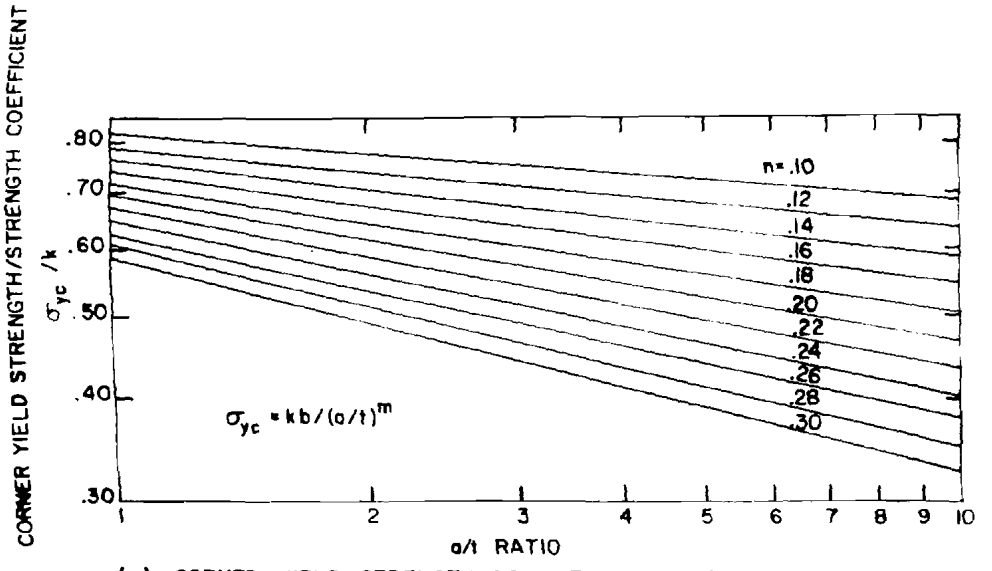

(a) CORNER YIELD STRENGTH AS A FUNCTION OF THE a/t RATIO

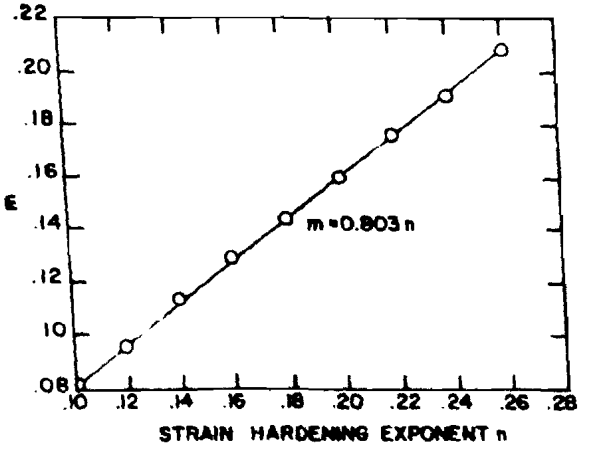

(b) THE CONSTANT m AS A FUNCTION OF THE STRAIN HARDENING EXPONENT n

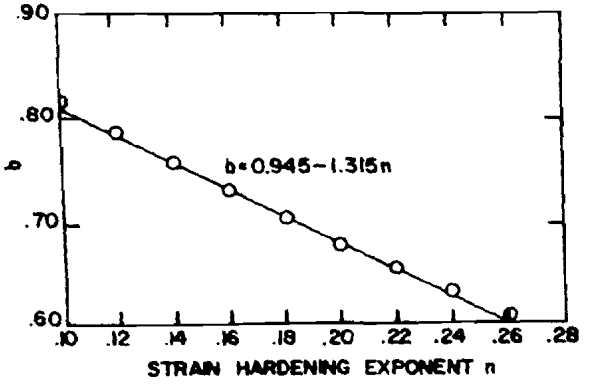

(c) THE CONSTANT b AS A FUNCTION OF THE STRAIN HARDENING EXPONENT n

FIG. 8. YIELD STRENGTH FOR CORNER MODEL SUBJECTED TO PURE FLEXURAL LOADS.

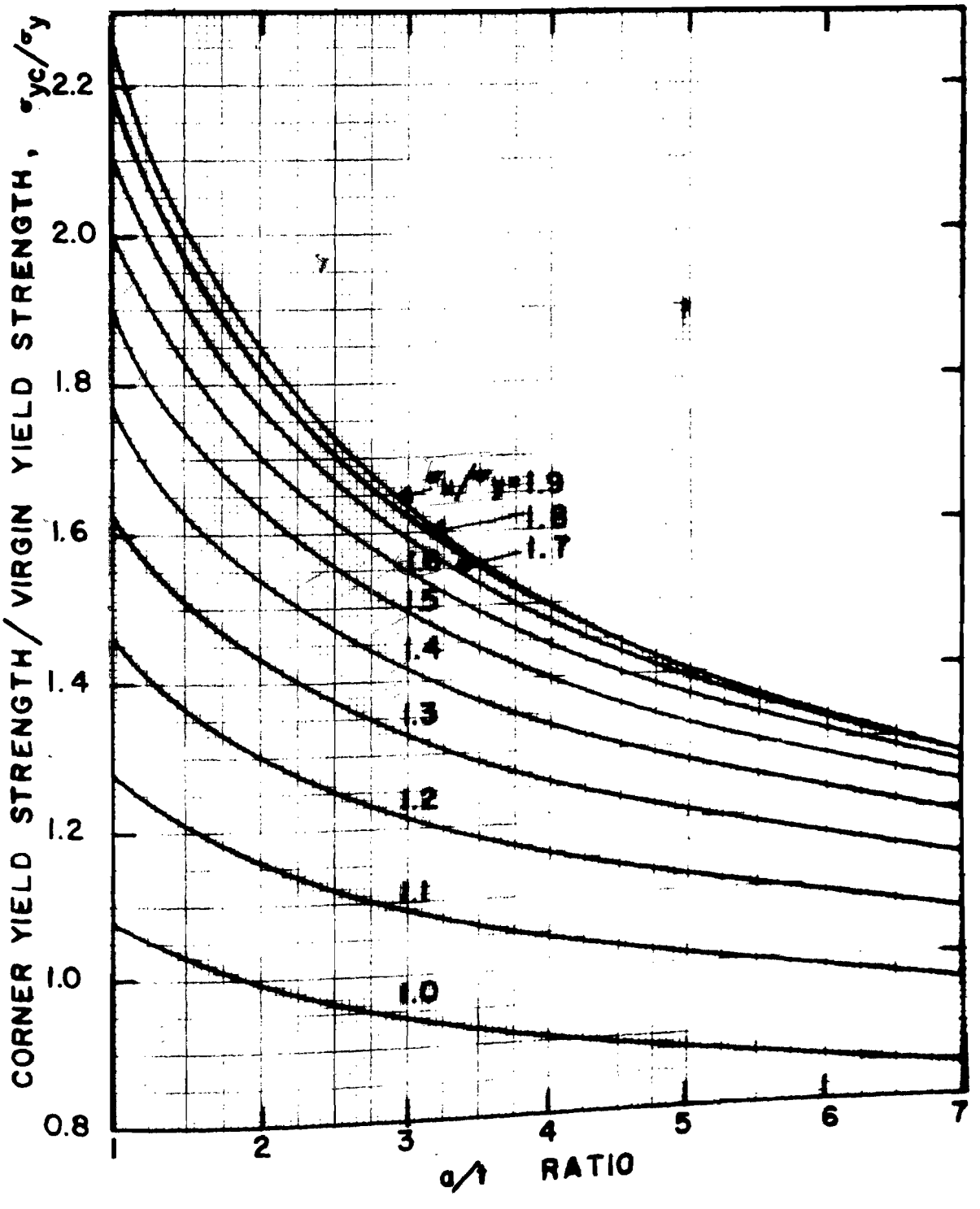

FIG. 8(d). CORNER YIELD STRENGTH DESIGN CHART.
(BASED ON THE SECOND CORNER MODEL).

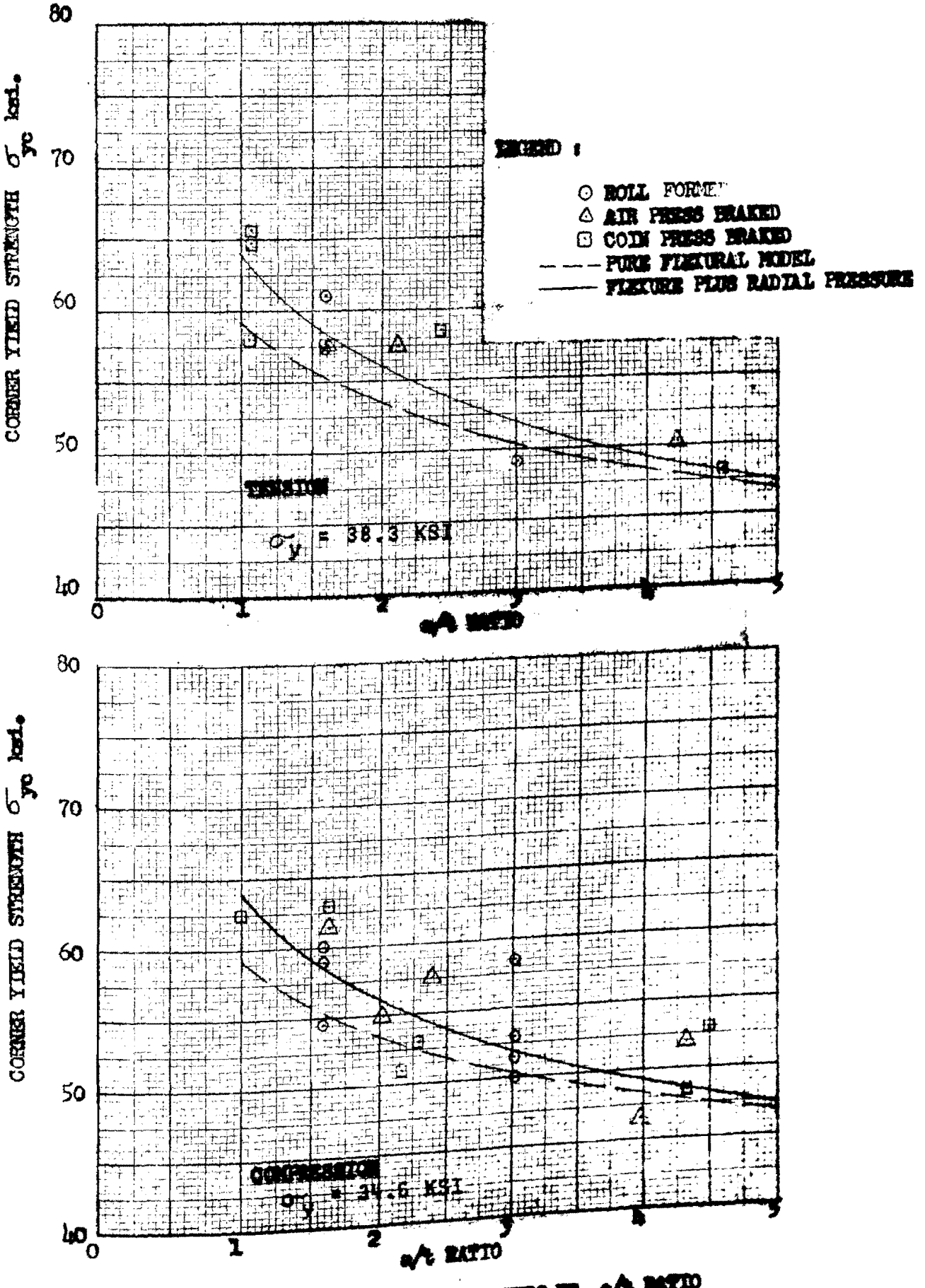

FIG. 9. YIELD STRENGTH OF CORNERS VS. σ/t RATIO
(CHK 16-36.3)

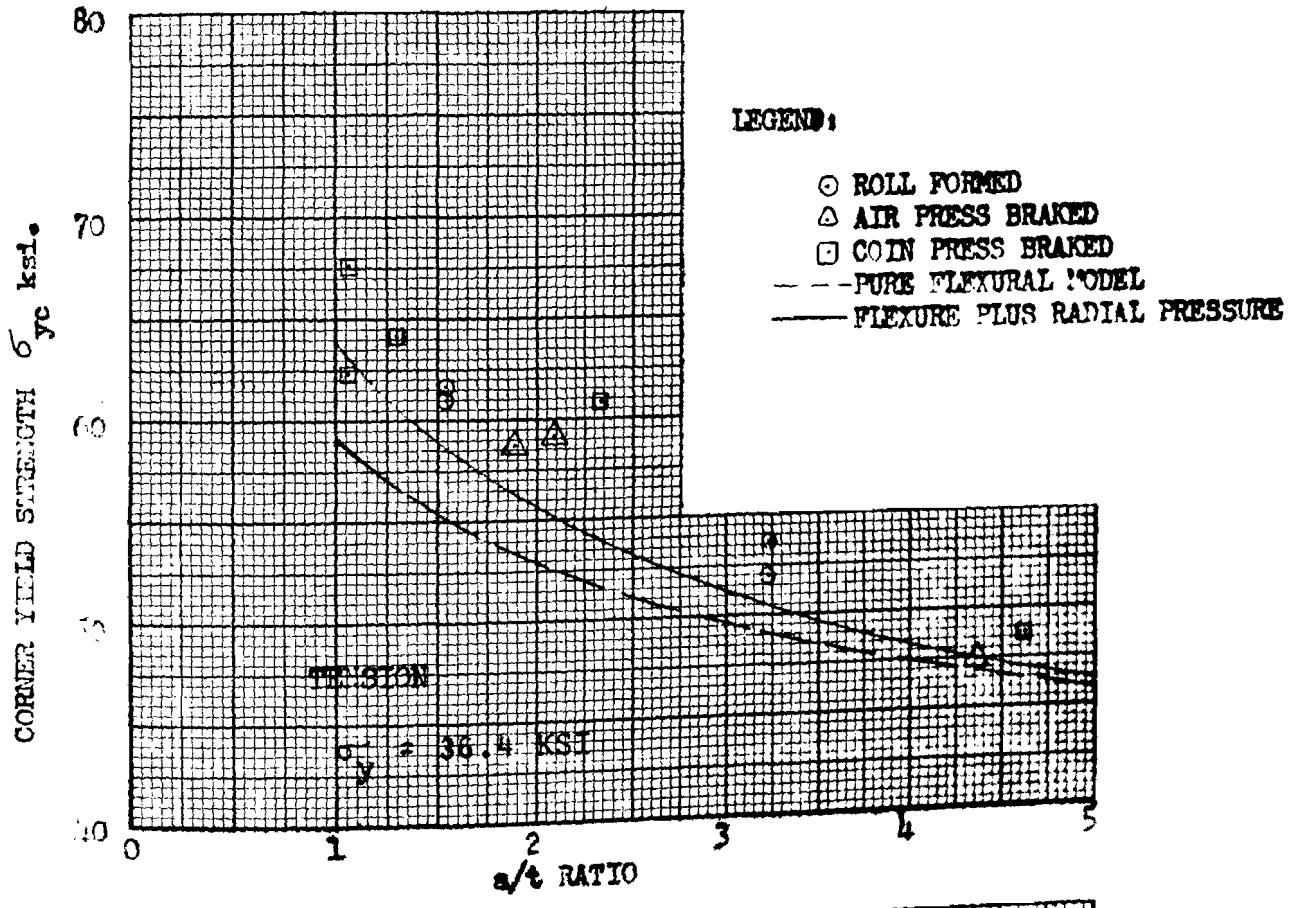

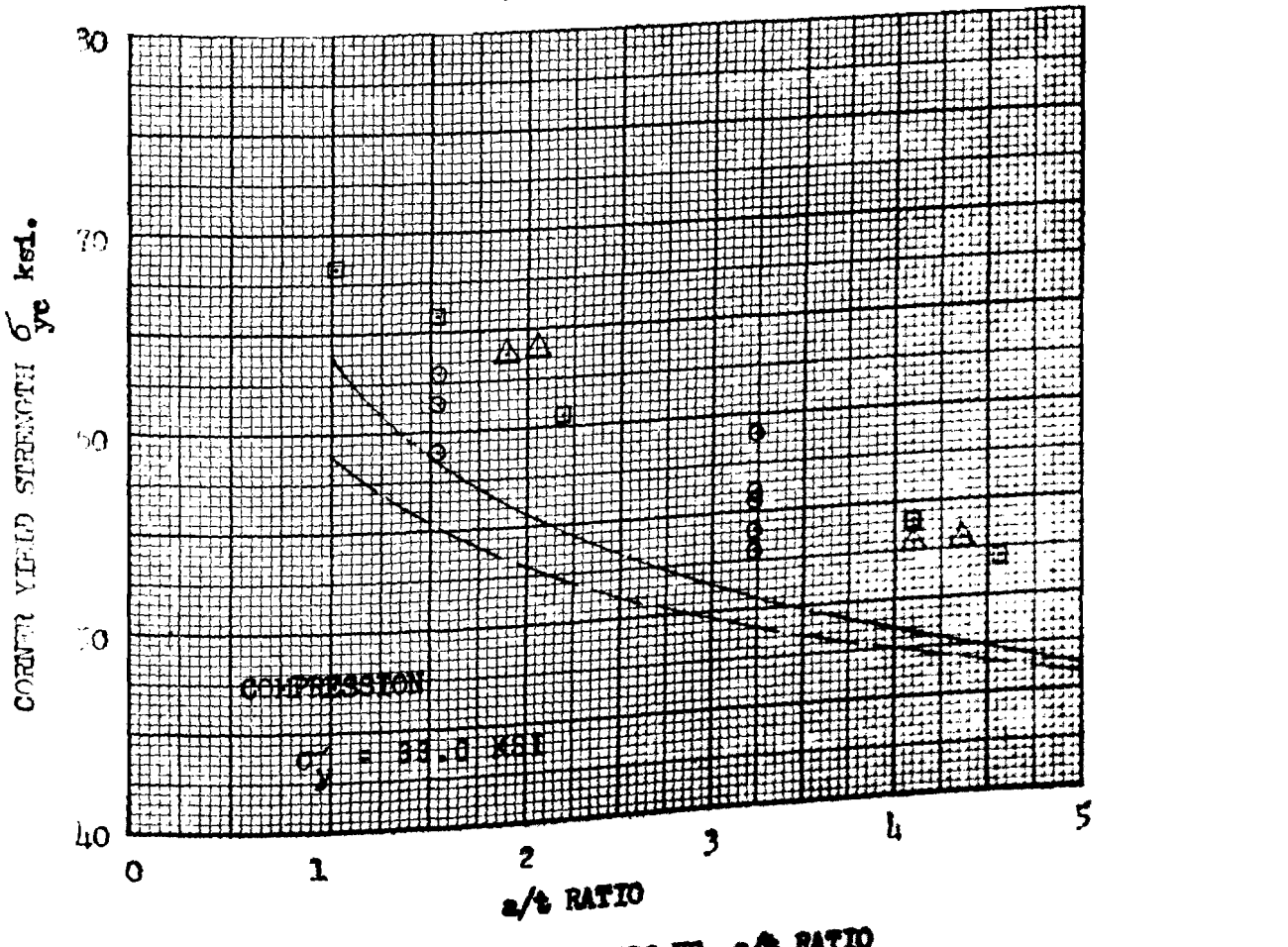

FIG. 10. YIELD STRENGTH OF CORNERS VS. a/t RATIO

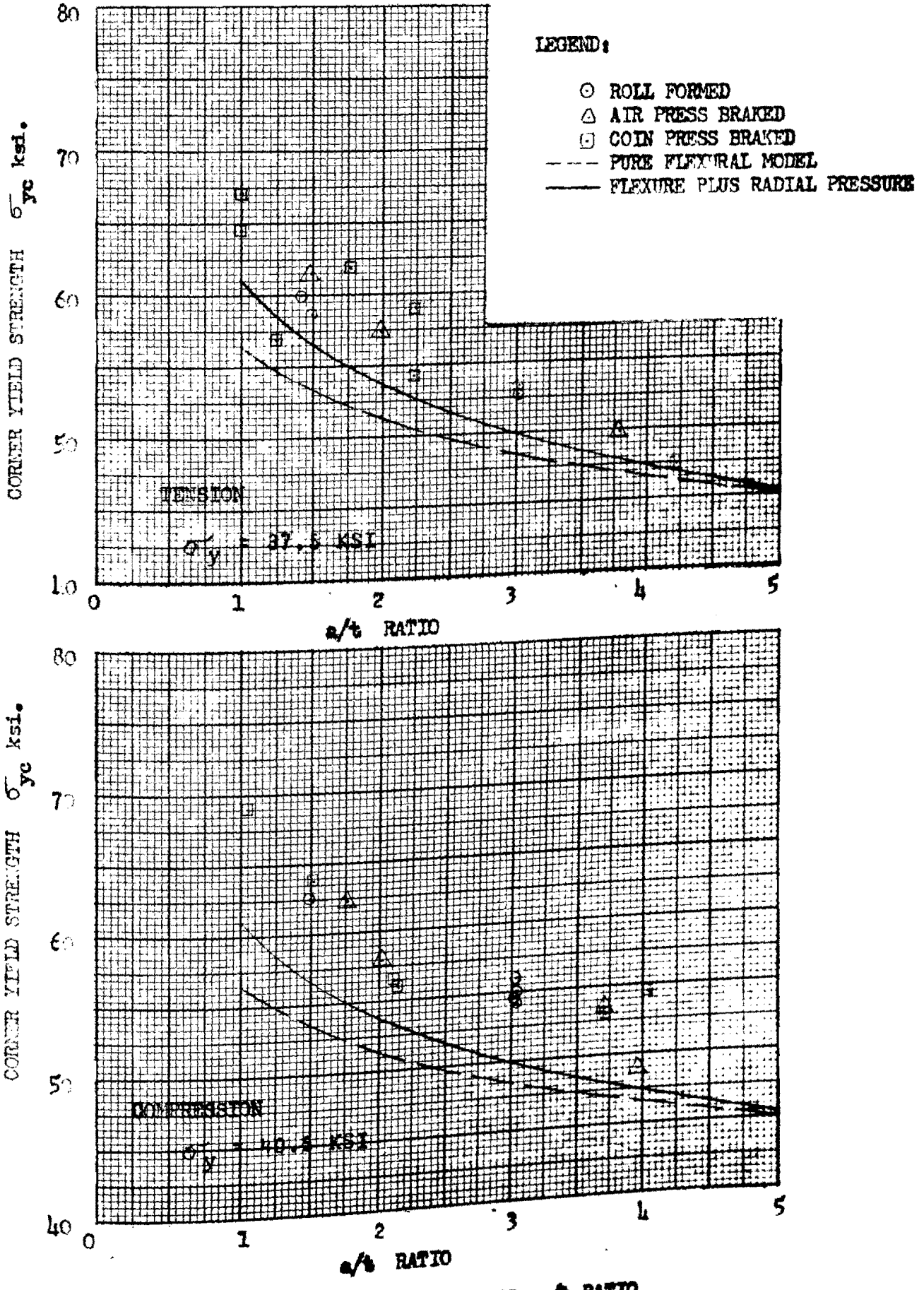

FIG. 11. YIELD STRENGTH OF CORNERS VS. a/t RATIO

(HS50D6-37.5)

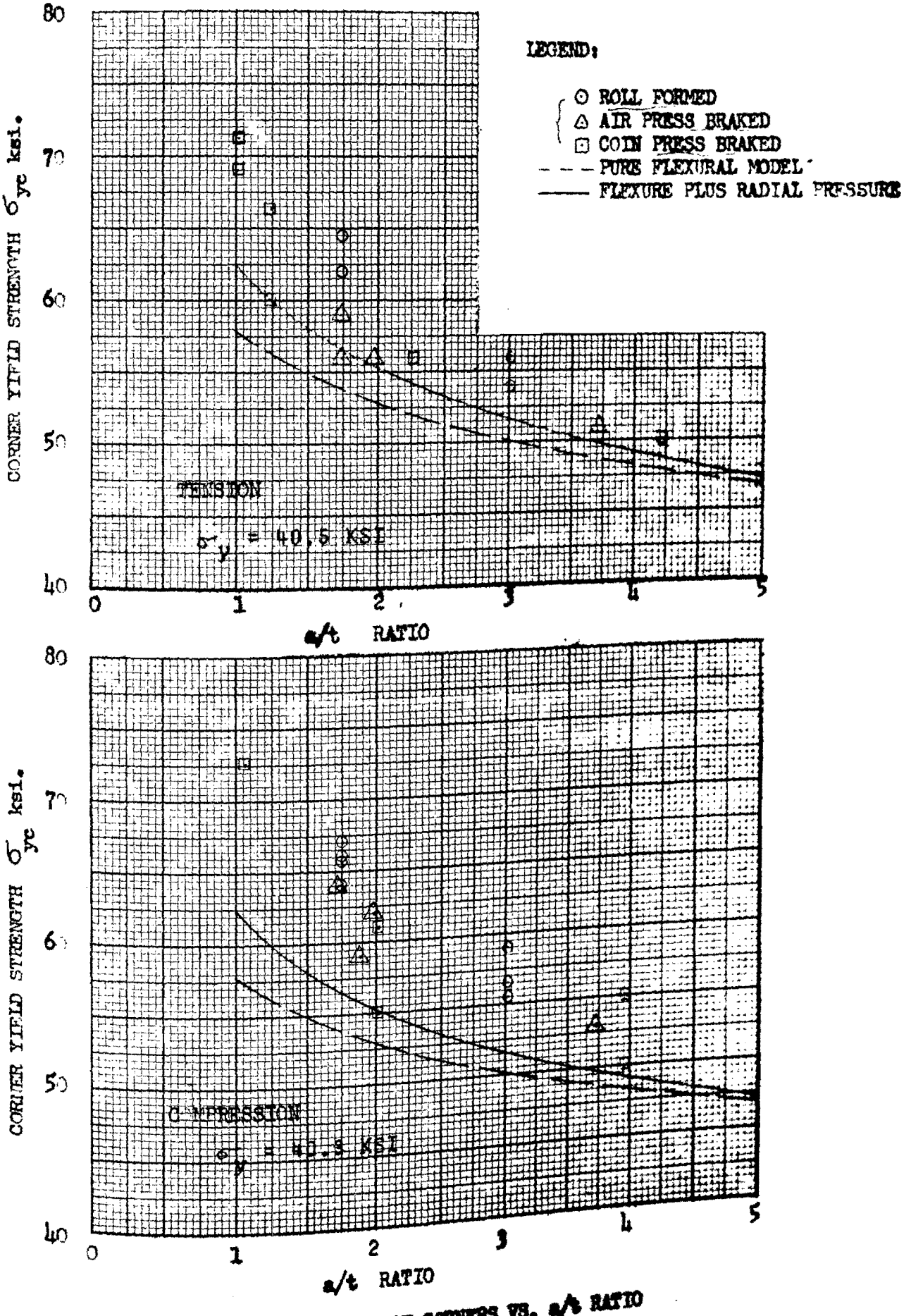

FIG. 12. YIELD STRENGTH OF CORNERS VS. a/t RATIO
(HRR 16-40.5)

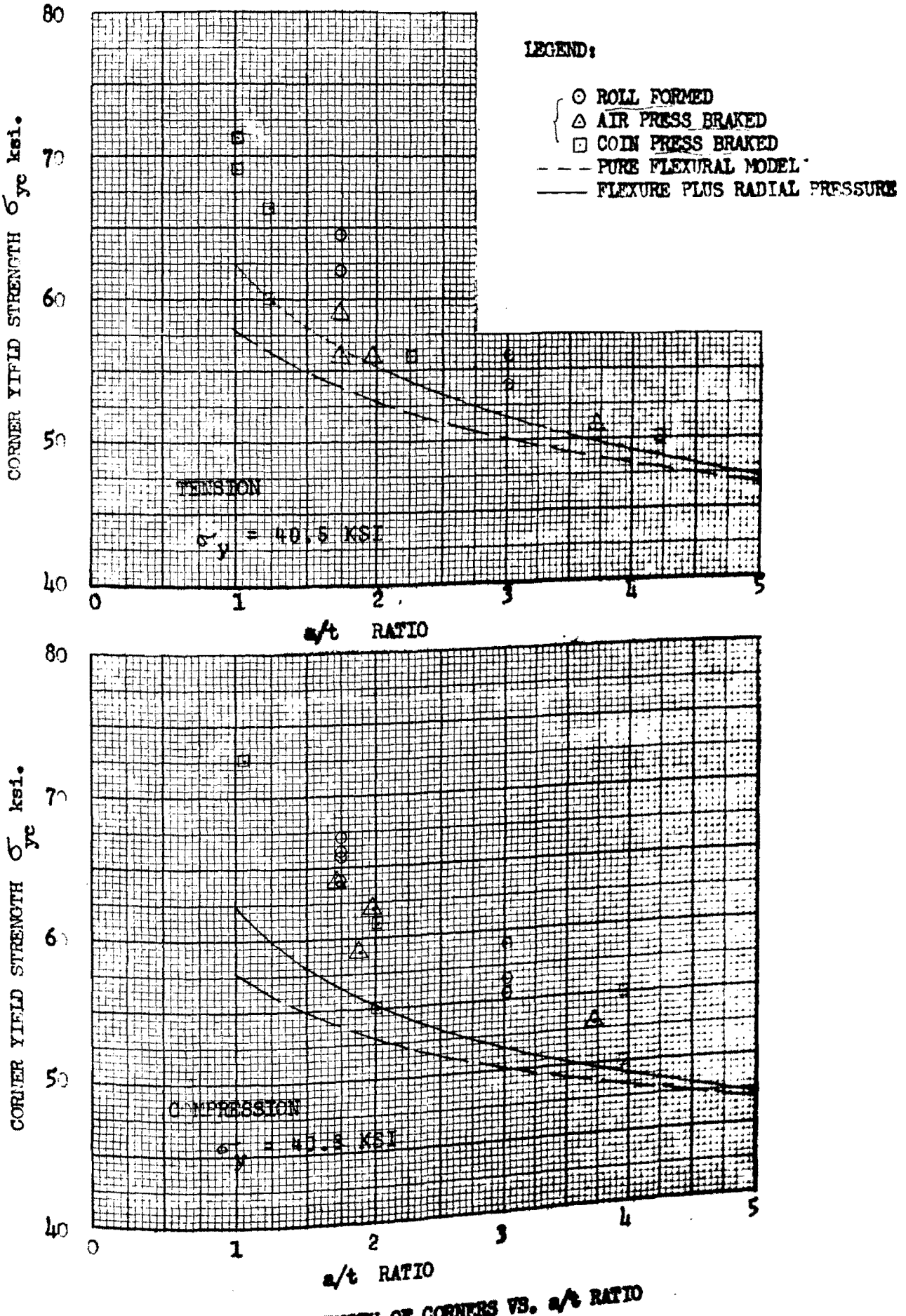

FIG. 12. YIELD STRENGTH OF CORNERS VS. a/t RATIO
(HRR 16-40.5)

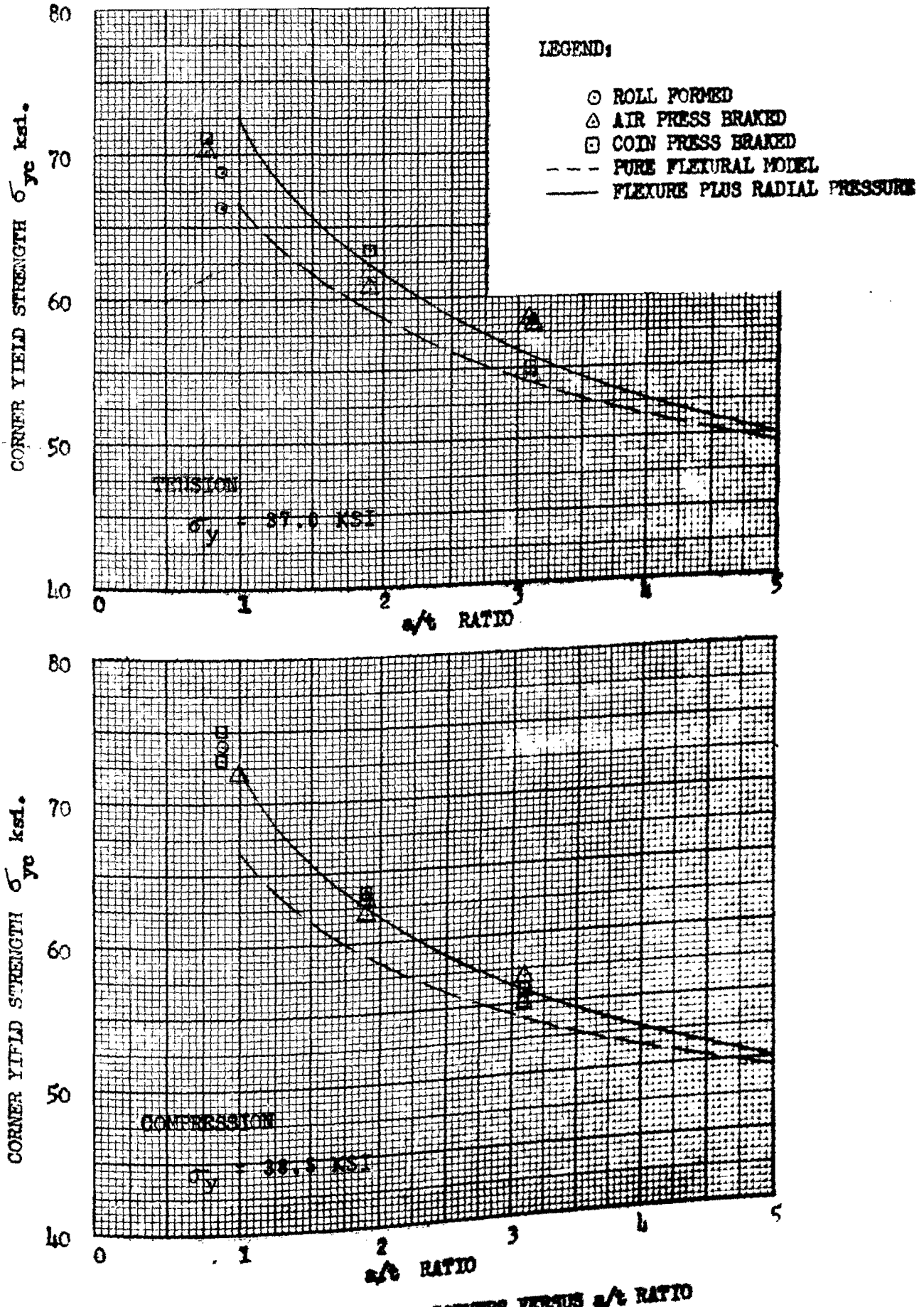

FIG. 13. YIELD STRENGTH OF CORNERS VERSUS B/t RATIO (HRSK 10-37.0)

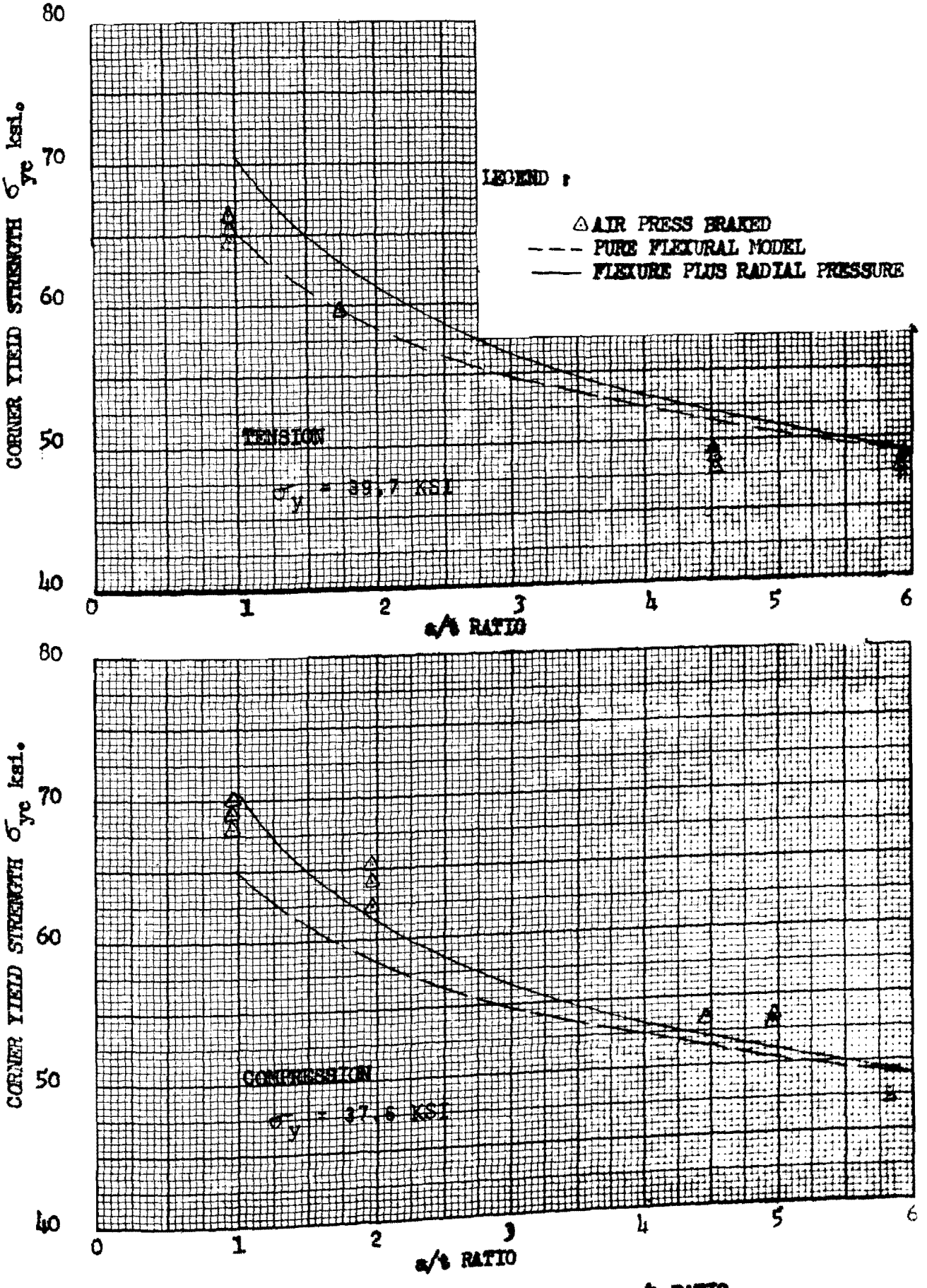

FIG. 14. YIELD STRENGTH OF CORNERS VS. a/t RATIO
(HRSK 16-39.7)

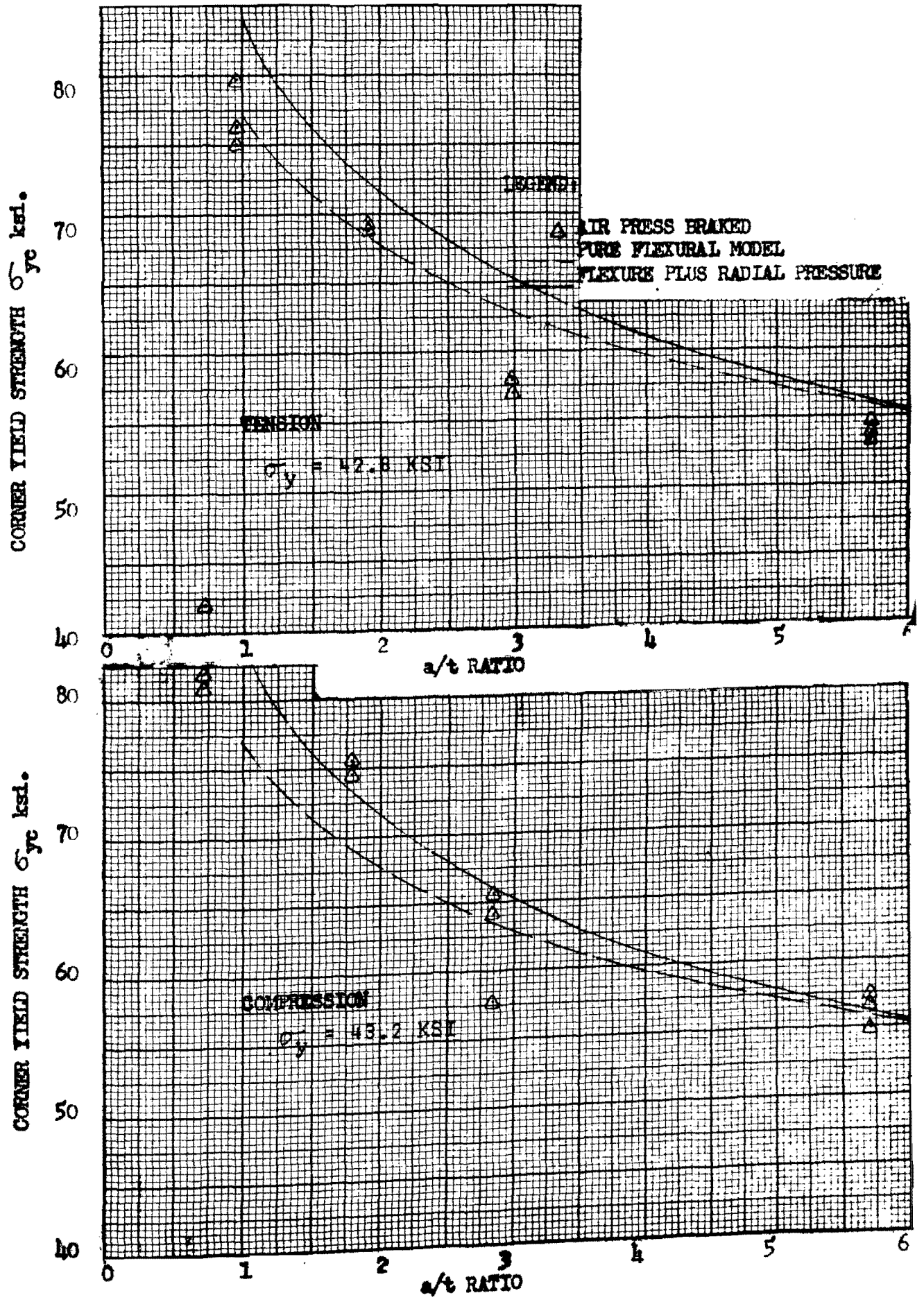

FIG. 15. YIELD STRENGTH OF CORNERS VS. a/t RATIO
(HRSM 10-42.8)

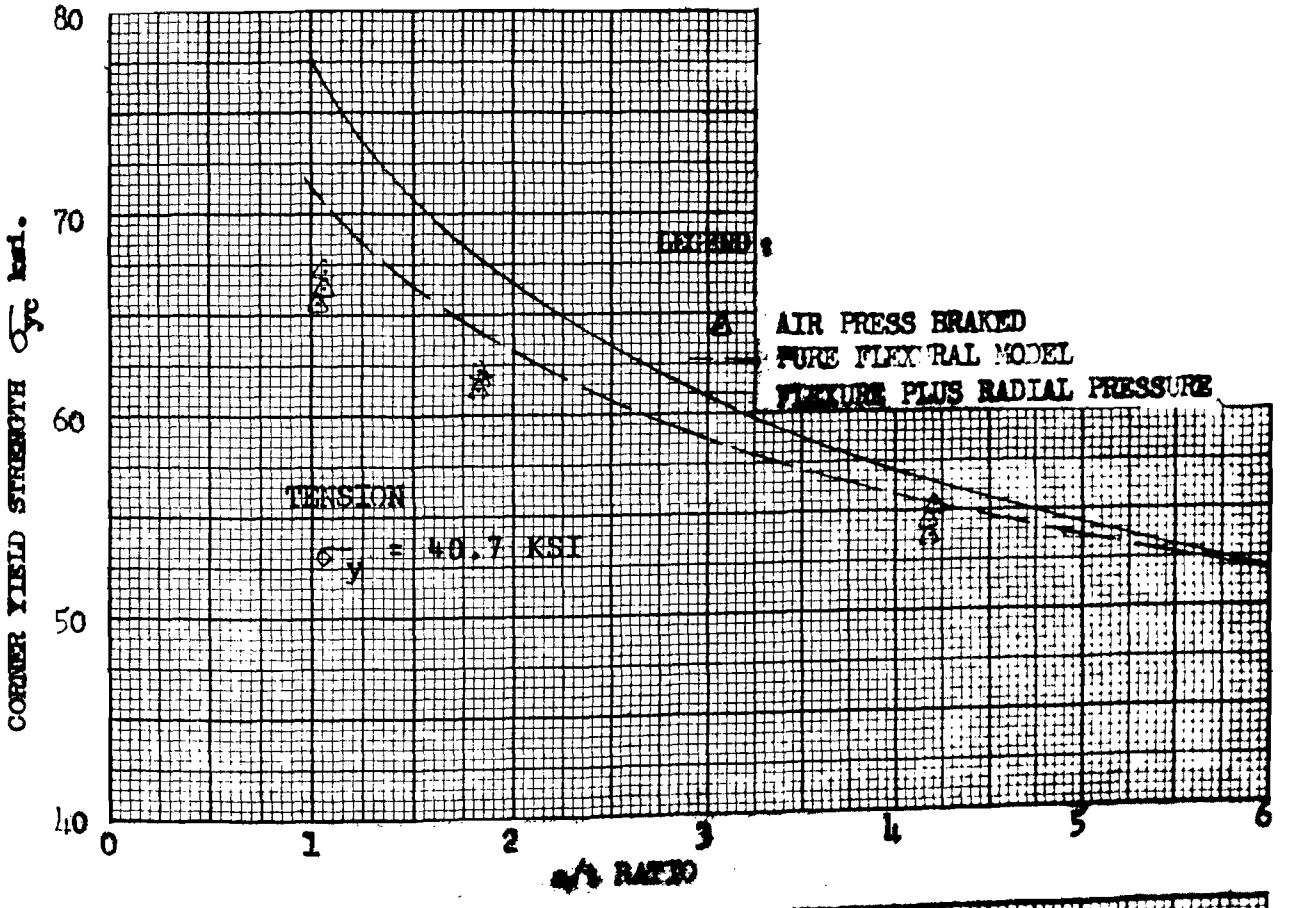

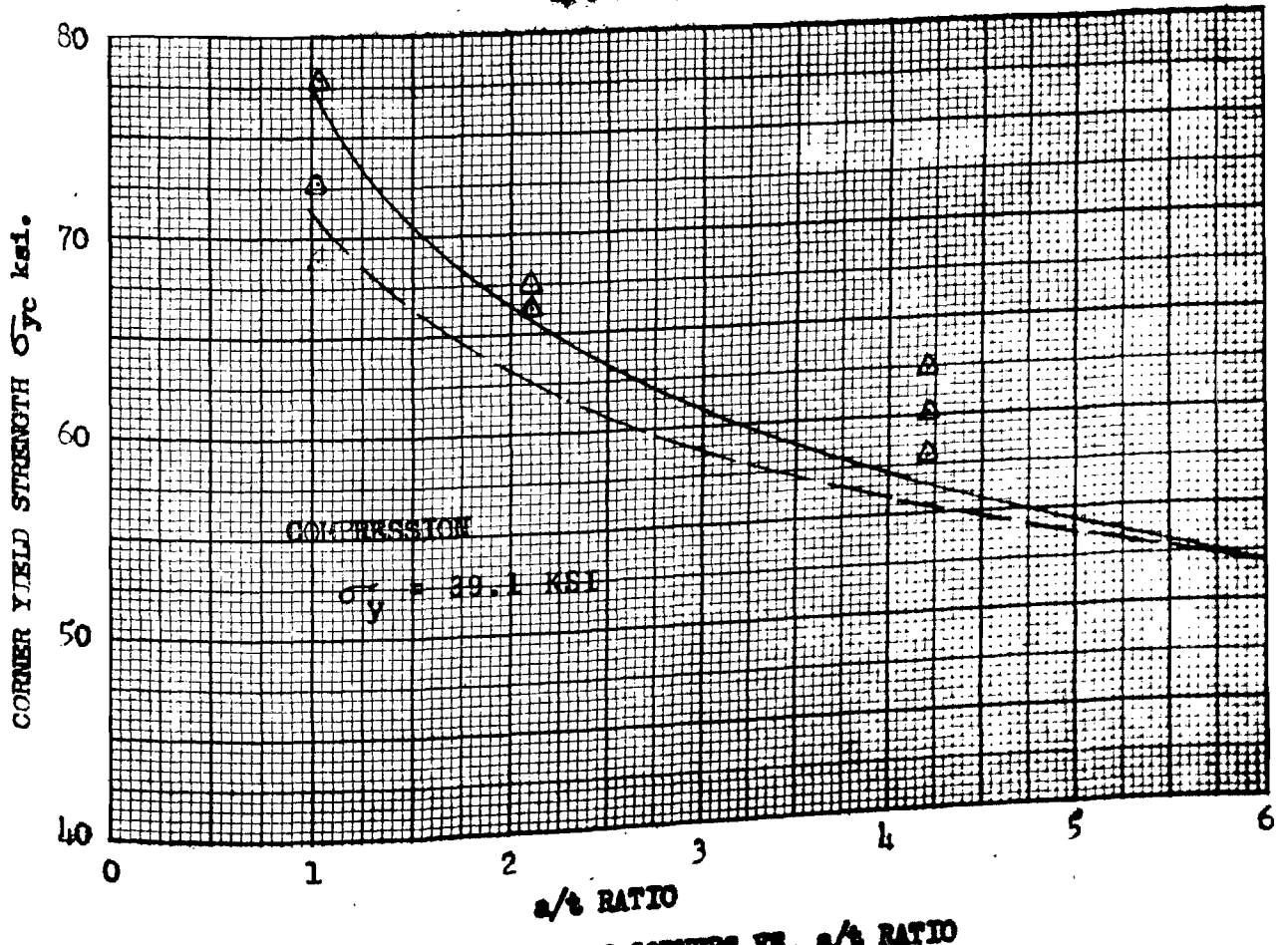

FIG. 16. YIELD STRENGTH OF CORNERS VS. a/t RATIO

(HRSK 16-40.7)

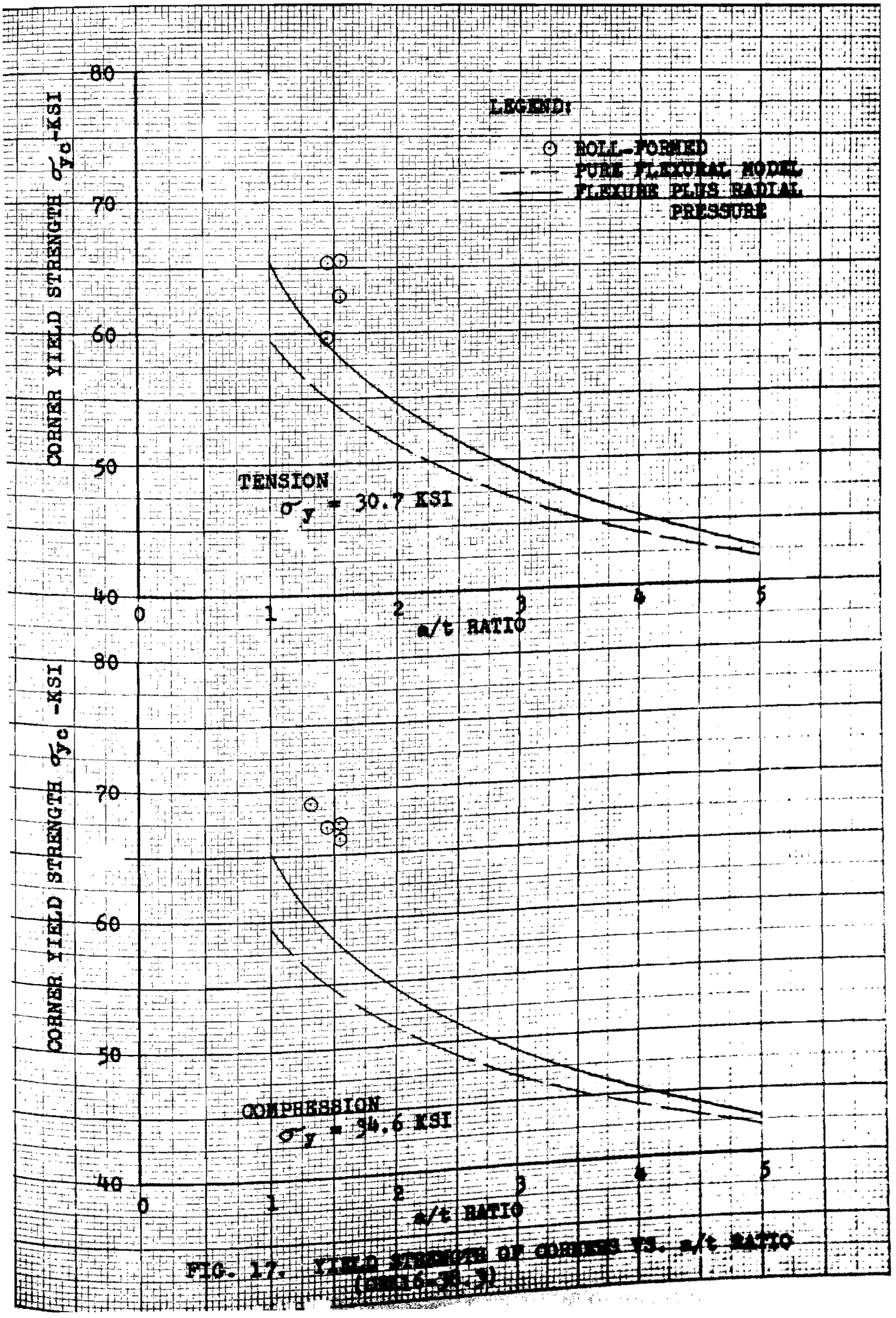

FIG. 17. YIELD STRENGTH OF CORNERS VS. a/t RATIO
(SAMPLE-36-3)

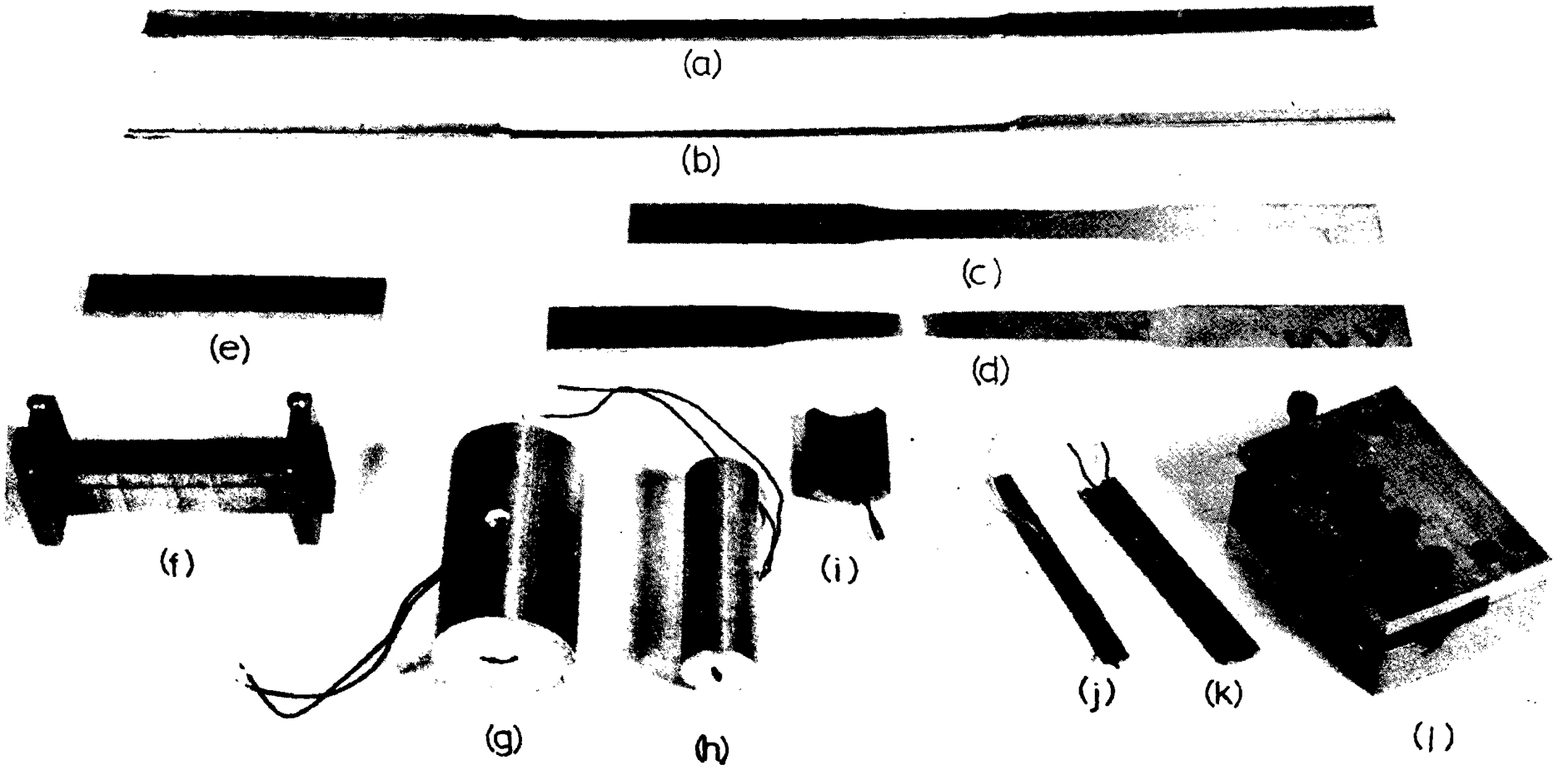

FIG. 18. TEST SPECIMENS. (a) TENSILE SPECIMEN-INSIDE RADIUS=1/4 IN., (b) TENSILE SPECIMEN-RADIUS=1/8 IN., (c) STANDARD FLAT TENSILE SPECIMEN, (d) FLAT TENSILE SPECIMEN AFTER TESTING, (e) FLAT COMPRESSIVE SPECIMEN, (f) JIG FOR COMPRESSIVE SPECIMEN, (g) AND (h) COMPRESSIVE CORNER SPECIMENS CAST IN HYDROSTONE, (i), (j), AND (k) COMPRESSIVE CORNER SPECIMENS OF 7/16, 1/8, AND 1/4 IN. RADII, WITH FOIL TYPE SR-4 STRAIN GAGES, (l) STEEL JIG FOR COMPRESSIVE CORNER SPECIMENS.

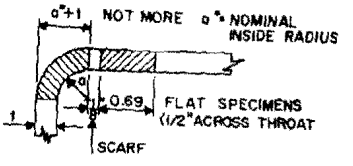

(a) CROSS SECTIONAL DIMENSIONS OF SPECIMENS

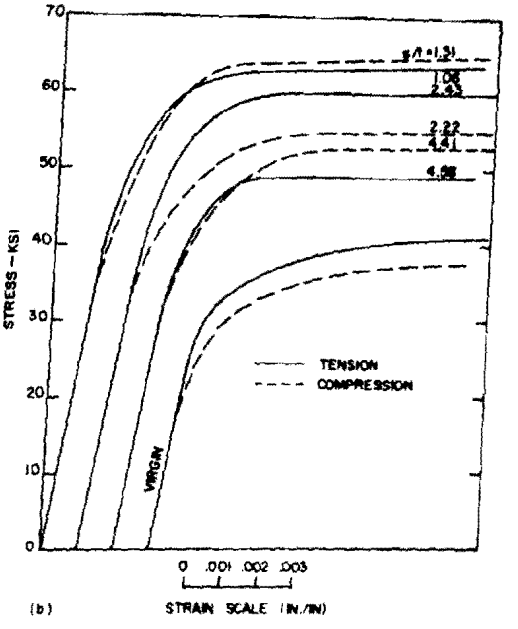

(b)

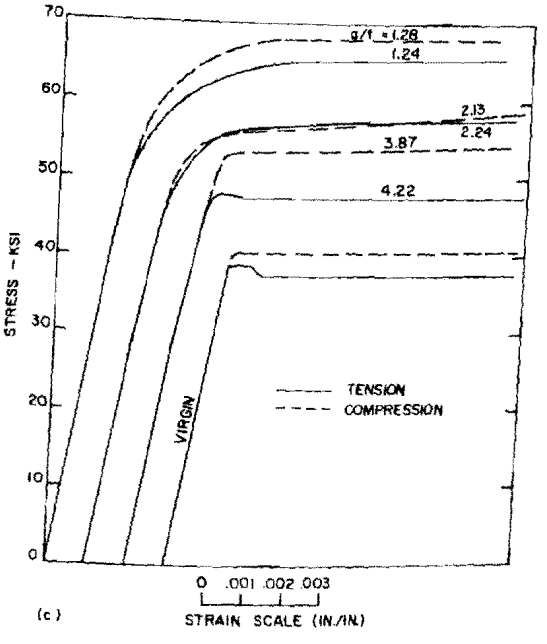

(c)

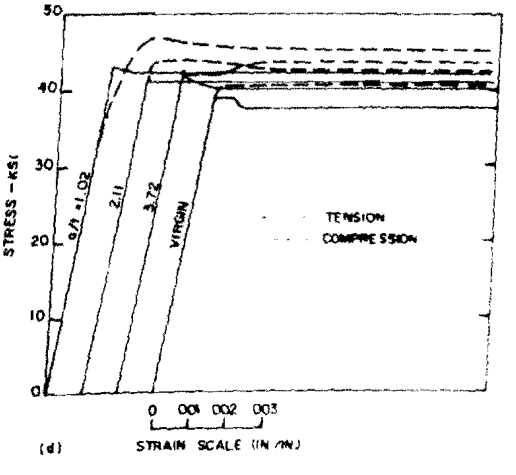

(d)

FIG. 19. TESTS OF CORNERS AND ADJACENT FLATS FROM COIN PRESS BRAKED ANGLES. (a) CROSS SECTIONAL DIMENSIONS OF SPECIMENS. (b) CRK16-38.3 AND (c) HRSK16-TYPICAL STRESS-STRAIN CURVES FOR (b) CRK16-38.3 AND (c) HRSK16-37.5 CORNERS. (d) STRESS-STRAIN CURVES FOR HRSK16-37.5 FLATS.

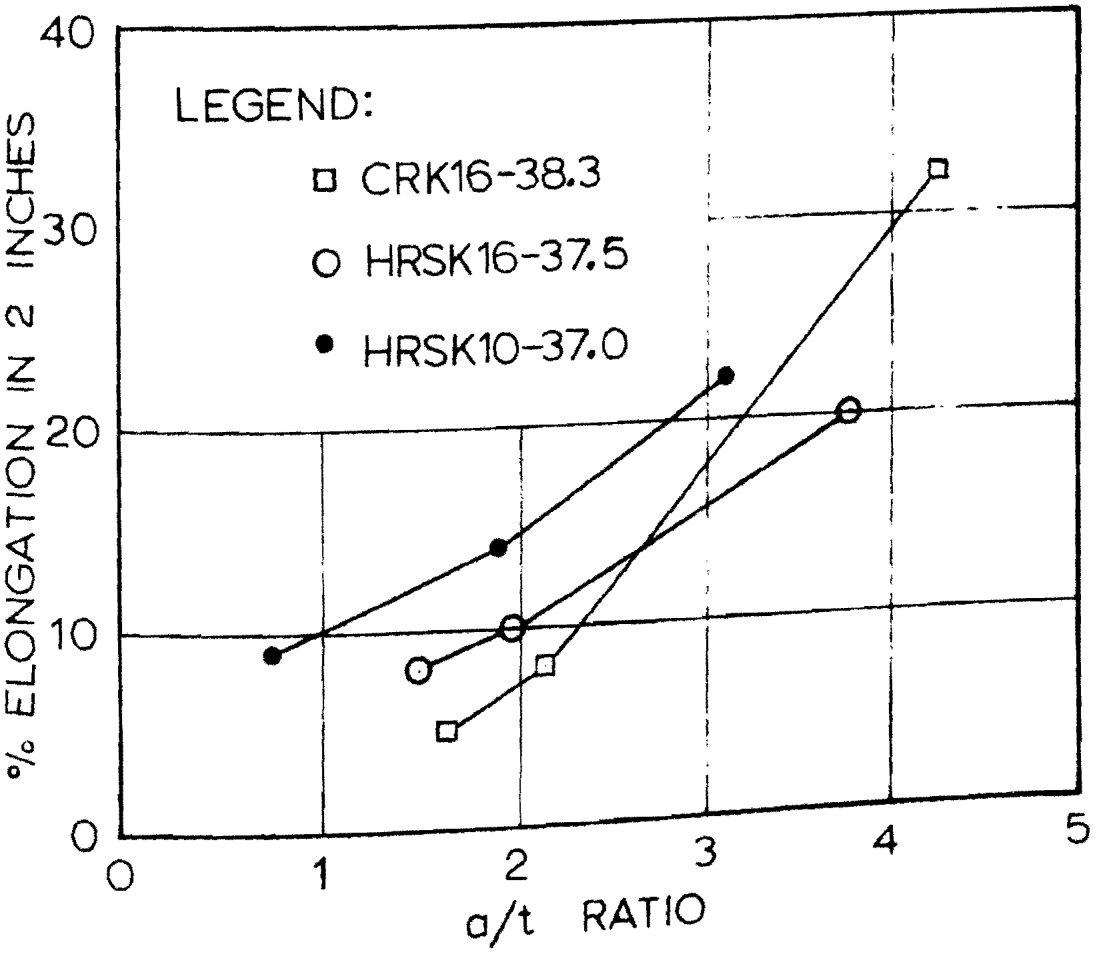

FIG. 20. PERCENT ELONGATION FOR CORNERS.

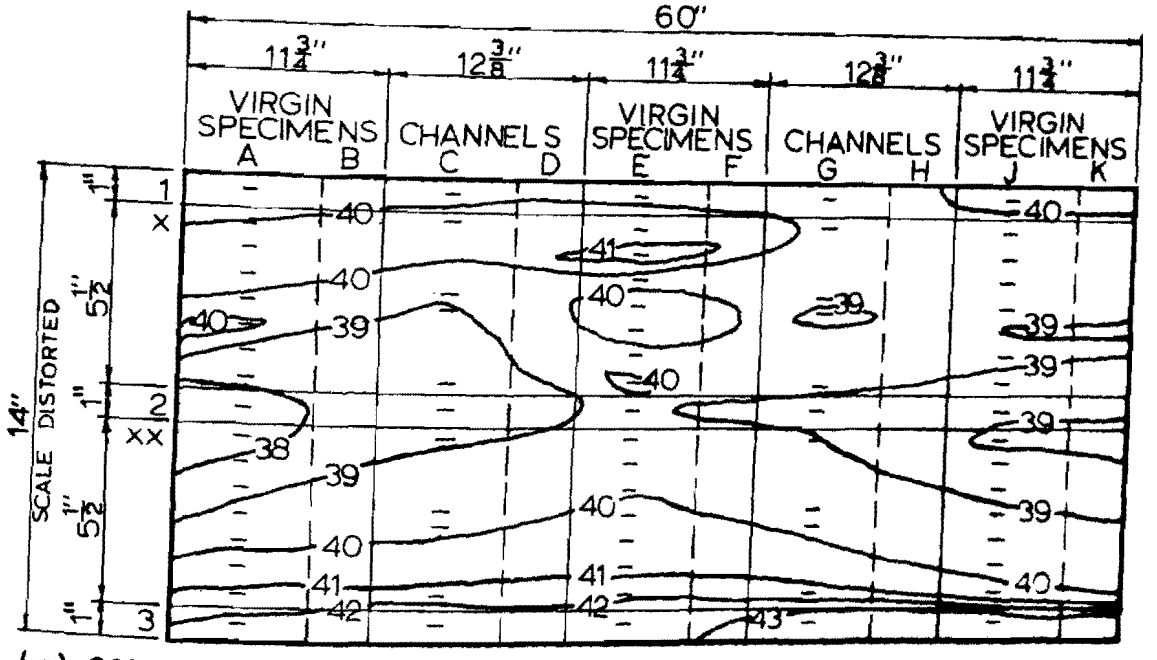

(a) CONTOUR VARIATION OF TENSILE YIELD STRENGTH (KSI) IN VIRGIN 14" X 60" HRSK 10-37.0 SHEET

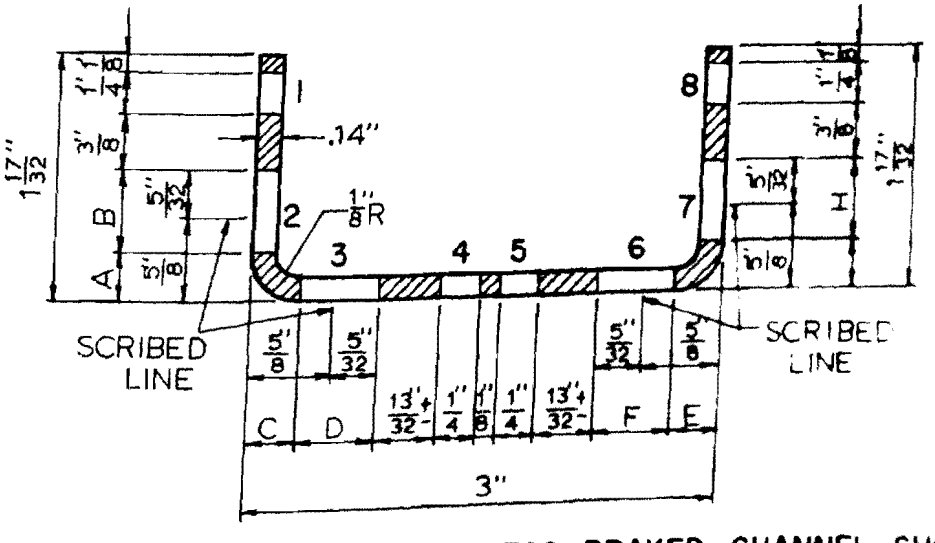

(b) TYPICAL CROSS SECTION OF PRESS BRAKED CHANNEL SHOWING TENSILE SPECIMEN LOCATIONS

FIG. 21. SPECIMENS FOR INVESTIGATION OF EXTENSION OF CORNER PLASTIC STRAIN EFFECTS INTO ADJACENT FLATS.

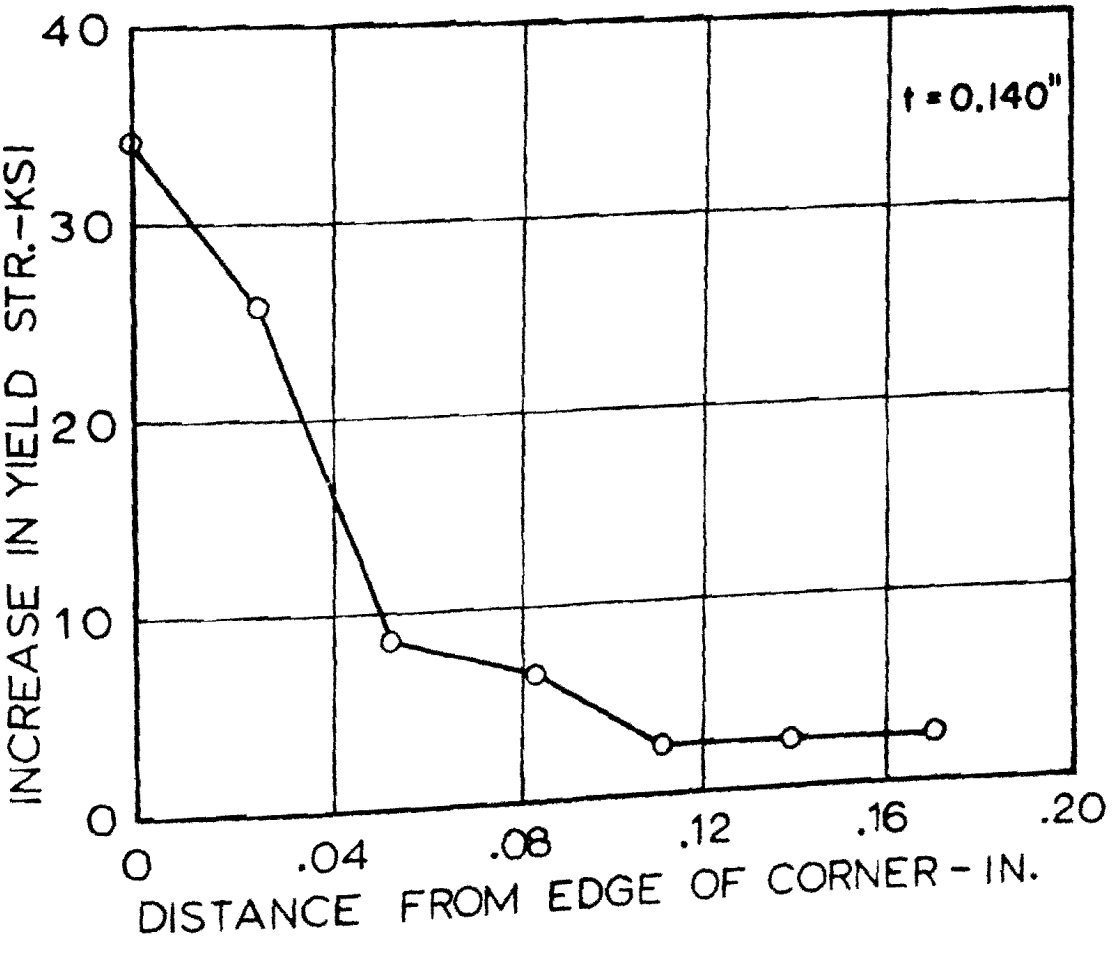

FIG. 22. VARIATION IN YIELD STRENGTH IN THE TRANSITION ZONE OF FLATS.

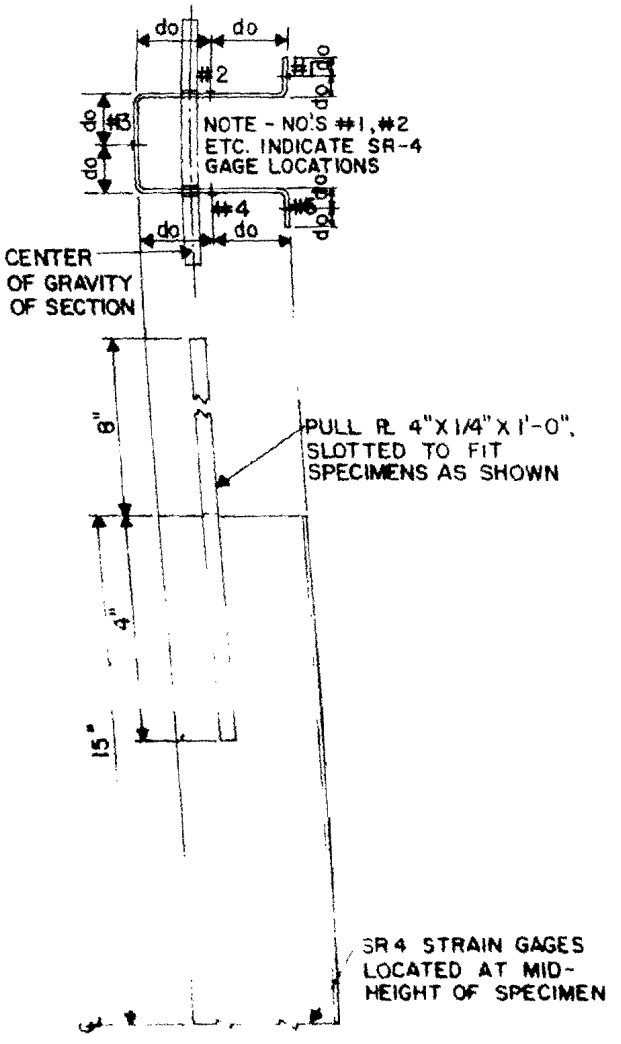

(a) TYPICAL FULL SECTION TENSION SPECIMEN

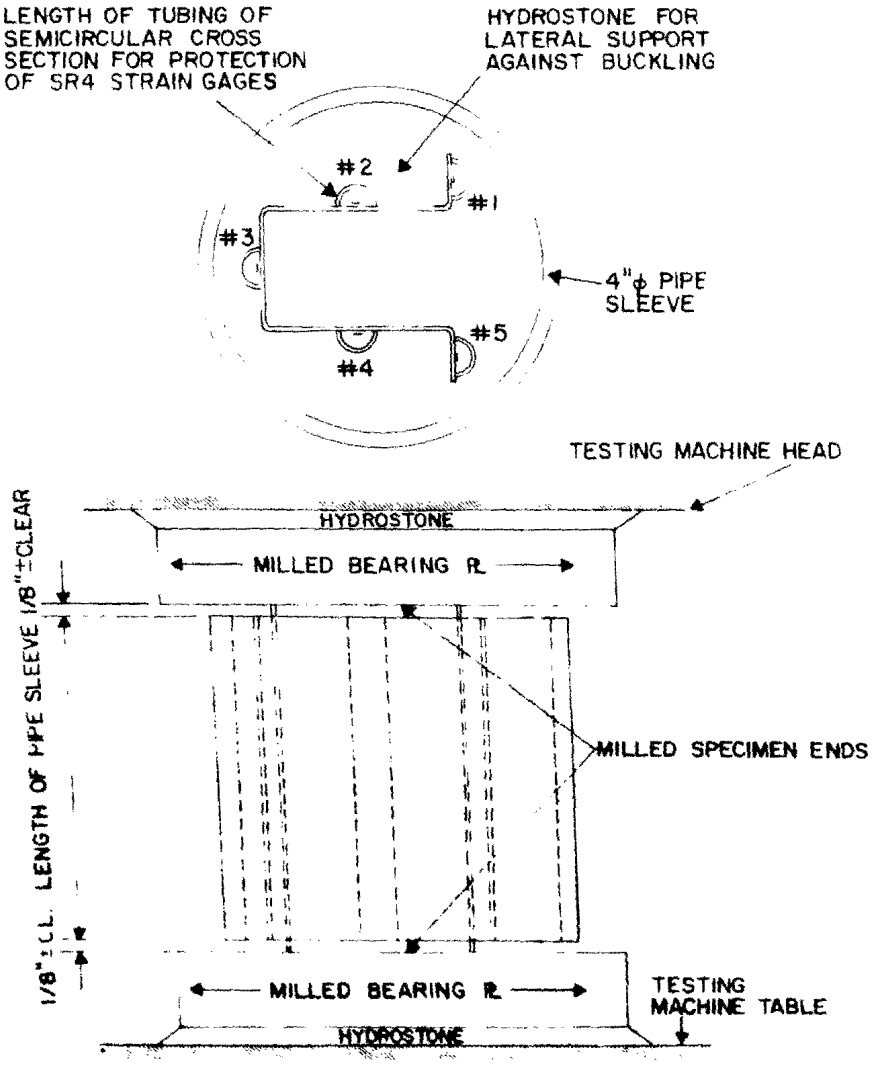

(b) FULL SECTION COMPRESSION TEST

FIG. 23. FULL SECTION TEST METHODS.

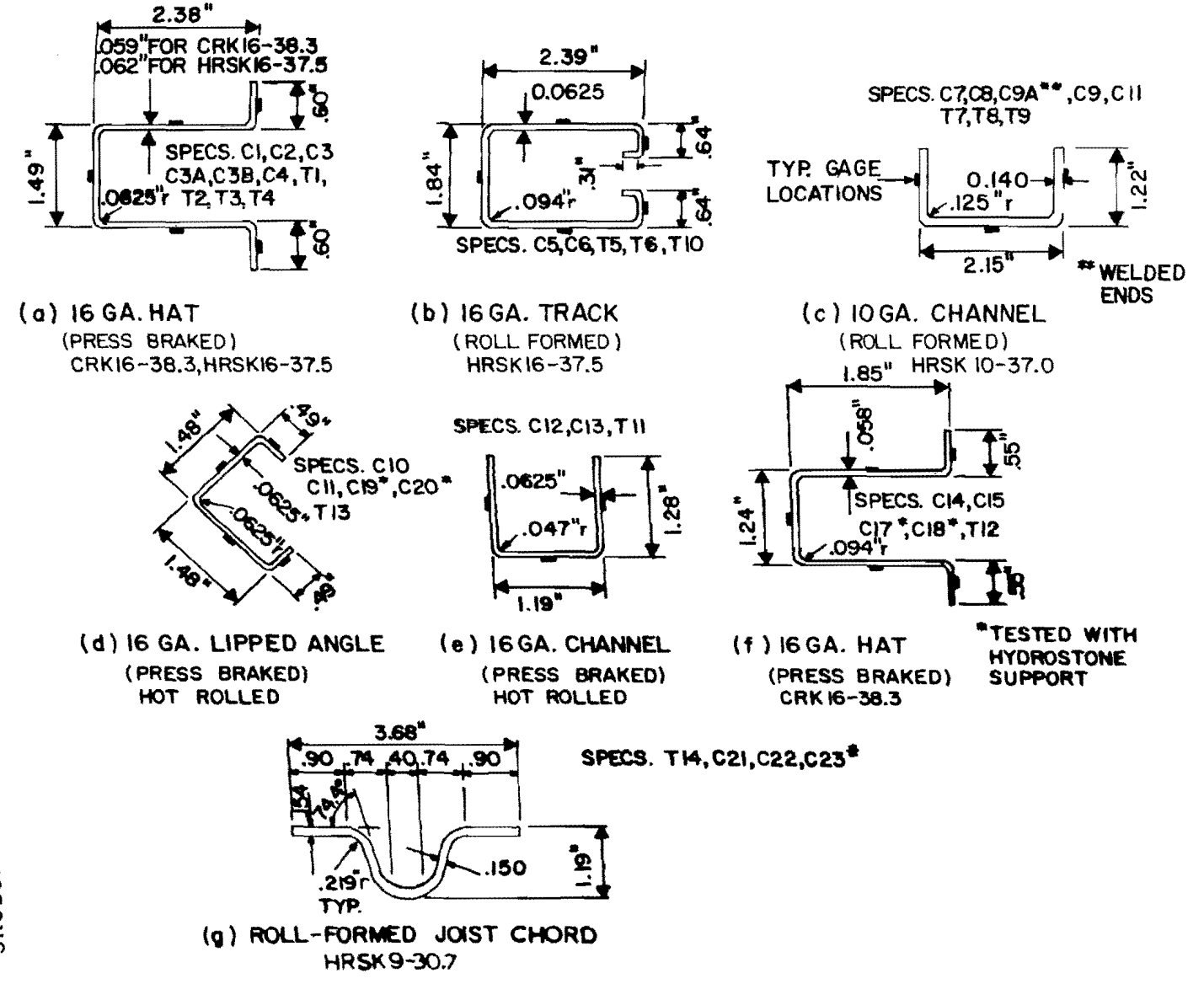

FIG. 24. FULL SECTION SPECIMENS AND AVERAGE DIMENSIONS

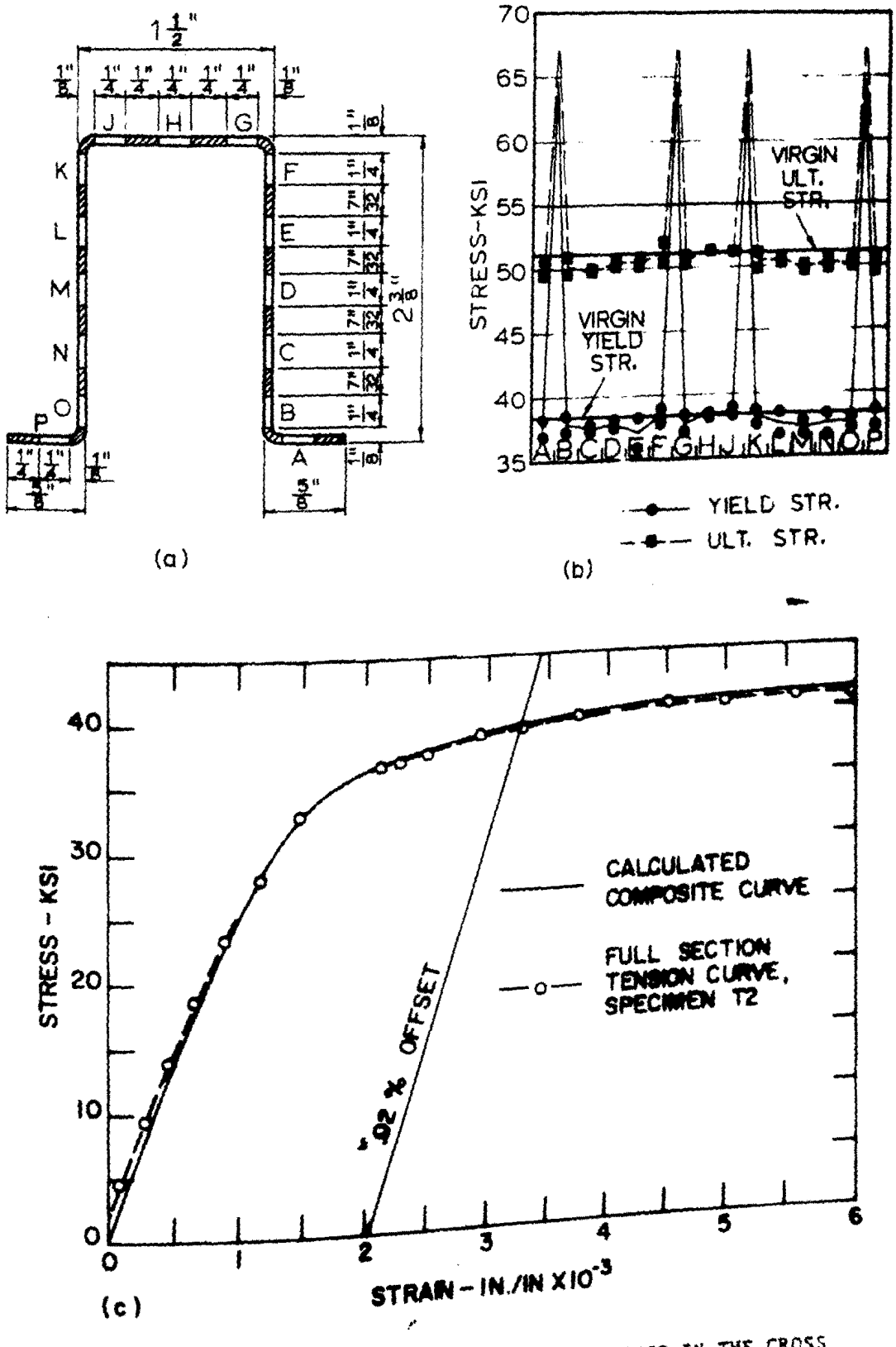

FIG. 25. TENSILE STRESS-STRAIN CHARACTERISTICS IN THE CROSS SECTION OF A PRESS BRAKED CRK16-38.3 HAT. (a) TENSILE STRIP SPECIMEN LOCATIONS. (b) VARIATION OF TENSILE YIELD AND ULTIMATE STRENGTHS. (c) COMPOSITE VERSUS FULL SECTION TENSION STRESS-STRAIN CURVES.

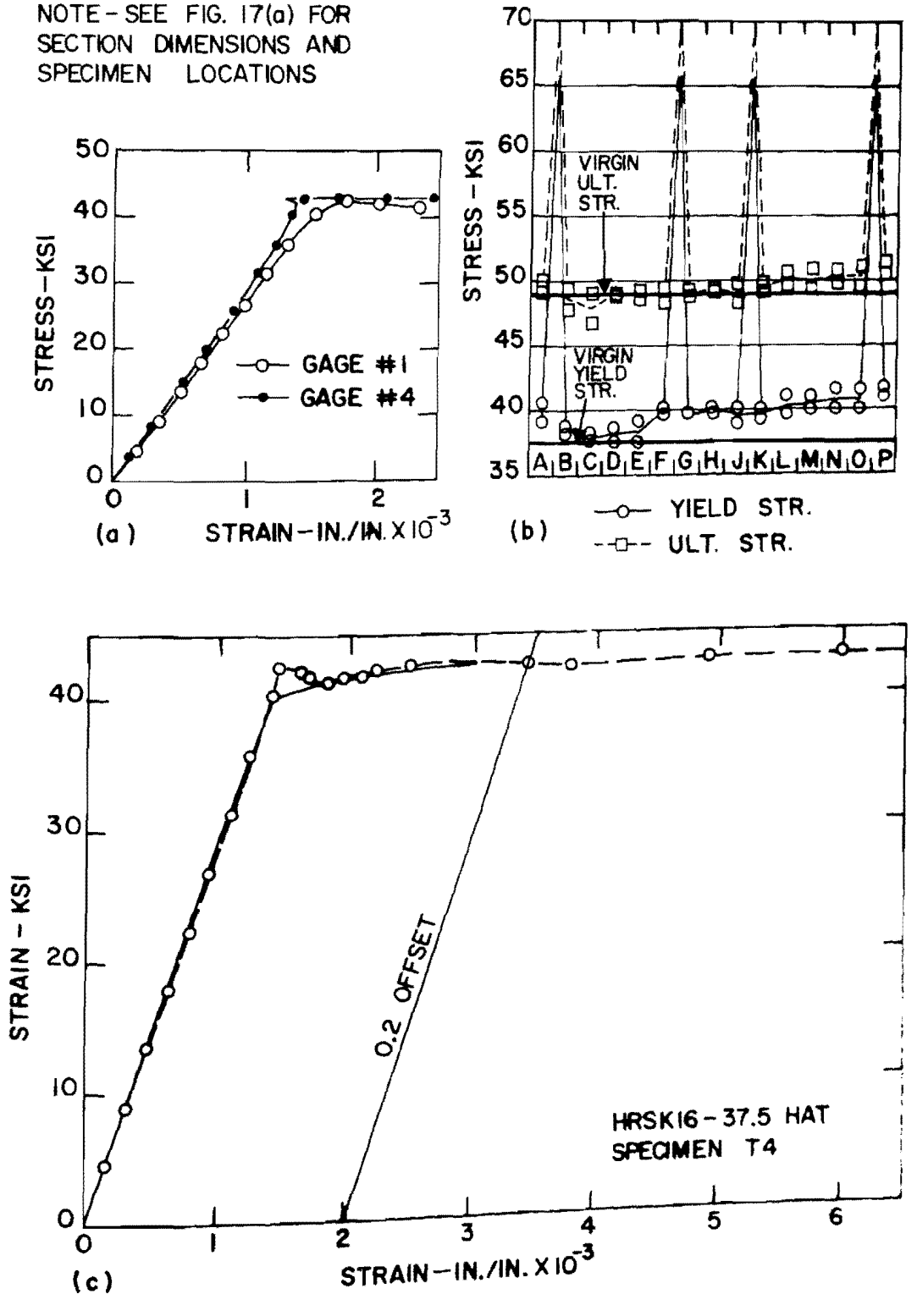

FIG. 26. TENSILE STRESS-STRAIN CHARACTERISTICS IN THE CROSS SECTION OF A PRESS BRAKED HRSK16-37.5 HAT. (a) STRESS-STRAIN CURVES FOR INDIVIDUAL STRAIN GAGES OF FULL SECTION TENSILE HAT SPECIMEN T4. (b) VARIATION OF TENSILE YIELD AND ULTIMATE STRENGTHS. (c) COMPOSITE VERSUS FULL SECTION TENSION STRESS-STRAIN CURVES.

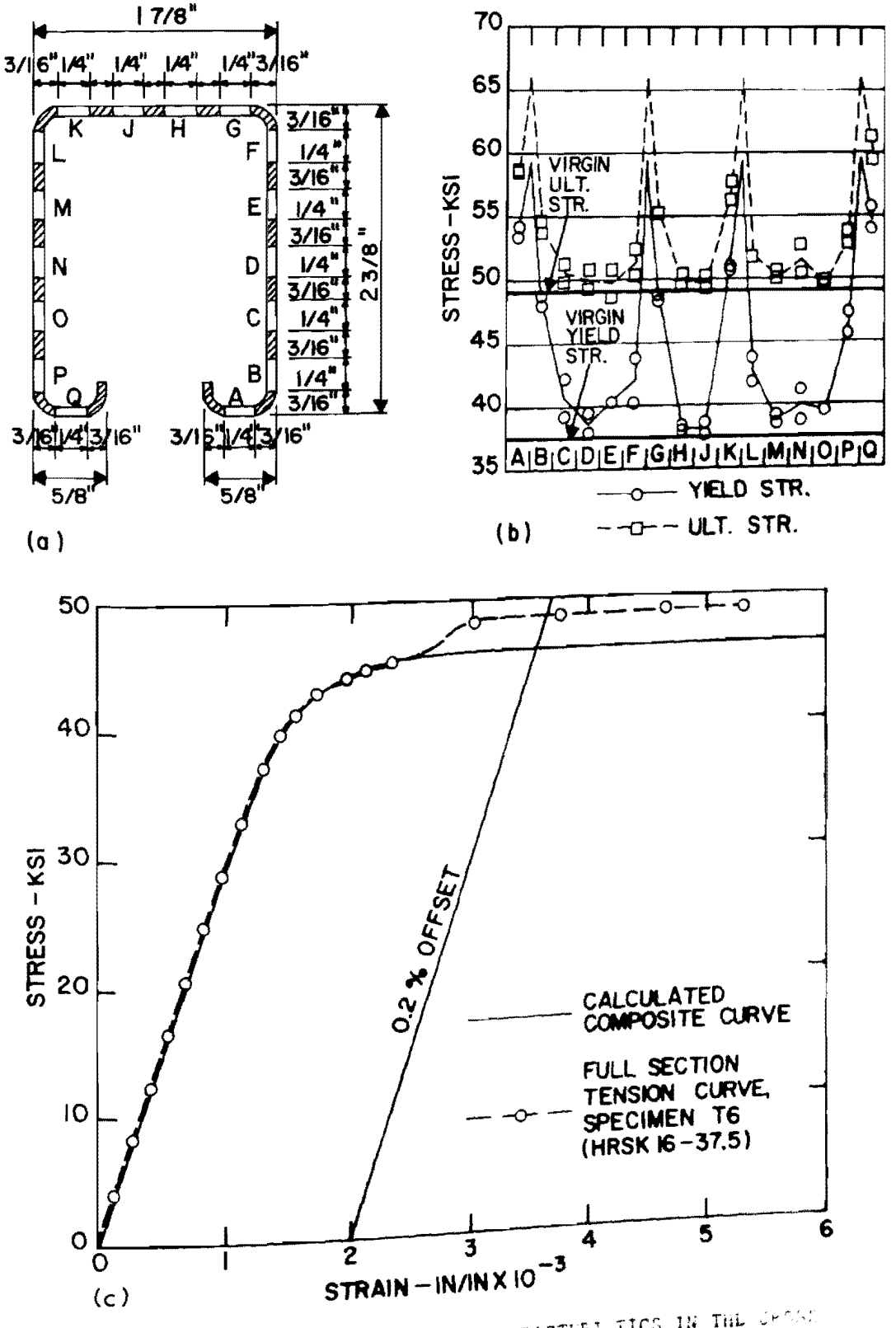

FIG. 27. TENSILE STRESS-STRAIN CHARACTERISTICS IN THE CROSS SECTION OF A ROLL-FORMED HRSK16-37.5 TRACK. (a) TENSILE STRIP SPECIMEN LOCATIONS. (b) VARIATION OF TENSILE YIELD AND ULTIMATE STRENGTHS. (c) COMPOSITE VERSUS FULL SECTION TENSION STRESS-STRAIN CURVES.

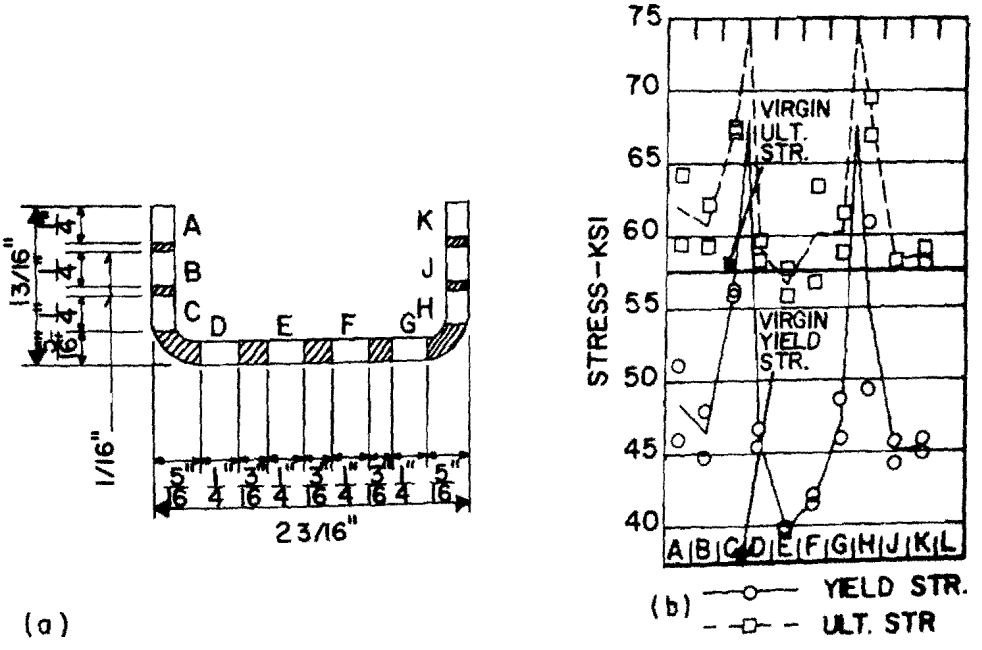

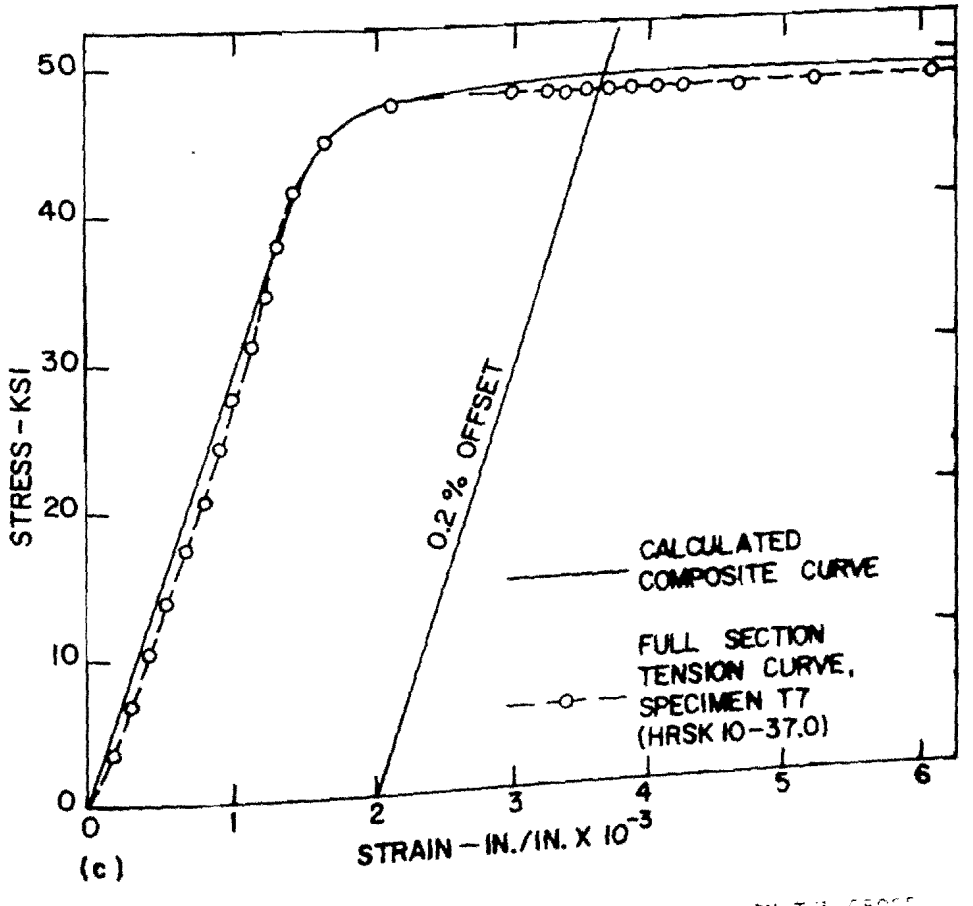

FIG. 28. TENSILE STRESS-STRAIN CHARACTERISTICS IN THE CROSS SECTION OF A ROLL-FORMED HRSK10-37.0 CHANNEL. (a) TENSILE STRIP SPECIMEN LOCATIONS. (b) VARIATION OF TENSILE YIELD AND ULTIMATE STRENGTHS. (c) COMPOSITE VERSUS FULL SECTION TENSION STRESS-STRAIN CURVES.

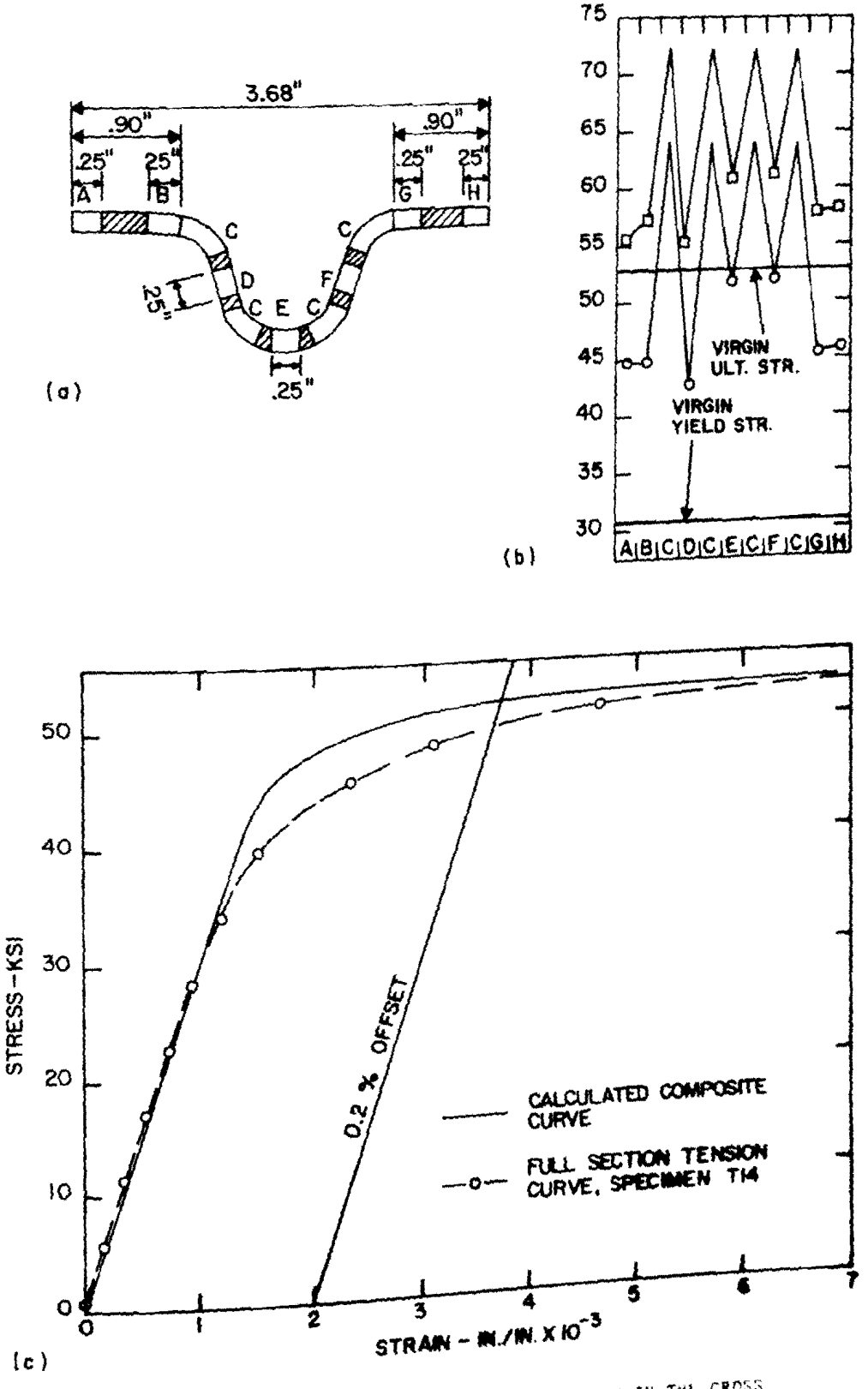

FIG. 29. TENSILE STRESS-STRAIN CHARACTERISTICS IN THE CROSS SECTION OF A ROLL-FORMED HRSK9-30.7 JOIST CHORD. (a) TENSILE STRIP SPECIMEN LOCATIONS. (b) VARIATION OF TENSILE YIELD AND ULTIMATE STRENGTHS. (c) COMPOSITE VERSUS FULL SECTION TENSION STRESS-STRAIN CURVES.

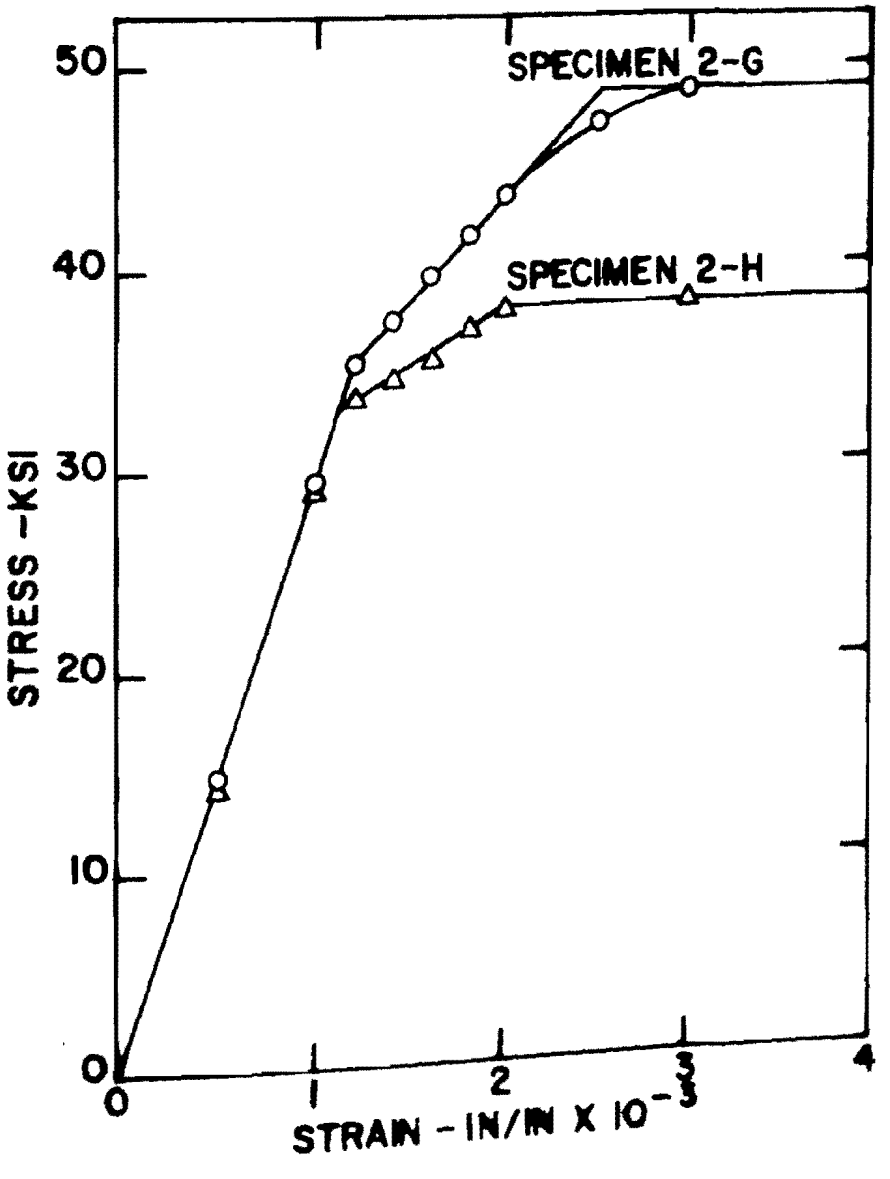

FIG. 30. TENSILE STRESS-STRAIN CURVES FOR 1/4 BY 1[illegible] INCH STRIP SPECIMENS FROM FLATS OF ROLL-FORMED [illegible] 37.5 TRACK SECTION.

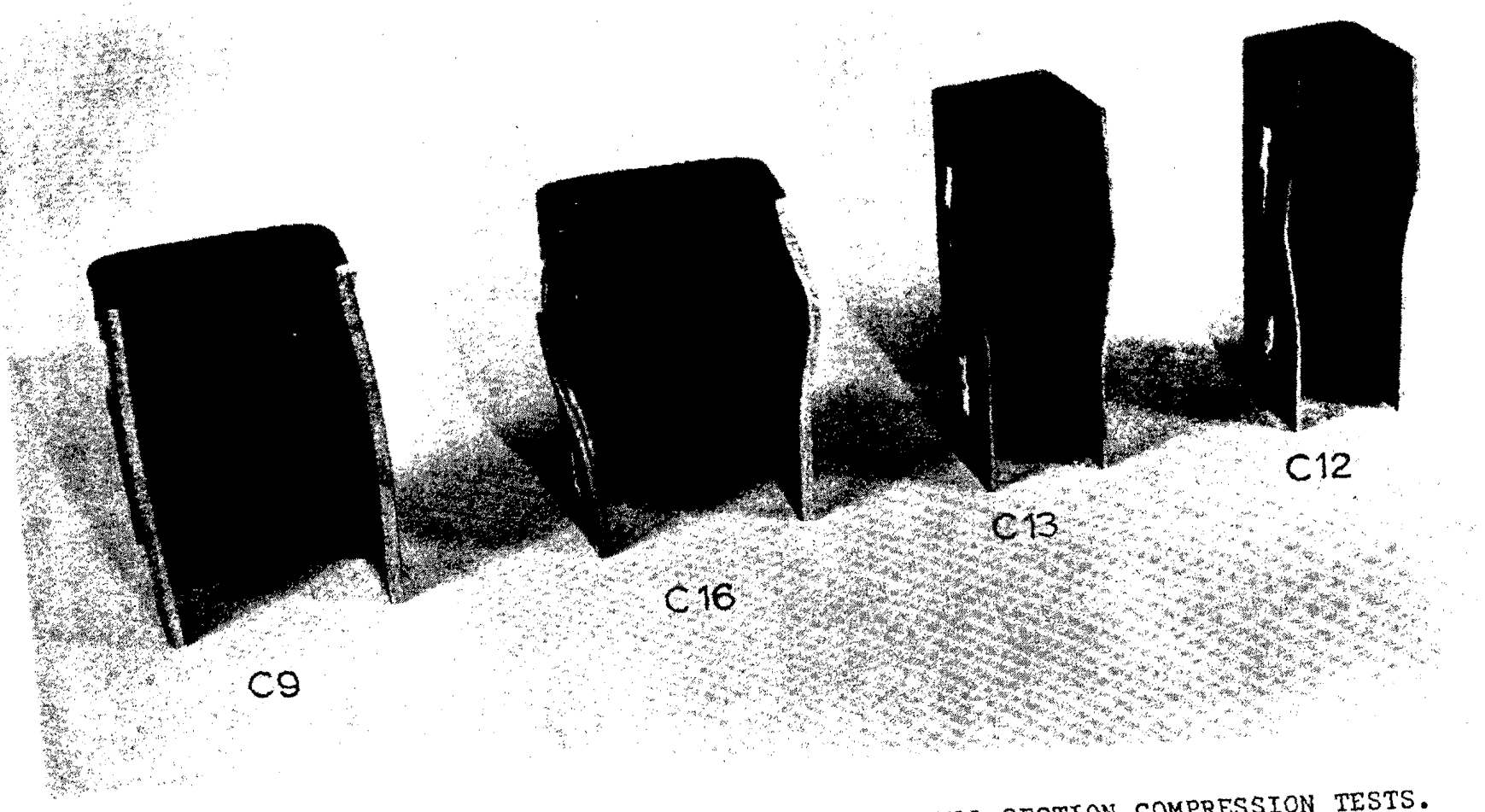

FIG. 31. LOCAL BUCKLING OF LATERALLY UNSUPPORTED FULL SECTION COMPRESSION TESTS.

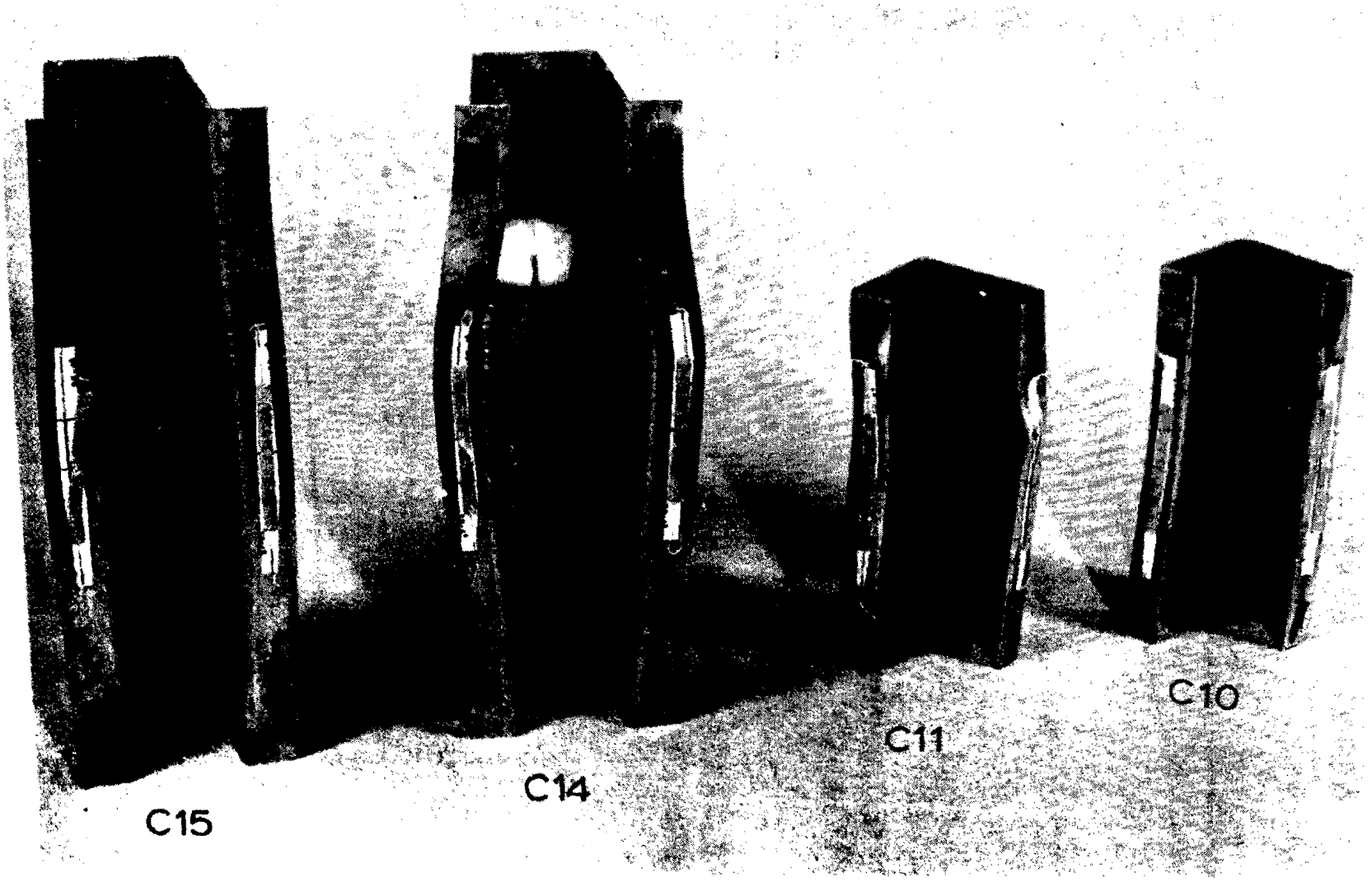

FIG. 32. LOCAL BUCKLING OF LATERALLY UNSUPPORTED FULL SECTION COMPRESSION SPECIMENS

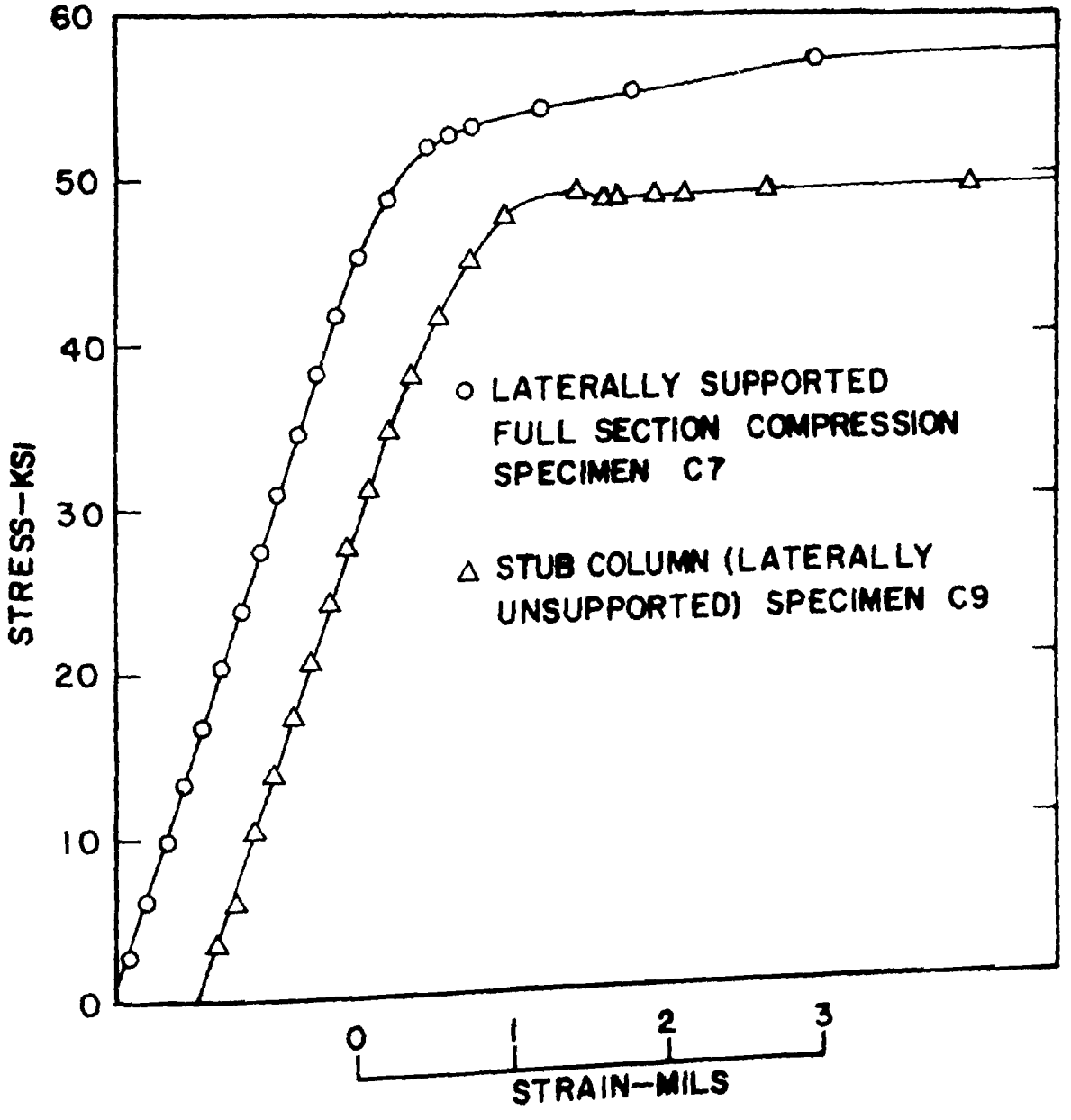

FIG. 33. COMPARISON OF FULL SECTION COMPRESSIVE STRESS-STRAIN CURVES FOR HRSK10-37.0 ROLL-FORMED CHANNELS.

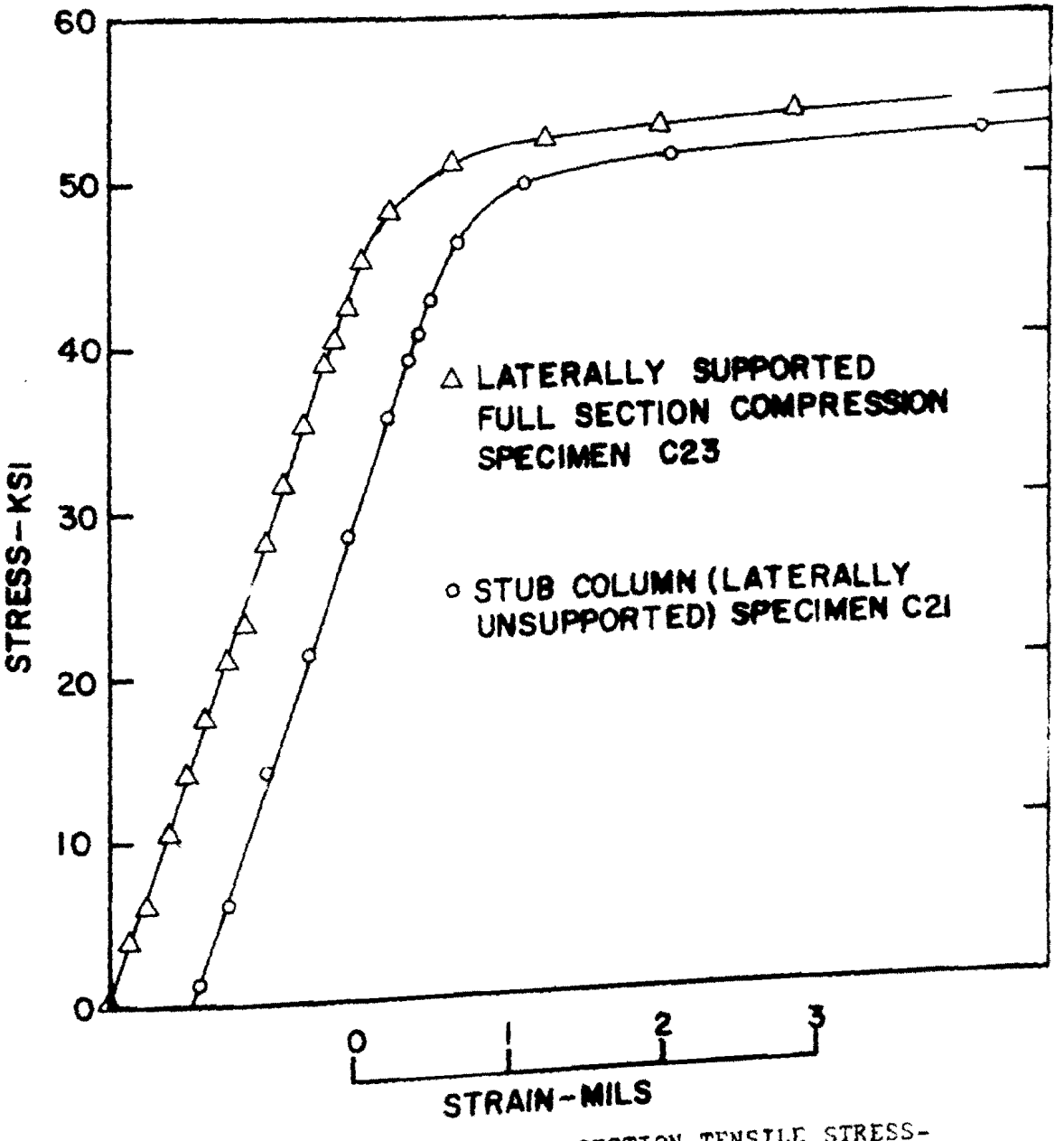

FIG. 34. COMPARISON OF FULL SECTION TENSILE STRESS-STRAIN CURVES FOR HRSK9-30.7 ROLL-FORMED JOIST CHORDS.

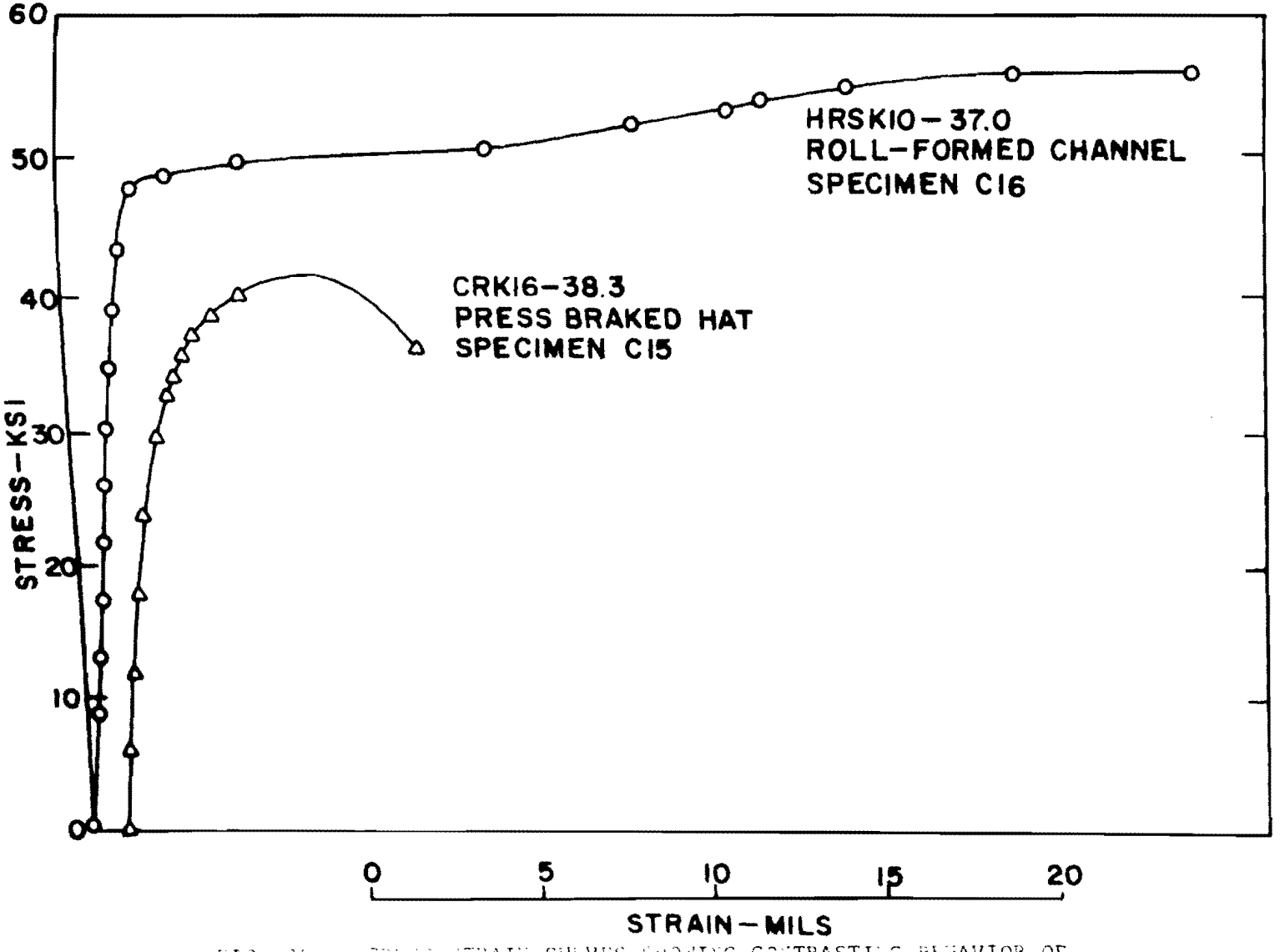

FIG. 35. STRESS-STRAIN CURVES SHOWING CONTRASTING BEHAVIOR OF COMPACT AND NON-COMPACT 10ft COLUMN SPECIMENS.

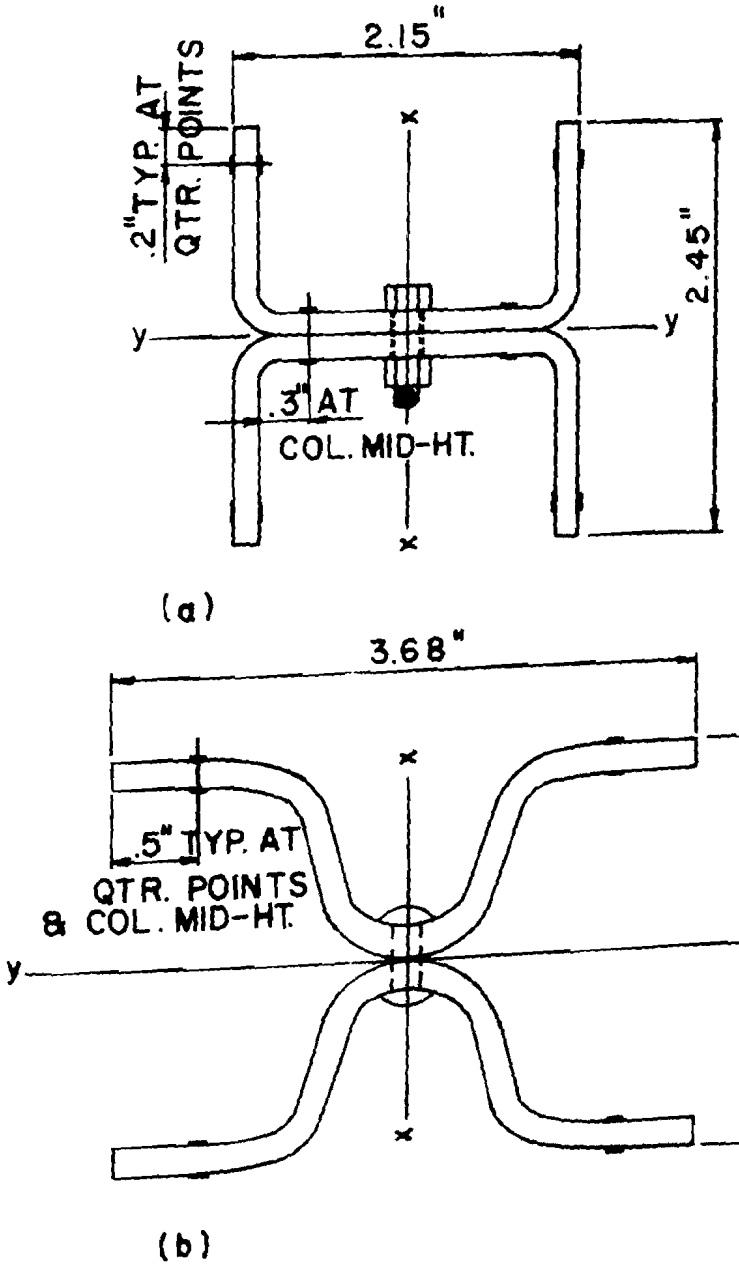

FIG. 36. SR-4 STRAIN GAGE LOCATIONS FOR COLUMN TEST SPECIMENS. (a) 10-GAGE HRSK10-37.0 ROLL-FORMED CHANNEL AND (b) 9-GAGE HRSK9-30.7 ROLL-FORMED JOIST CHORD.

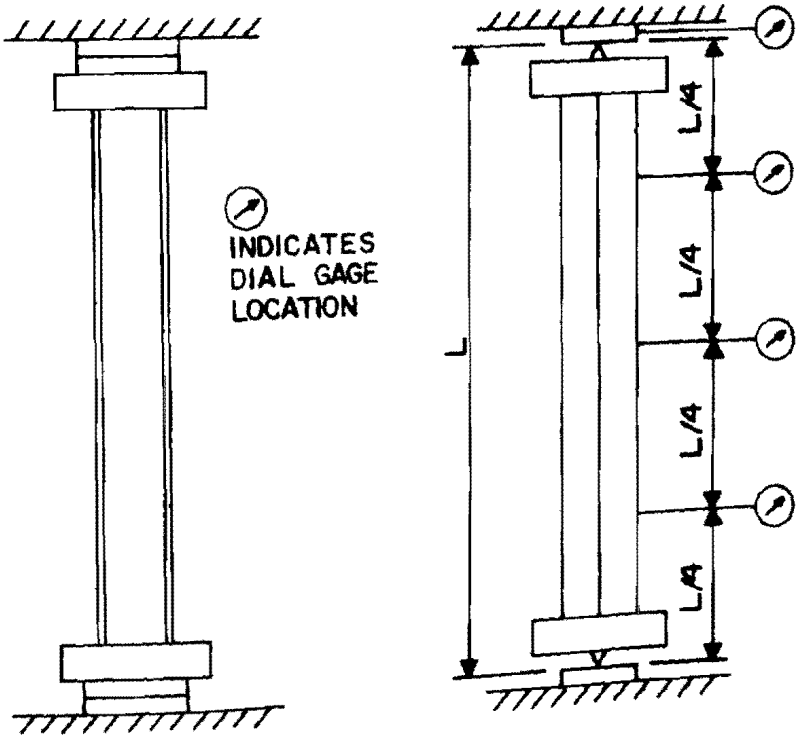

FIG. 37. SCHEMATIC OF TEST SET-UP FOR AXIALLY LOADED PIN-ENDED COLUMNS.

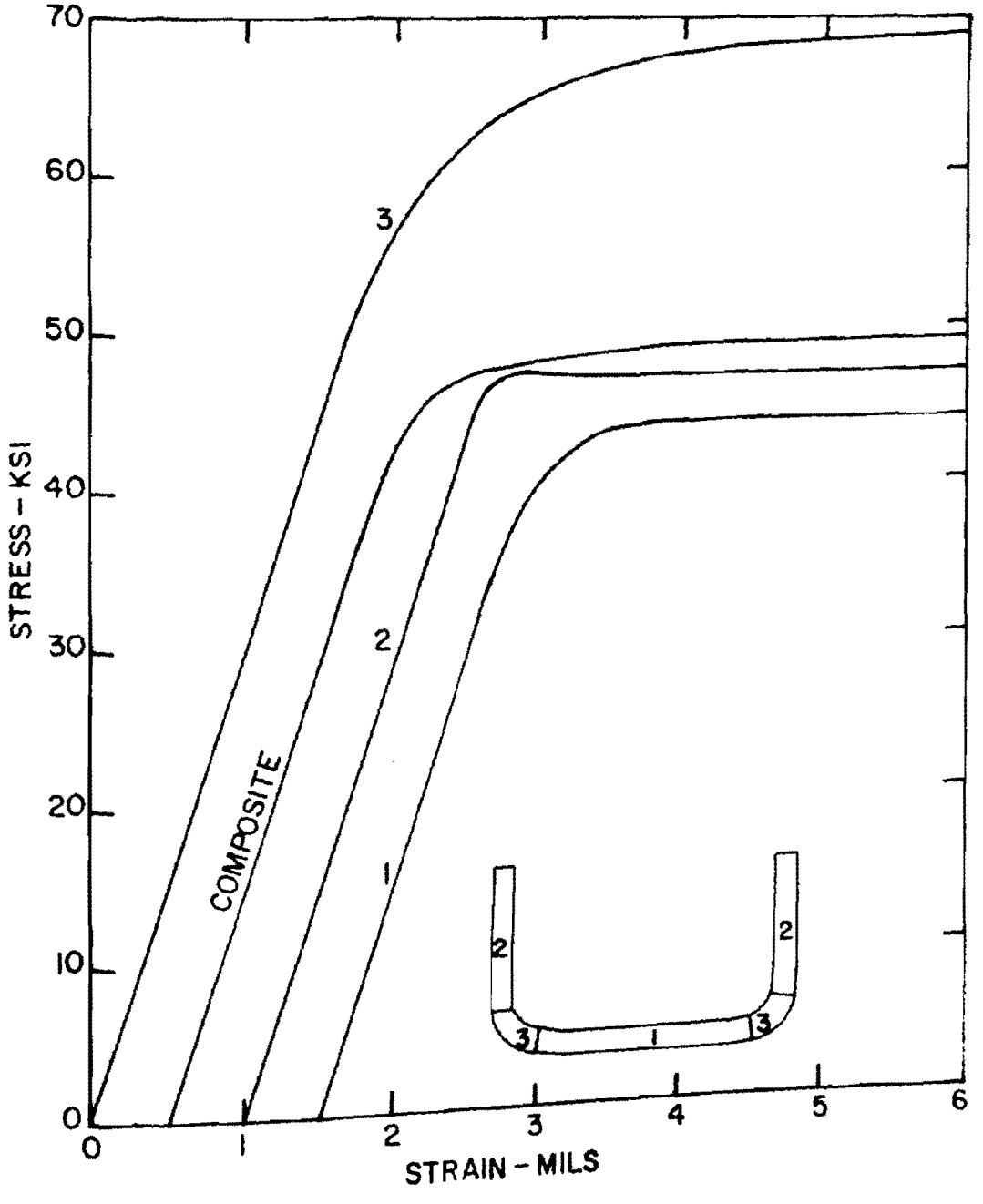

FIG. 38. TENSILE STRESS-STRAIN CURVES FOR ELEMENTS OF HRSK10-37.0 CHANNEL SECTIONS.

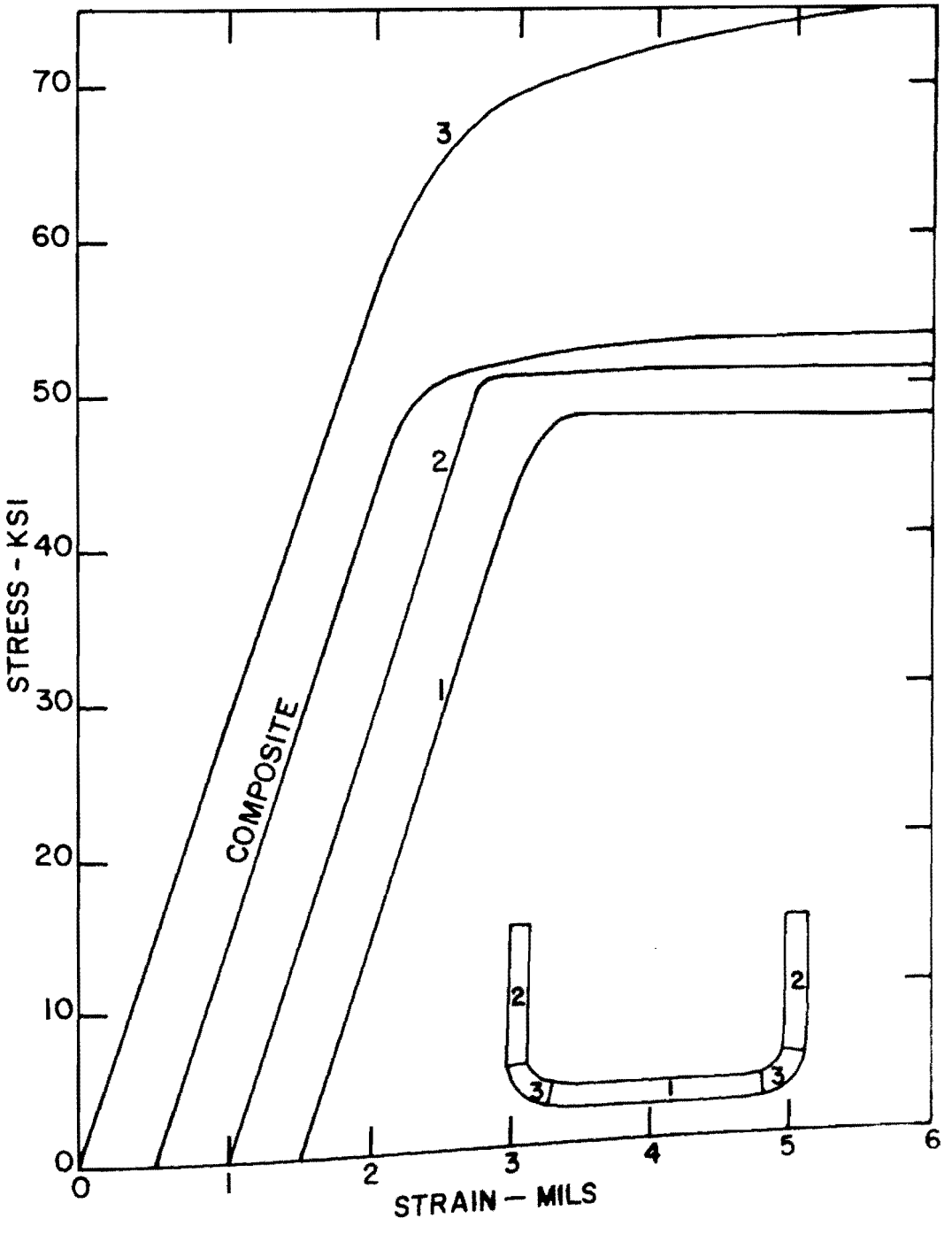

FIG. 39. COMPRESSIVE STRESS-STRAIN CURVES FOR [illegible]
OF HRSK10-37.0 CHANNEL SECTIONS.

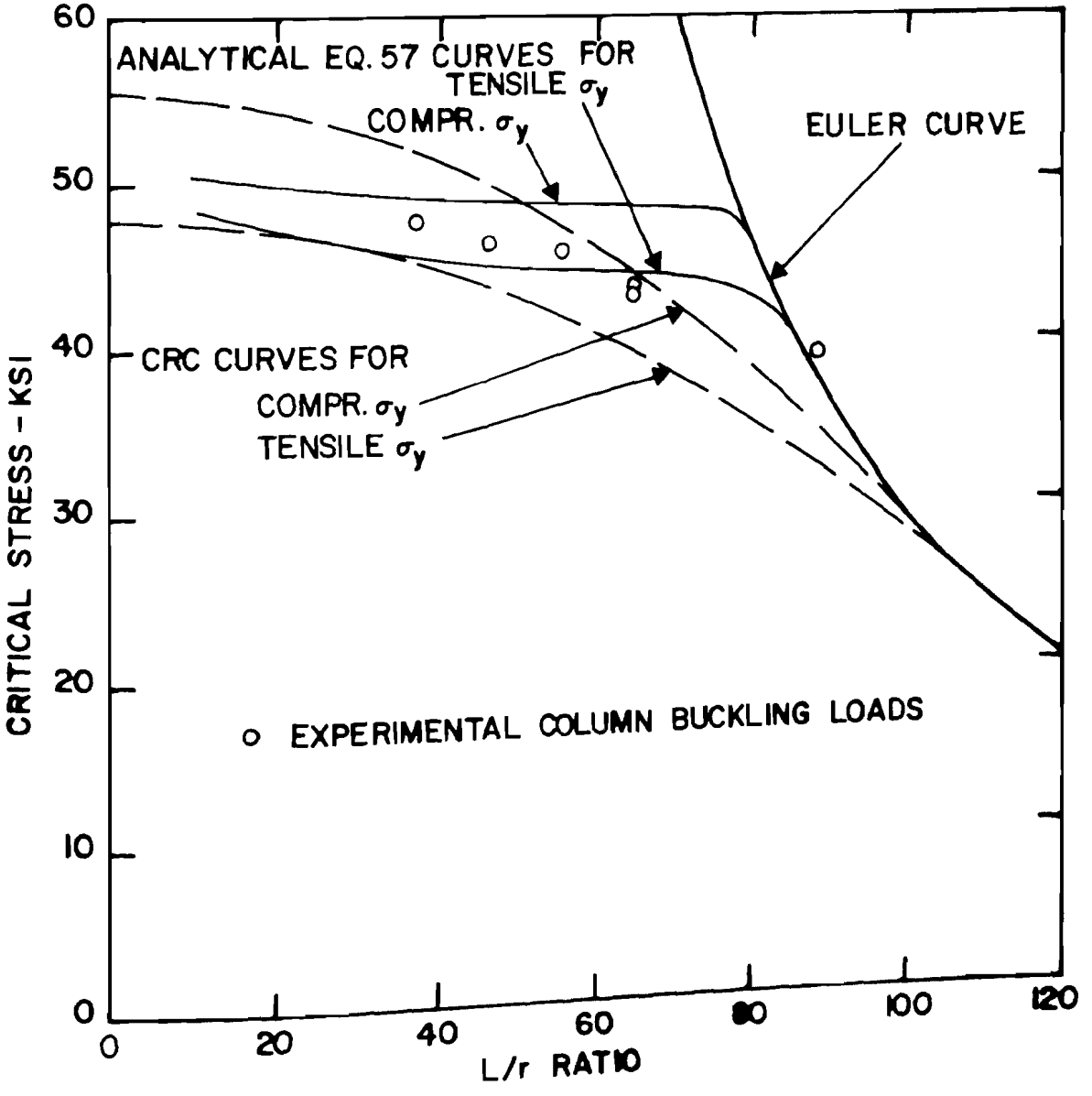

FIG. 40. TEST RESULTS FOR INELASTIC BUCKLING OF BOLTED AND COLD-RIVETED 10 GAGE CHANNEL COLUMNS.

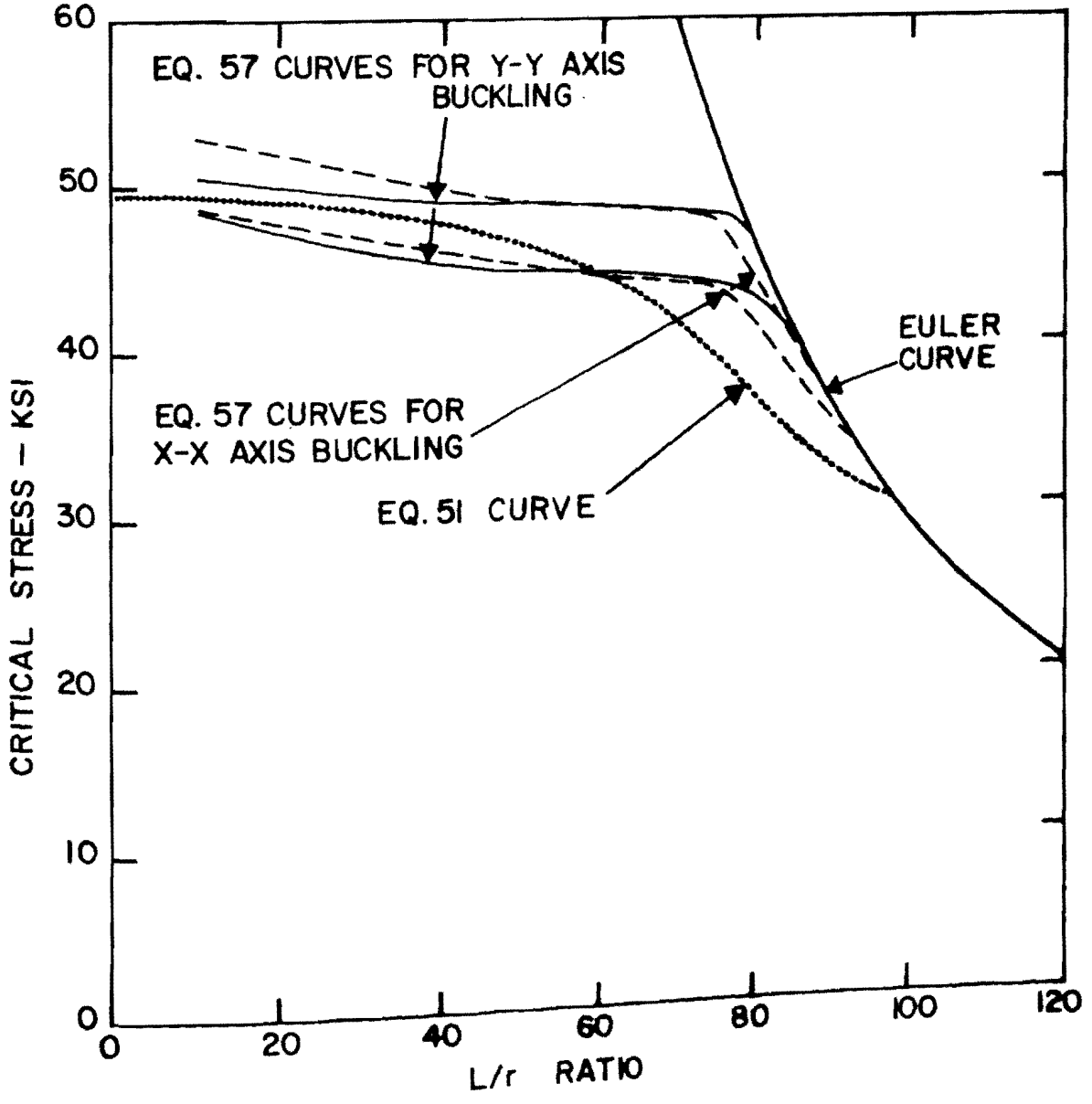

FIG. 41. COMPARISON OF COLUMN CURVES FOR BOLTED AND COLD-RIVETED 10 GAGE CHANNEL COLUMNS.

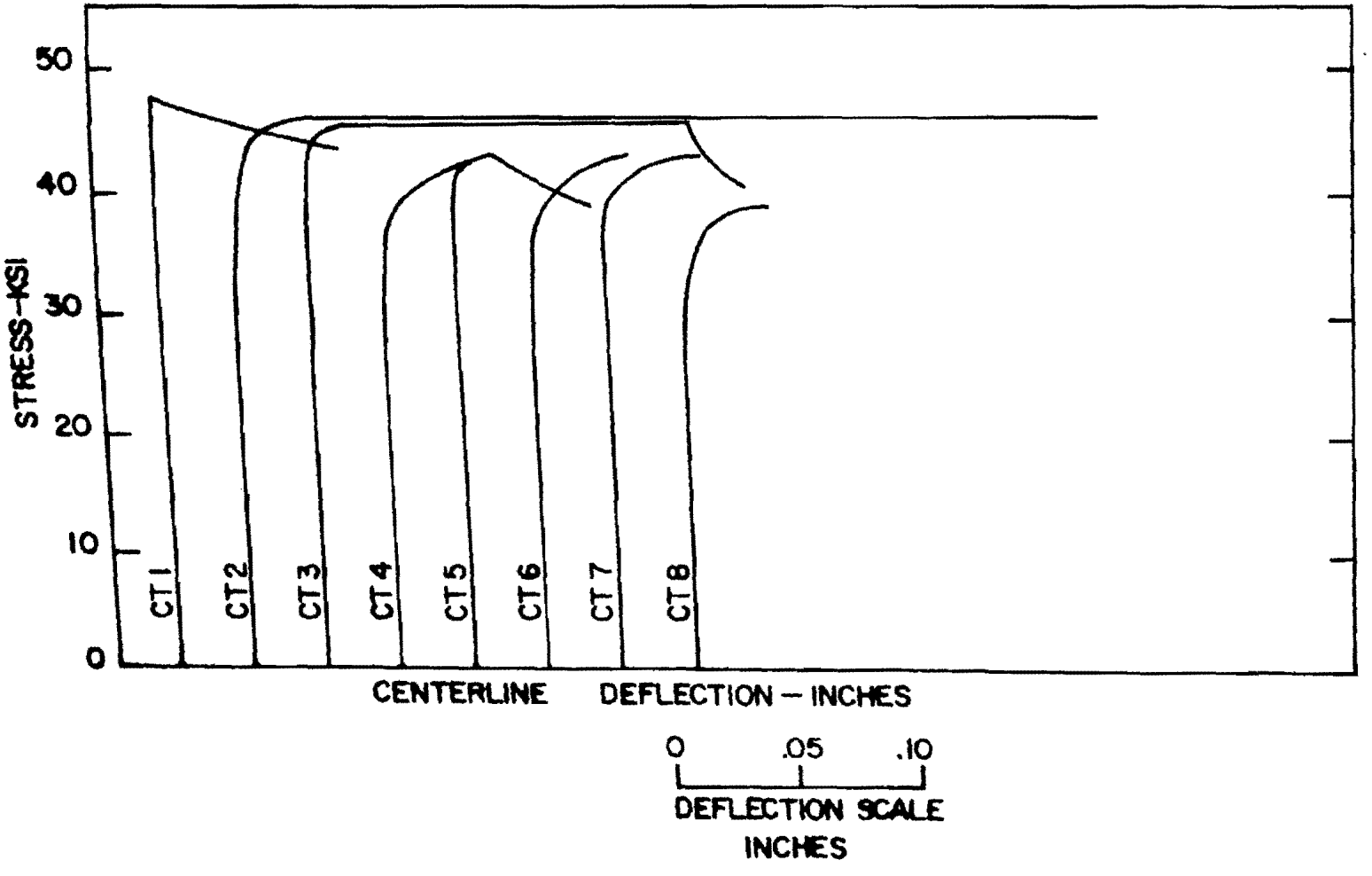

FIG. 42. LOAD-VERSUS CENTERLINE DEFLECTION CURVES FOR BOLTED AND COLD-RIVETED 10 GAGE CHANNEL COLUMNS.

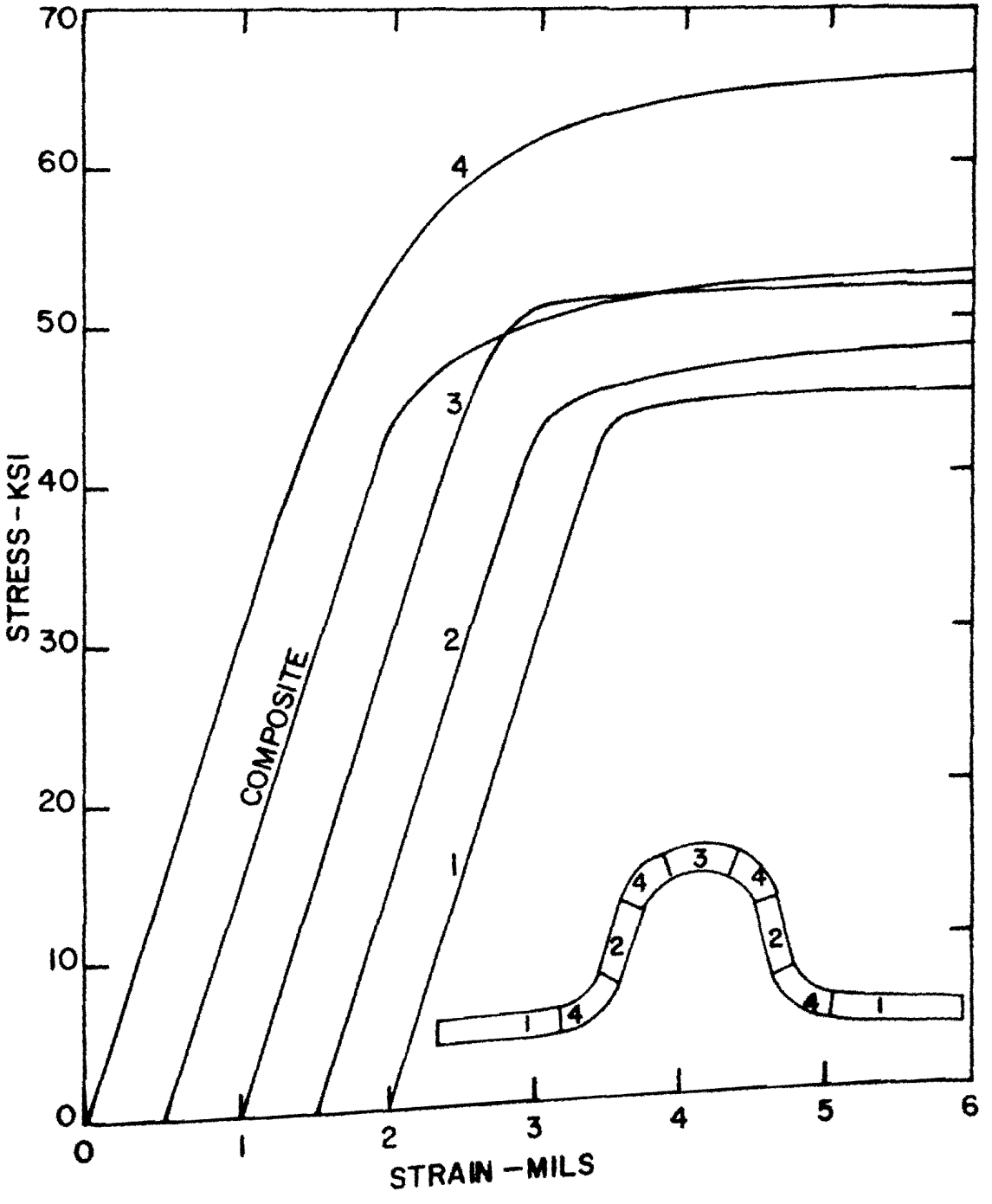

FIG. 43. TENSILE STRESS-STRAIN CURVES FOR ELEMENTS OF HRSK9-30.7 JOIST CHORD SECTIONS.

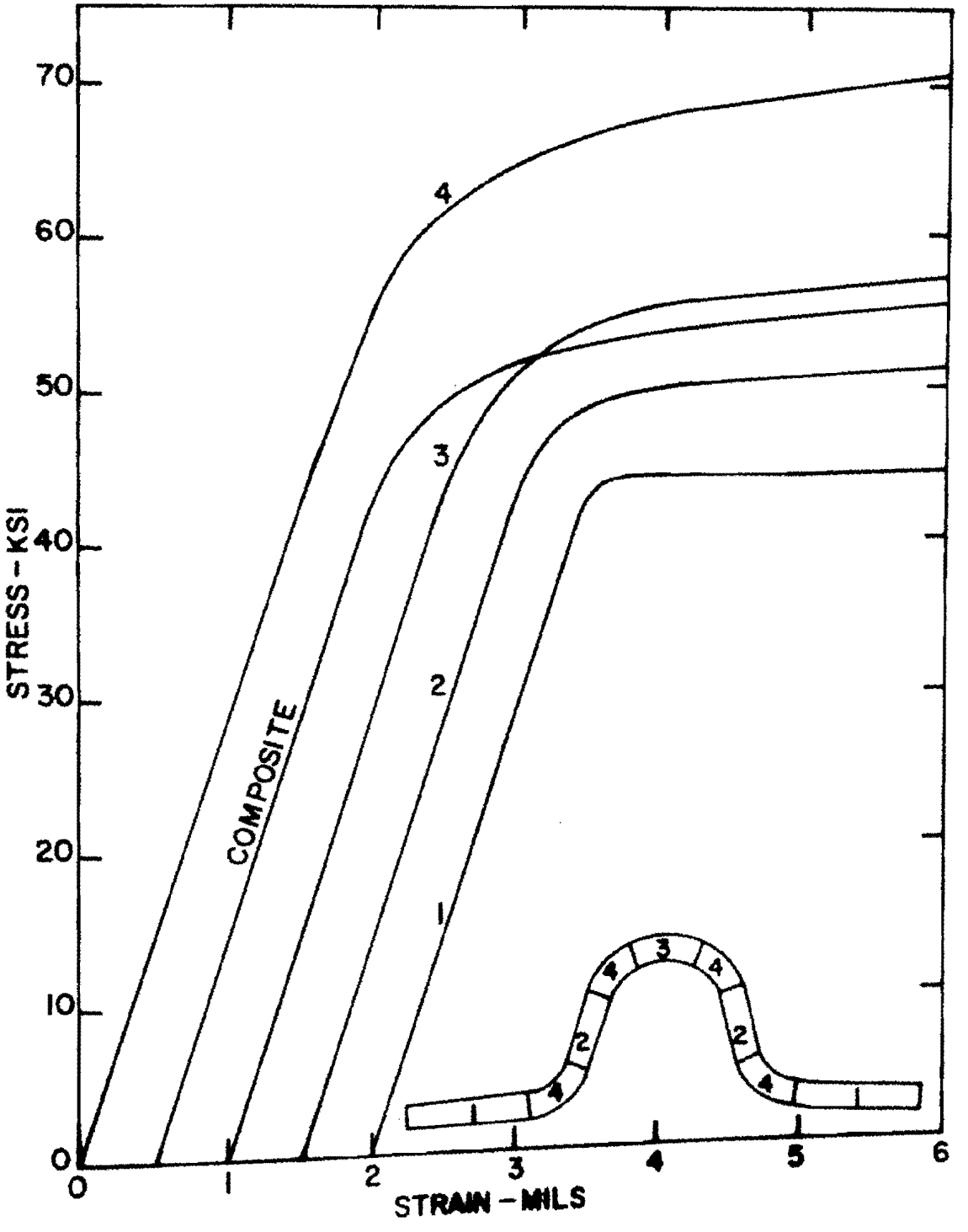

FIG. 44. COMPRESSIVE STRESS-STRAIN CURVES FOR ELEMENTS OF HRSK9-30.7 JOIST CHORD SECTIONS.

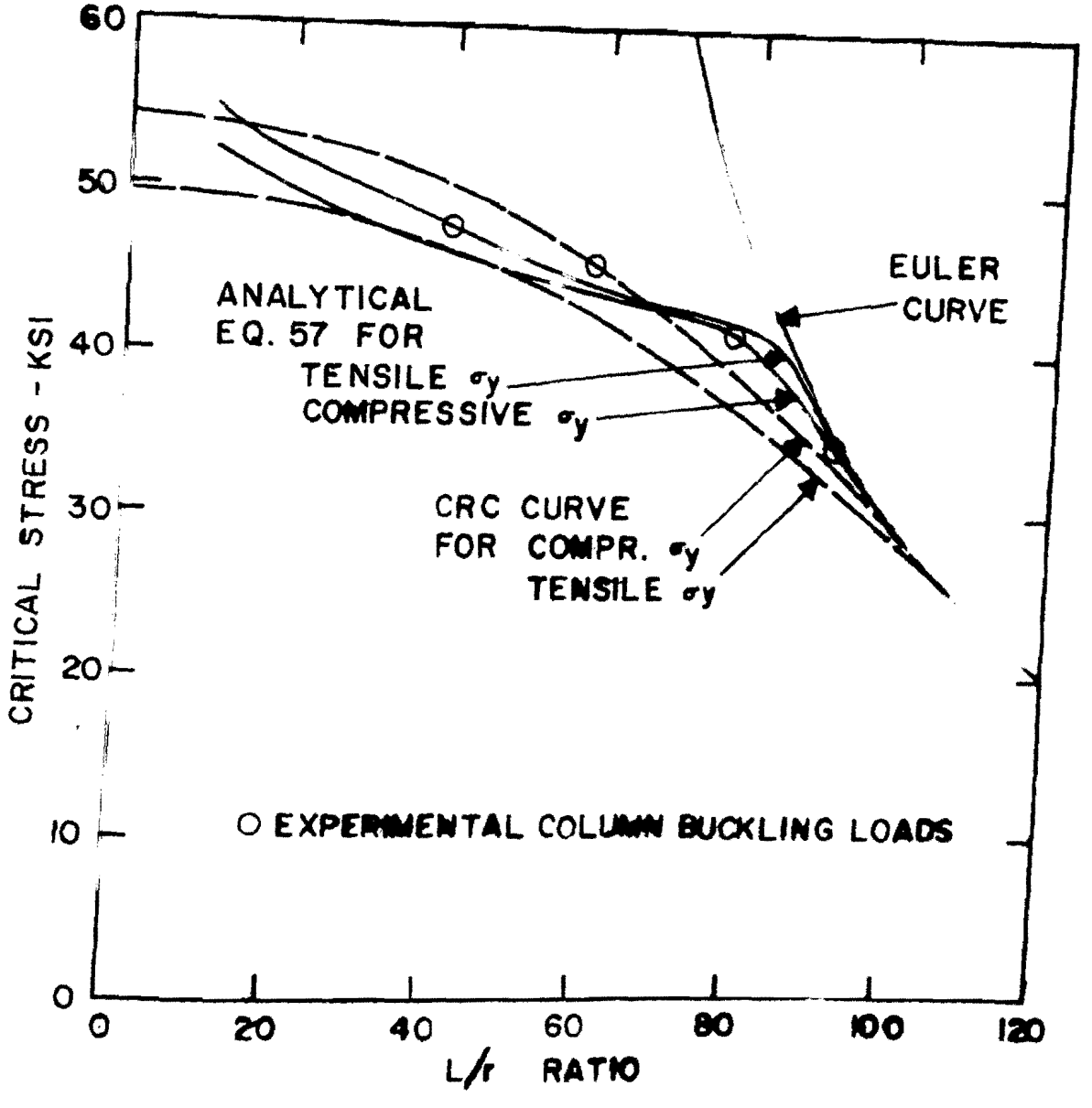

FIG. 45. TEST RESULTS FOR INELASTIC BUCKLING OF COLD-RIVETED 9 GAGE JOIST CHORD COLUMNS.

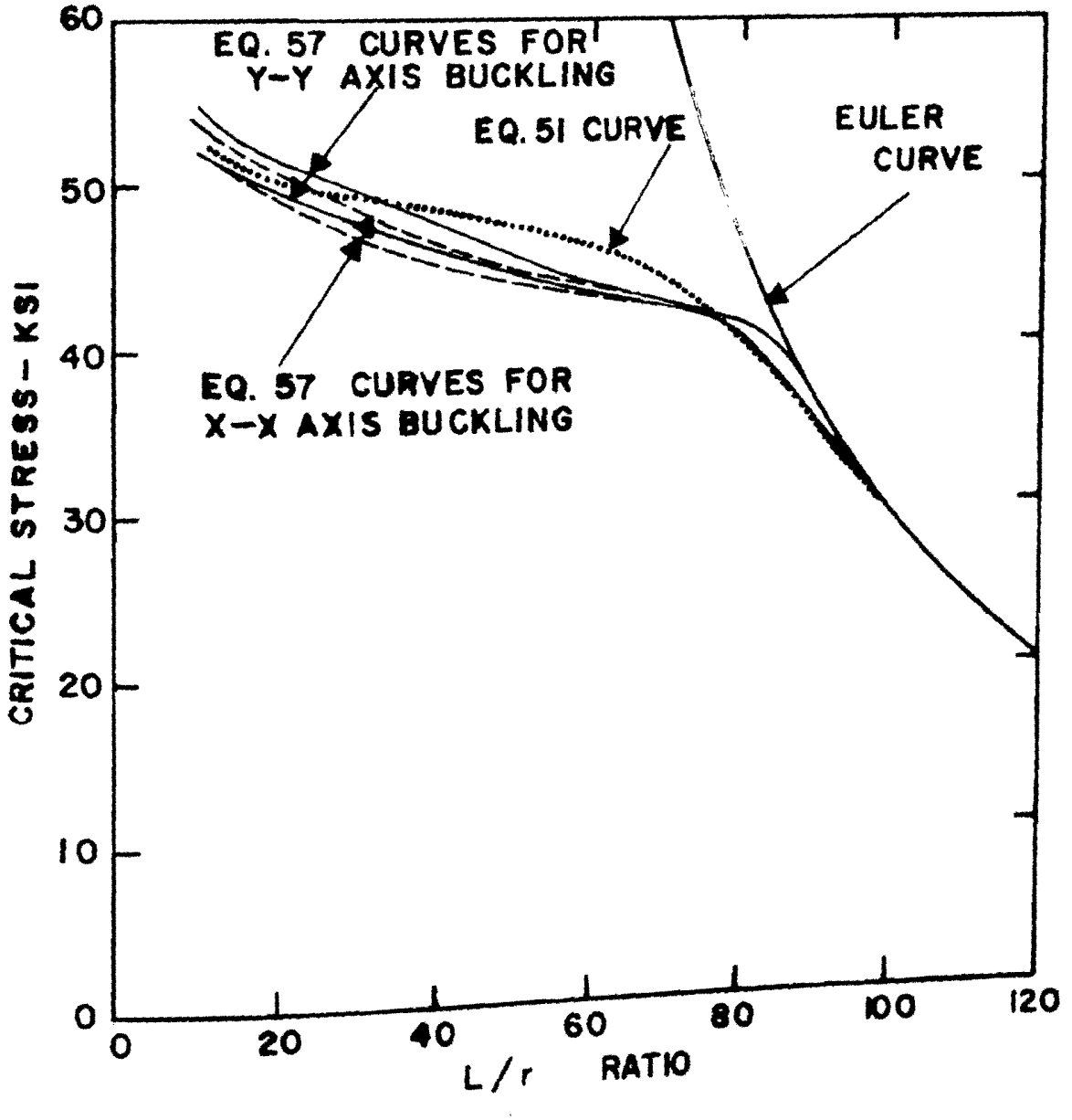

FIG. 46. COMPARISON OF COLUMN CURVES FOR COLD-RIVETED 9 GAGE JOIST CHORD COLUMNS.

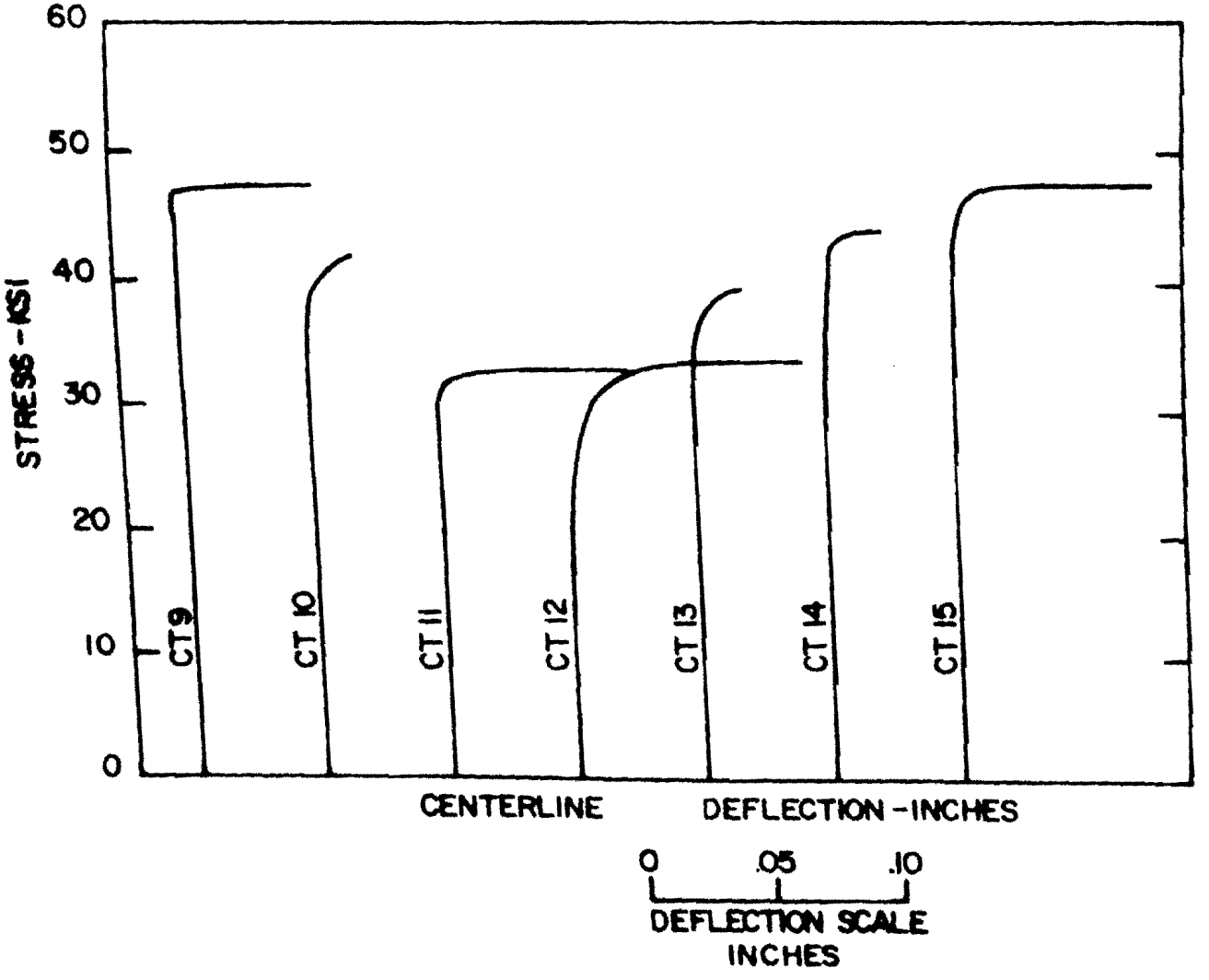

FIG. 47. STRESS VERSUS CENTERLINE DEFLECTION CURVES FOR COLD-RIVETED 9 GAGE HRSK9-30.7 JOIST CHORD COLUMNS.

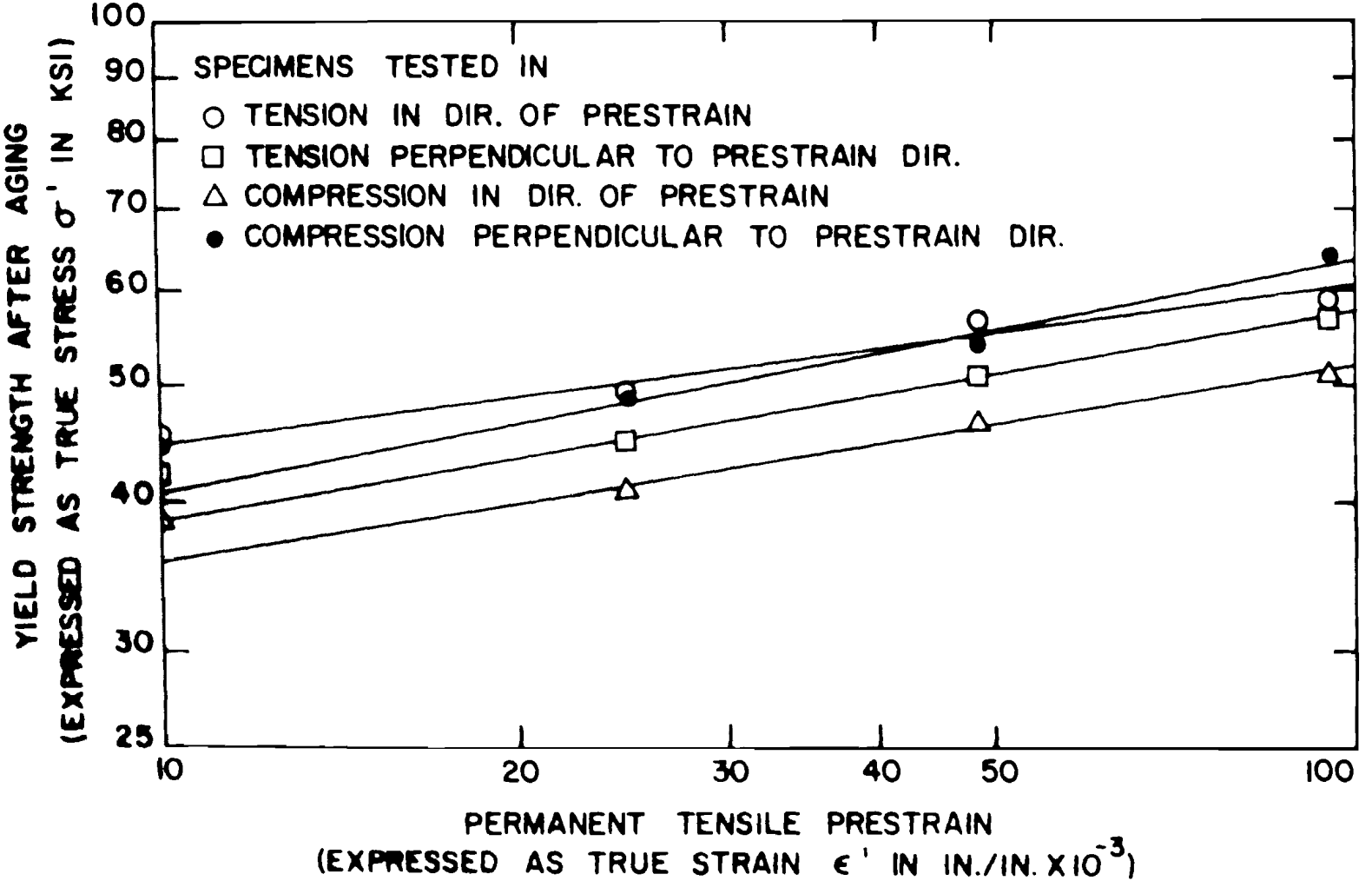

FIG. 48. TYPICAL CURVES OF YIELD STRENGTH-PLASTIC STRAIN RELATIONSHIPS OF UNIDIRECTIONALLY PRESTRAINED FLAT SHEETS.

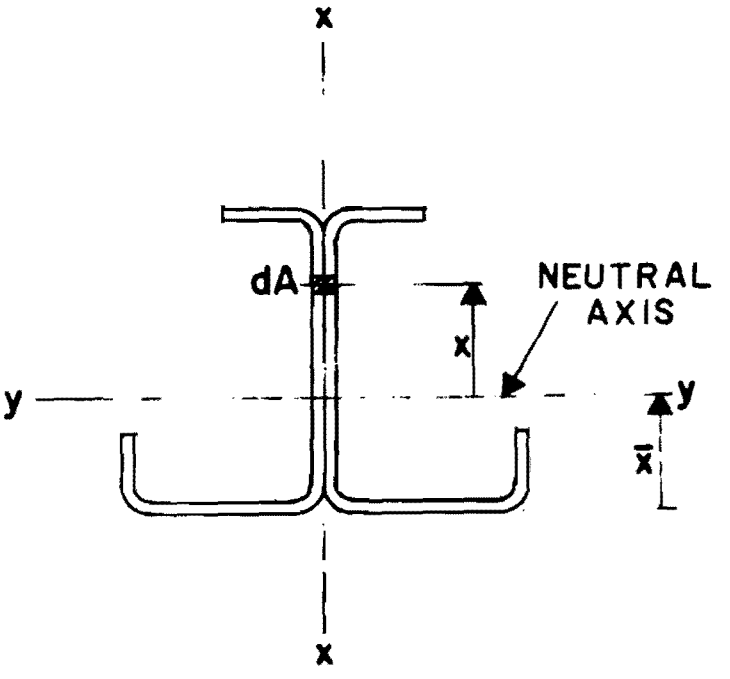

(a) COLUMN CROSS SECTION

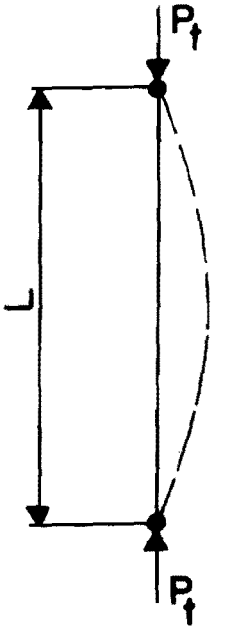

(b) PIN-ENDED COLUMN AND LOADS

FIG. 49. MONO-SYMMETRIC COLUMN